January 2016

DESIGNER COLLAGEN-FIBRIL BIOGRAFT MATERIALS FOR TUNABLE MOLECULAR DELIVERY

Rucha Joshi
Purdue University

Follow this and additional works at: https://docs.lib.purdue.edu/open_access_dissertations

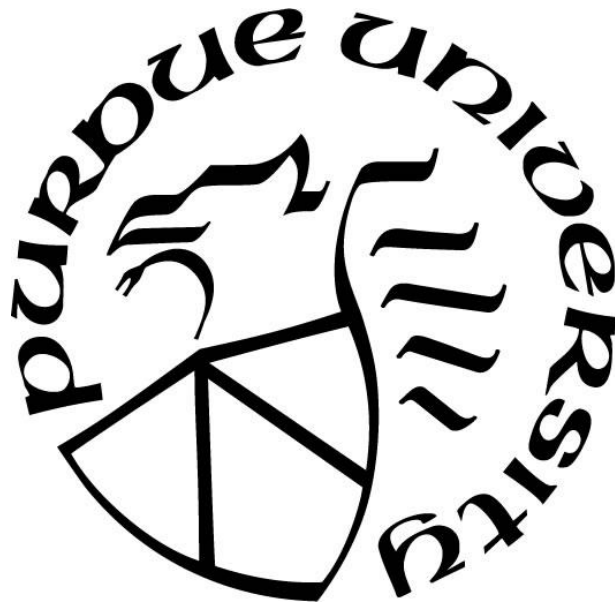# DESIGNER COLLAGEN-FIBRIL BIOGRAFT MATERIALS FOR TUNABLE MOLECULAR DELIVERY

by

Rucha V. Joshi

A Dissertation

Submitted to the Faculty of Purdue University

In Partial Fulfillment of the Requirements for the degree of

Doctor of Philosophy

Department of Biomedical Engineering

West Lafayette, Indiana

December 2016

THE PURDUE UNIVERSITY GRADUATE SCHOOL
STATEMENT OF DISSERTATION APPROVAL

Dr. Sherry Voytik-Harbin, Chair

     Department of Biomedical Engineering

Dr. Kinam Park

     Department of Biomedical Engineering

Dr. Bumsoo Han

     Department of Mechanical Engineering

Dr. Mervin C. Yoder

     School of Medicine, Indiana University

Approved by:

Dr. George R. Wodicka

     Head of the Departmental Graduate Program

I dedicate this work to all my mentors who have wonderfully ignited my mind in quest of science, and inspired me to take the paths less trodden with heart full of passion.

ACKNOWLEDGMENTS

and equipment needed in this research. I would also like to acknowledge the source of funding for research, the National Heart, Lung, and Blood Institute.

My special thanks go to my husband Dr. Shashank Tamaskar, for the incredible amount of support and help he has provided in completion of my Ph.D. From spending countless weekends with me in lab, lending a patient ear to my research talk, offering thoughtful solutions to any of my problems, and encouraging me to be calm and patient throughout my research, this biggest cheerleader of my life has helped me celebrate little victories of graduate student life on the roller-coaster of research. I owe him a life-time of happiness in return.

Last but not the least, I would like to thank my family, relatives, friend and teachers: my parents, parents-in law, brother in-law Shravan Tamaskar and all the relatives, teachers and friends for supporting me spiritually throughout this work and my life in general. I would like to express my immense gratitude to my father Dr. Vinay Joshi and mother Mrs. Deepa Joshi for their tremendous support throughout my Ph.D. I could not have been where I am today without their support, guidance, and love. I am also obliged to my school teachers, badminton coach and mentors for being my guiding light on multiple aspects of life.

TABLE OF CONTENTS

LIST OF TABLES

LIST OF FIGURES

ABSTRACT

Author: Joshi, Rucha, Vinay. Ph.D.
Institution: Purdue University
Degree Received: December 2016
Title: Designer Collagen-Fibril Biograft Materials for Tunable Molecular Delivery
Major Professor: Sherry L. Voytik-Harbin

One of the biggest challenges in tissue engineering currently is the formation of a functional microvascular network as part of an engineered tissue graft. Despite many advances in tissue engineering methods, the field still awaits biograft designs that enable neovascularization at clinically relevant size scales. Critical to the design of such materials are tissue-specific physico-mechanical properties and controlled local therapeutic molecular release.

The purpose of the current research is to develop such a multifunctional biograft material from type I collagen polymers. Although collagen-based biomaterials have been applied broadly to tissue engineering and local drug delivery applications, persistent shortcomings remain, including poor mechanical properties, rapid proteolytic degradation, and cursory control over physical properties and molecular release profiles. In large part, this is owing to 1) poor characterization of conventional formulations in terms of their molecular composition and 2) inability to fully capitalize on the inherent self-assembly or polymerization capacity of collagen.

Here we address current shortcomings through the development of self-assembling, collagen-fibril biograft materials through integrated tissue engineering and molecular delivery design. More specifically, collagen polymers specified by their intermolecular crosslink composition and self-assembly capacity were used to customize and design materials in terms of 1) collagen fibril microstructure and 2) proteolytic degradability, collectively defining overall local molecular release profiles. Application of the designed collagen biograft materials to control vascular endothelial growth factor (VEGF) release for promoting neovascularization and tissue regeneration was shown using an established *in-vivo* chicken egg chorioallantoic membrane (CAM) model.

Results indicated that the collagen polymers specified by their intermolecular crosslink composition and self-assembly capacity can be used effectively to fashion a broad range of multifunctional collagen-fibril biograft materials with tunable physical and molecular delivery properties in absence of excessive processing and exogenous crosslinking. Further, using heparin affinity-based VEGF retention in collagen constructs, we demonstrated improved and accelerated neovascularization as well as cellularization of the collagen biografts implanted on CAM. These highly porous collagen materials comprise D-banded fibrils, resembling those found in tissues, and maintain their inherent biological signaling properties, thereby providing an ideal platform for integrated tissue engineering and molecular therapy design.

CHAPTER 1.   INTRODUCTION

Soft tissue reconstruction is often required as a result of trauma, burns, tumor resection, congenital defects, and chronic wounds. Unfortunately, the lack or limited supply of autograft tissues remains a major surgical challenge[1]. While various types of scaffolds prepared from synthetic or natural materials have been used for simple reconstruction, their effectiveness remains limited by slow neovascularization ultimately contributing to poor functional integration, pain, and/or scarring. An ideal solution for clinicians would be a designer biologic graft material that provides appropriate multi-scale structure and function while fostering rapid vascularization for improved tissue integration and regeneration.

Our long-term goal is to develop a multifunctional soft tissue graft material that provides 1) tissue-specific physico-mechanical properties and 2) controlled, local therapeutic molecular release for accelerated neovascularization and functional tissue integration and regeneration. Type I collagen, the predominant and major structural component of the ECM represents an ideal natural polymer candidate for such integrated tissue engineering and local molecular delivery strategies [2]. It possesses several advantages over other materials, such as inherent self-assembly and biological signaling capacities, proteolytic biodegradability, and low immunogenicity [3].

Despite the advantages of collagen as a natural biomaterial, its application as a multifunctional delivery vehicle has been limited by the inability to precisely and predictably control its microstructure, mechanical properties, and proteolytic degradability [4, 5]. Shortcomings associated with conventional collagen-based drug delivery formulations include poor mechanical integrity, rapid proteolytic degradation, and burst release of molecules. Exogenous processing and crosslinking, including treatment with glutaraldehyde, polyepoxy compounds, or carbodiimides, are often used to slow down degradation and prolong the release of molecules [6-8]. Unfortunately, such strategies have been reported to have deleterious effects on the inherent biological signaling capacity of collagen resulting in adverse tissue responses [4, 9-13]. Thus, in order to harness the true potential of collagen as an ideal material for soft tissue repair

and regeneration, there is an urgent need to remedy shortcomings in existing collagen based formulations.

We plan to address this gap through development of designer polymerizable collagen fibril matrices, capable of tunable therapeutic delivery, using self-assembling collagen building blocks. The advantage of using self-assembling material is that it provides ability to tailor specific bulk material properties, such as matrix stiffness, proteolytic degradability, release profiles, at a molecular level. Recently, the Voytik-Harbin laboratory has developed and characterized an uncommon set of collagen polymer building blocks that demonstrate such a self-assembly, and can be used in the hierarchical design and customization of collagen-fibril materials. These fundamental collagen molecule building blocks predictably and reproducibly control the relevant fibril- and matrix-level properties such as matrix pore size, permeability and diffusivity, stiffness, and cell-instructive signaling [14, 15]. The unique feature of this technology is that it capitalizes on the differential self-assembly or matrix-forming capacity of these collagen polymer building blocks. Furthermore, no exogenous crosslinking is required to improve mechanical integrity or slow proteolytic degradation. As such, resultant materials display supramolecular fibril assemblies and biological signaling capacity inherent to *in-vivo* extracellular matrices.

We now propose to extend this work by testing the central hypothesis that collagen polymer building blocks specified by their intermolecular crosslink composition and self-assembly capacity can be used to modulate microstructure and proteolytic degradability of collagen-fibril materials to create functional soft tissue grafts with tunable molecular delivery, as illustrated in Figure 1.

The **objective** of the proposed work is to design and develop a self-assembling, multifunctional collagen graft material that supports accelerated vascularization and tissue integration and regeneration.

We decided to accomplish our objective by pursuing the following AIMS:

AIM 1: Design self-assembling collagen-based drug delivery system and define how its specific molecular and fibril level features modulate molecular release.

AIM 2: Demonstrate application of self-assembled collagen graft materials towards enhancing local neovascularization in an *in-vivo* chorioallantoic membrane model

(CAM), through retention of heparin and vascular endothelial growth factor (VEGF) molecules.
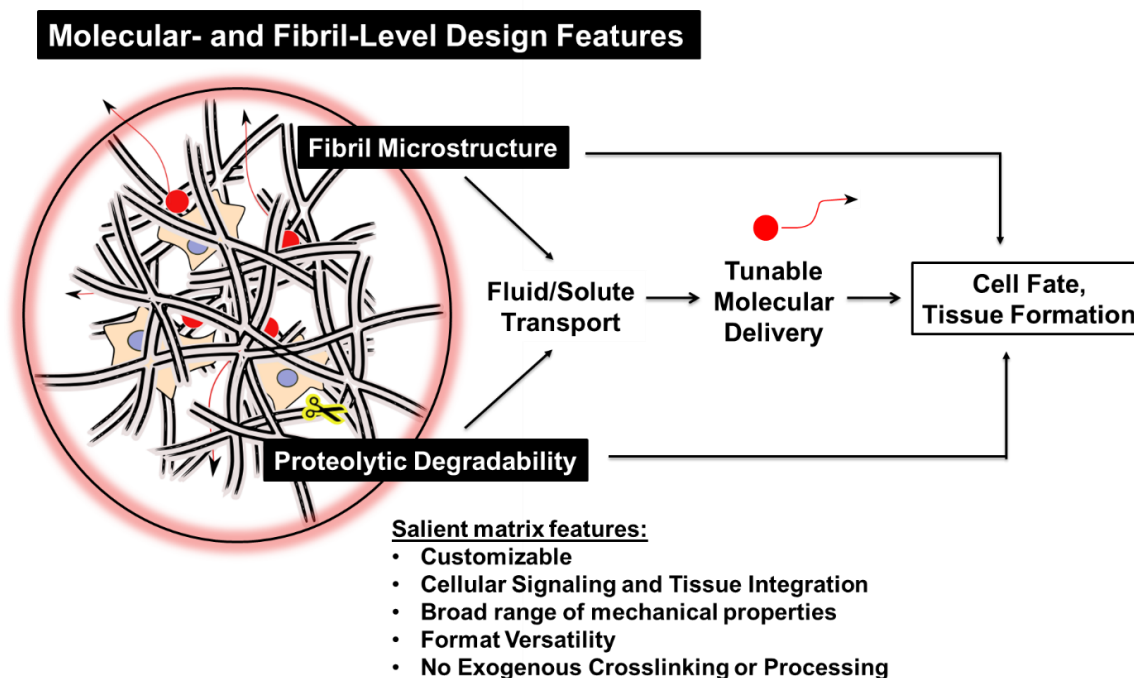
Figure 1: Schematics of design strategy for creating designer collagen biografts with tunable molecular delivery. The strategy to achieve a multi-functional collagen biograft from type I collagen is presented. It involves 1) modulation of collagen microstructure at molecular and fibrillar level and 2) altering proteolytic degradability of matrix, as both these parameters affect 1) solute/fluid transport and 2) cell fate and tissue formation.

1.1   Background

1.1.1   Motivation for applying collagen towards integrated tissue engineering and molecular delivery

Chronic wounds, defined by the presence of a skin defect or lesion that persists longer than 6 weeks or has a frequent recurrence [16], affect around 6.5 million patients in the United States alone [17], and as many as 37 million globally [18]. Chronic wounds pose a tremendous burden to the patients' health as well as the economic system. An excess of US$25 billion is spent annually on treatment of chronic wounds, and the burden is escalating due to increasing health care costs, an aging population and a higher incidence of diabetes and obesity [19].

A common yet seriously challenging example of chronic wounds is a diabetic foot ulcer (DFU) which due to its suboptimal healing properties, increases the risk of infection and if not cured in timely manner, leads to leg amputation [20]. In 2010, about 73,000 non-traumatic lower-limb amputations were performed due to DFUs [21]. Costing $38,077 per amputation procedure, approximately 3 billion dollars are spent per year on diabetes-related amputations [22]. An estimated 12% of individuals with a foot ulcer require foot amputation , which is a serious concern considering the fact that the 5-year survival rate after one major lower extremity amputation is about 50% [19].

Chronic wounds fail to heal because of the disruption of the orderly sequence of events during the wound healing process. To understand pathophysiology of chronic wound, it is necessary to know the physiology of normal wound healing process first. Wound healing normally involves a complex interaction between epidermal and dermal cells, the extracellular matrix (ECM), angiogenesis, and plasma derived proteins, all coordinated through an array of cytokines and growth factors. This dynamic process can be classified into four overlapping phases, including hemostasis, inflammation, proliferation, and remodeling [23, 24], as depicted in Figure 2 and described briefly below.

i) **Hemostasis:** After tissue injury, thrombus formation requires an interaction between endothelial cells, platelets, and coagulation factors to achieve hemostasis. Trapped platelets within the clot trigger an inflammatory response through the release of vasodilators, chemoattractants and activation of complement cascade.

ii) **Inflammation:** In the early phase of inflammation, neutrophils predominate and remove bacteria and other foreign material from the wound by phagocytosis and release of enzymes. Later in the inflammatory phase neutrophils reduce in number and are replaced by macrophages. This stage lasts until about 48 h after injury.

iii) **Proliferation:** In this phase, fibroblasts play an important role in the synthesis of new type I collagen and ECM. Additionally, tenascin, fibronectin, and proteoglycans are also produced. Production of ECM is clinically seen as formation of granulation tissue. The formation of new tissue combined with the contraction of surrounding tissues is essential for the healing of wounds. While new matrix is synthesized, existing matrix in and around the wound margin is degraded by several enzyme systems such as matrix

metalloproteinases (MMPs) and plasminogen activators. This stage occurs about 2–10 days after injury.

iv) Remodeling: In this phase, type I collagen replaces fibronectin, becoming the predominant ECM constituent and resulting in a more mature ECM. Once closure of the wound has been achieved, remodeling of the resulting scar occurs over months or years, with a reduction of cell content and blood flow in the scar tissue.
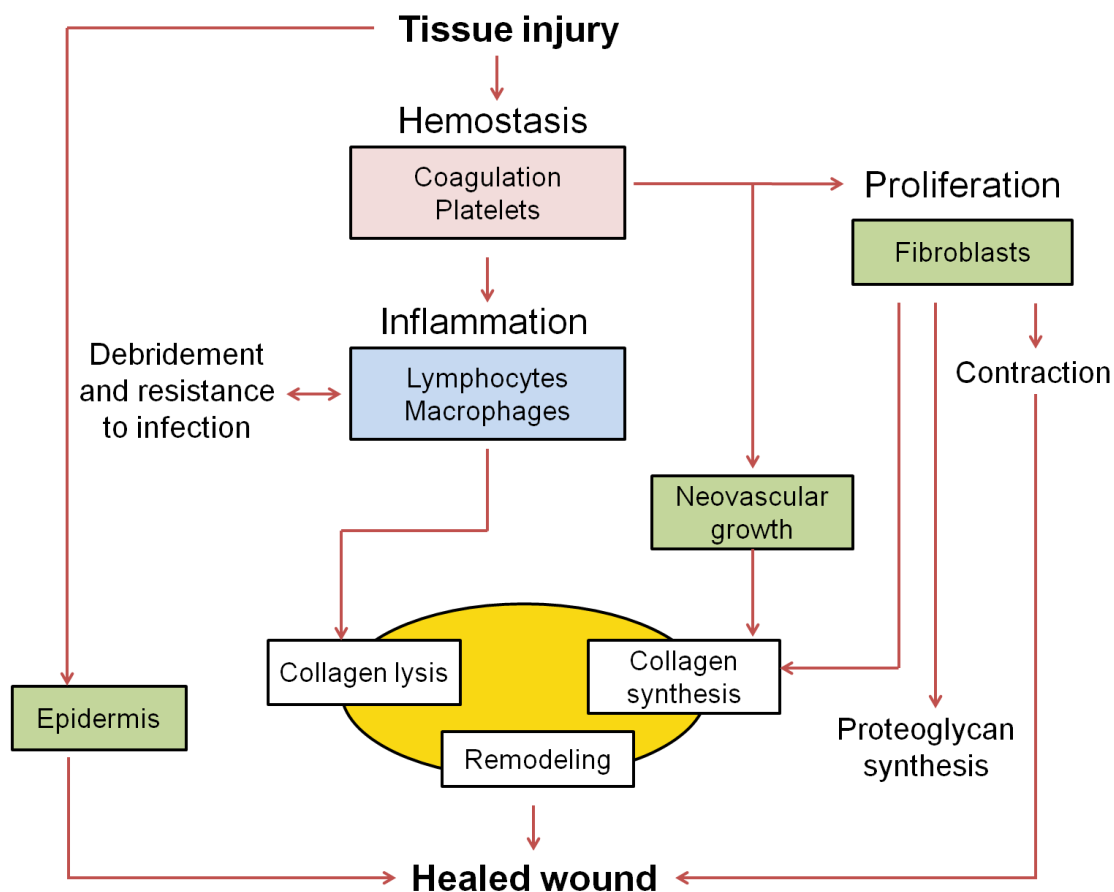
Figure 2: Fundamental interrelation of the wound healing phases: Hemostasis (red), inflammation (blue), proliferation (green), and tissue remodeling (yellow). Figure adopted from [23].

An important feature of the proliferation phase in normal wound healing is neovascularization. The dynamic interactions between endothelial cells, various soluble angiogenic cytokines, and the ECM environment promote neovascularization in the wound as shown in Figure 3A [24]. Angiogenic capillaries sprout and invade the

fibrin/fibronectin-rich wound clot and organize into a microvascular network throughout the granulation tissue within a few days.
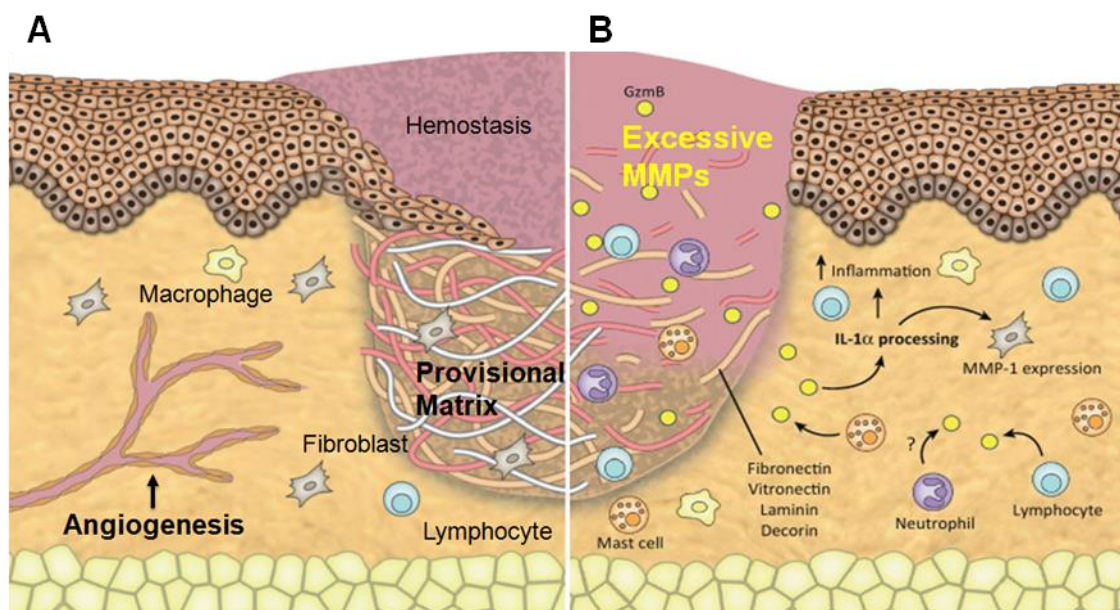
Figure 3: Normal versus impaired wound healing. Normal wound healing (A) versus impaired wound healing (B). In a normal wound healing, fibroblasts construct new ECM necessary to support cell ingrowth, and blood vessels that carry oxygen and nutrients necessary for cell survival. The provisional ECM promotes granulation tissue formation. Macrophages, fibroblasts, and blood vessels move into the wound space as a unit, through dynamic biologic interactions contributing to tissue repair. Fibroblasts contribute to new type I collagen synthesis. While MMP levels decrease through the normal wound-healing process, chronic wounds continue to show a significantly higher level of proteases and pro-inflammatory cytokines. As a result, inflammation persists longer and higher levels of MMPs cause excessive breakdown of type I collagen and ECM. Chronic wound is healing is then further impaired by lack of neovascularization, and an impaired re-epithelialization. Figure adapted from [29].

However, in chronic wounds, this dynamic spatio-temporal interaction between endothelial cells, angiogenesis factors, and surrounding ECM proteins is impaired. The chronic skin defect is usually in a permanent inflammatory state due to a hyper stimulated neutrophil response[16]. Along with an elevated level of proinflammatory cytokines, permanent increased proteolytic activity is typical for chronic wounds, contributed by excessive production of matrix metalloproteinases (MMPs) in the wound [25, 26]. MMPs are said to be responsible for poor healing by breaking down too many components of the ECM and by inhibiting growth factors that are essential for tissue synthesis [27]. This

imbalance between ECM deposition and degradation, and deficiencies in growth factor and cytokine receptors, lead to impaired progenitor cell recruitment and angiogenesis and delay wound epithelialization [28].

Typically, wound debridement followed by its compression with sterile gauze is the classic treatment for treating acute wounds [30, 31]. However, when this method is not effective enough, chronic wounds have to be dressed with adequate biomaterials to protect the long-term healing from infection and aiding in tissue regeneration [31, 32].

An intervention from alternative multifunctional tissue engineering strategy can therefore offer a potential solution, by providing a strong structural template for cell infiltration and growth of new tissue, and at the same time, providing local exposure of growth factors, that can coordinate angiogenic response for full functional tissue recovery. The ultimate goal for treating these wounds is scar-free healing and timely restoration of tissue function [33].

1.1.2 Collagen based materials as wound dressings available commercially

As a major natural constituent of our body, collagen is seen to play an integral role in the repair and replacement of soft tissue by providing an extracellular scaffold, stimulating certain growth factors, and propagating tissue granulation [34]. As a result, numerous efforts have been put into developing collagen implants and wound dressings to specifically accelerate the natural process of wound healing and promote tissue regeneration. Variety of products have been commercially developed and reviewed in detail previously [34-40]. Selective examples of these products, including Oasis, Alloderm, and Integra Dermal Regeneration Template products are described below. It is claimed that the collagen in these products promotes the deposit of newly formed collagen in the wound bed. These dressings come in variety of formats, including pads, gels and particle forms. They can be used on surgical wounds, in deep wounds to fill dead space, to absorb exudate and to provide a moist environment.

Alloderm (TM), distributed by the LifeCell Corporation, is a processed acellular dermal matrix derived from human cadavers [41]. Cadaveric tissue samples are first screened for a host of transmittable pathogens. The decellularization is achieved through use of detergent solution, that leaves only the dermal matrix and associated basal lamina intact,

removing all other cellular components [42]. Following decellularization, samples are lyophilized for storage, and must be rehydrated before use [43]. Upon grafting, host fibroblasts and associated vasculature infiltrates the Alloderm matrix. However, the full extent of vascularization is said to be uncertain [44, 45]. The clinical use of Alloderm also requires subsequent application of an ultrathin split-thickness autograft immediately following implantation, since Alloderm lacks an epidermal component and has limited barrier properties [44]. Other disadvantages of Alloderm are said to be requirement of multiple applications and a theoretical risk of transmission of human pathogens [46].

Oasis(TM), developed by Cook Biotech, is an acellular dermal scaffold derived from porcine small intestinal submucosa (SIS). It contains numerous dermal components including collagen, glycosaminoglycans (hyaluronic acid), proteoglycans, fibronectin, and bioactive growth factors such as fibroblast growth factor-2, transforming growth factor β1, and vascular endothelial growth factor (VEGF) present naturally in the SIS [47]. Following application to the wound bed, this acellular matrix is infiltrated by fibroblasts and associated vasculature, which gradually replace the material with new ECM components over time [48]. It should be noted that while the material has a limited porosity, it does not provide a moisture barrier and must be protected by an appropriate secondary dressing [49]. Oasis limitations therefore include possible higher infection rate, and need for multiple applications [46]. Clinical data with Oasis is also limited. A clinical trial comparing the application of Oasis in 73 patients with diabetic foot ulcer showed only slight statistical superiority ($p=0.055$) when compared with Regranex - a carboxymethylcellulose-based topical gel containing recombinant human platelet-derived growth factor (rhPDGF-BB) [50] .

Integra(TM) is a composite acellular collagen product developed by the Integra Life Science Corporation. It is composed of an outer layer of silicone and a cross-linked bovine type I collagen glycosaminoglycan dermal matrix and was originally described by Yannas and Burke [51, 52]. The collagen-GAG matrix is gradually invaded by host fibroblasts upon implantation in an excised wound bed [44]. Tissue integration is said to take place in approximately 3-6 weeks, resulting in production of a 'neodermis' with associated vasculature [44]. During this time the silicone layer acts as a protective barrier, limiting moisture loss through the membrane [42]. Once the dermal layer regenerates,

the silicone layer has to be removed and the wound is permanently closed with a split thickness skin graft [34].

While Integra has shown promise in the treatment of chronic wounds and burns, it has a number of limitations that hinder its clinical use. When compared with AlloDerm in a mouse wound model, the Integra matrix induced more foreign body response and giant cells, owing to the fact that it is a chemically cross-linked material [53]. Integra scaffold needs to be first cleared by macrophages in order to allow deposition of collagen fibers. Since Integra has no intrinsic immunological defenses, it can be easily infected by bacteria and requires daily monitoring for signs of bacterial growth until the bio integration process is complete [54]. In the incidence of infection, wound debridement and reapplication are typically necessary, which further lengthens the time required for healing [54]. Another concern is a two-step process required for Integra based therapy. Since the silicone layer of Integra functions only as a temporary covering, it must be replaced by an ultrathin autograft following neodermal formation [36]. Given that the average acceptance rate of Integra is at least 10% lower than for a standard split-thickness graft, patients might prefer to undergo the latter procedure directly instead of opting for a riskier two-step process, if they have sufficient donor skin [36]. Furthermore, technical difficulty in Integra application necessitates physician training, and as a result, it may only be used by practitioners that have undergone a company sponsored training program [55]. In an early trial, incidences of hematoma and seroma formation occurred due to improper application of Integra, highlighting the level of skill required for proper use of the material [52].

Thus, it is seen that despite the advantages of collagen based advanced wound dressings, undesirable outcomes limit the use of these products in treatment of chronic wound ulcers. In general, peripheral ischemia, which is a pathological characteristics of chronic ulcers, critically affects collagen based biomaterial transplantations [56, 57]. Many diabetic patients need surgical revascularization to achieve timely and durable healing. However, with collagen-based wound therapies, it currently takes 3-4 weeks for engineered dermal substitutes to be sufficiently vascularized, before a split-thickness skin graft can be placed on the neodermis [58]. **Thus, slow vascularization along with the**

inability of collagen based dressings to serve as stand-alone therapy adds to the current limitations of collagen-based wound healing products, including frequent surgical interventions, high costs of treatment, and inflammation mediated response that leads to scar formation rather than tissue regeneration [34-39]. Thus, there is acute need to improve vascularization period, and tissue regeneration capacity of collagen-based products for clinical therapies.

1.1.3   Drug delivery from conventional collagen formulations: state of the art

To address the issue of slow vascularization and tissue regeneration through collagen based products, alternative of combining growth factors into collagen [59-61] has gained interest of researchers since many growth factors have been recently recognized as key signaling molecules inducing wound healing [28]. For example, platelet-derived growth factor-BB (PDGF-BB) is important for the granulation tissue formation and for stem cell recruitment, vascular endothelial growth factor-A (VEGF-A) is needed to induce blood vessel growth for sustaining the granulation tissue, and fibroblast growth factors (FGFs) are crucial for both wound reepithelization and angiogenesis [62]. However, none of these growth factor-loaded collagen matrices have reached commercial market as a treatment available to patients. The reasons could be associated with the rapid clearance from the matrix and/or degradation of soluble VEGF at the implant site [63, 64]. This raises an important question on the ability of collagen to serve as a matrix to achieve controlled release of growth factors.

Interestingly, to date, numerous studies report applications of collagen for controlled drug delivery as ophthalmological shields, antibiotic-loaded sponges, drug loaded microspheres and injectable collagen gels, and have been extensively reviewed previously [4, 5, 65, 66]. Select representative examples of these formulations reported in research articles are given in Appendix 1. Despite this wide research, close inspection shows that only a few collagen-based drug delivery formulations have made it into clinical trials or are currently marketed [4, 67, 68]. The selective examples of these commercially available products are given in Table 1. It was observed that the majority of these products are restricted to the delivery of an antimicrobial agent, silver (to prevent infection in chronic wounds), and ethylenediaminetetracetic acid (EDTA) (to form a

chelating complex with MMPs and to prevent them from excessively degrading matrix) [69]. Thus, despite the numerous advantages and wide research on collagen as an excellent natural biomaterial [4, 65, 67, 70, 71], its use as a vehicle for controlling local growth factor release is seen to be limited [72, 73]. This points to yet another gap in existing collagen based biomaterials - **inability to achieve controlled release of biomolecules.**
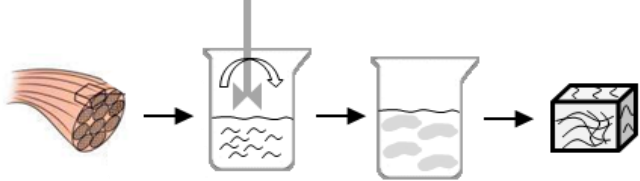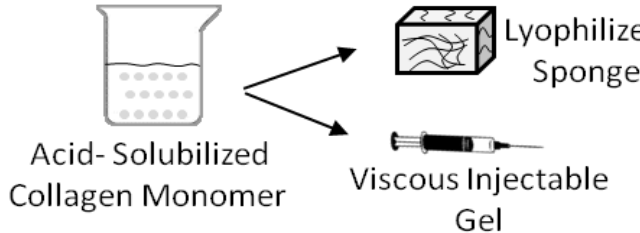
Table 1: Examples of collagen based drug delivery products in market
(Source: Company based literature and BCC Market Research[74])

Drug Delivery System	Company	Drug Incorporated	Dressing format	Application
Cogenzia	Innocoll	Gentamicin	Lyophilized sponge	Treatment of diabetic foot infections
XaraColl	Innocoll	Bupivacaine Hydrochloride		Local Anesthetic Sponge for postoperative pain relief
Vitagel™	Orthovita Inc.	Thrombin	Suspension of bovine collagen and bovine thrombin in CaCl2 buffer	Surgical Hemostatic gel
ColActive ® Plus Ag	Covalon	EDTA and silver ions	Lyophilized collagen sponge made with collagen, carboxyl methyl cellulose (CMC) and sodium alginate	Chronic wound healing
Promogran Prisma™ Ag	Acelity	Silver-ORC containing 25 % w/w ionically bound silver (Ag)	Lyophilized sponge consisting of 44% oxidized regenerated cellulose (ORC), 55% collagen and 1% silver-ORC	Healing chronic wounds such as diabetic venous and pressure ulcers
Biostep Ag	Smith & Nephew	EDTA and silver (Ag)	Lyophilized sponge made from porcine type I collagen and gelatin	Healing chronic wounds such as diabetic, venous, and pressure ulcers, and burns

The scarcity of collagen based drug delivery systems in market is concerning, considering the wealth of information that exists on research-based collagen's drug delivery systems. In deciphering why collagen based products might not be reaching their full clinical potential, we reviewed the formulations of collagen used in current collagen-based biomaterials. As such, two main categories of formulations were identified, as shown in Table 2. These are:

1. Non-dissociated Fibrillar Collagen- These formulations contain decellularized collagen ECM particulate matter, which is mechanically homogenized, acid-swollen, and finally lyophilized to form sponge which may or may not be cross-linked. Such collagen formulations do not undergo polymerization since collagen fibers are never dissociated during this preparation method.

2. Soluble Collagen- These are obtained from pepsin or acid solubilization of mammalian tissues to form viscous collagen solutions, which are then lyophilized to form cross-linked or non-cross-linked sponge or injectable viscous gel. They exhibit fluid like behavior under shear stress, and become entangled again when the suspension is at rest.

Table 2: Major collagen formulations used in commercial drug delivery applications of collagen-based biomaterials

Collagen Formulation	Preparation
Non dissociated, Fibrillar Collagen	Collagen Fiber → Homogenized Slurry → Acid Swollen → Lyophilized Sponge
Solubilized Collagen	Acid-Solubilized Collagen Monomer → Lyophilized Sponge / Viscous Injectable Gel

The major limitation of these formulations is that they do not capture and capitalize the inherent fibril self-assembly of collagen that occurs *in vivo*, and are limited by their poor molecular characterization. As a result, the matrices formed from such formulations lack interfibril branching and simply represent entanglements of long individual fibrils, that lead to their poor shape definition, low mechanical integrity, poor handling, cell-induced contraction, and rapid proteolytic degradation [4, 75-77]. To improve these properties, materials are subjected to exogenous cross-linking, which is achieved through chemical, enzymatic or physical methods [4].

Chemical cross-linking of type I collagen matrices is typically performed using agents, such as glyoxal, formaldehyde, methylene diphenyl diisocyanate, hexamethylene diisocyanate, and most commonly glutaraldehyde [4]. Glutaraldehyde and formaldehyde treatment provides an advantage of cross-linking dry collagen material with reagent in vapor phase instead of treatment in liquid phase [9]. Although these agents achieve the goal of cross-linking, they also exhibit detrimental effects on cells and tissues [78] such as cytotoxicity [6, 79] or tissue calcification [80-82]. For example, depolymerization of polymeric glutaraldehyde cross-links has been reported to releases highly cytotoxic glutaraldehyde and monomer fragments into the recipient [80, 83-85]. Cross-linking with other chemical agents, for example, diphenylphosphoryl azide, 1-ethyl-3-(3-dimethylaminopropyl) carbodiimide (EDC)/N-hydroxysuccinimide (NHS), and oxygen species, were proved to be nontoxic, but the cross-linked fibers were unstable in water and collapsed into films in aqueous or high humidity environments [86]. Besides, cross-linking can reduce porosity [82], limiting the nutrient transport to cells.

Researchers have also attempted to use physical cross-linking techniques such as photooxidation, dehydrothermal treatments (DHT) and ultraviolet irradiation with photosensitizers (e.g., riboflavin) to avoid introducing potentially cytotoxic chemical residuals into the system and retain the biocompatibility of collagen materials [4]. However, most of these physical treatments cannot yield enough high cross-linking degree to meet mechanical strength demand of drug delivery devices [77]. Furthermore, collagen is reported to have been partially denatured by these physical treatments [8].

Enzymatic cross-linking agents such as lysyl oxidase and tissue transglutaminase has also been used however limited due to feasibility issues [87] and concerns of apoptosis [88] respectively.

Thus, while materials formed without any cross-linking are characterized as mechanically unstable, too soft to handle, and unable to resist cell-induced contractions, exogenous crosslinking has been shown to have detrimental effects on cells and tissues [78], such as cytotoxicity [6, 79] or tissue calcification [80-82] and partial denaturation of collagen itself [86] [8].

1.1.4   Drug incorporation method in collagen delivery systems

While reviewing the application of collagen formulations in drug delivery [4],[65],[5],[66], it was realized that the methods through which drugs are entrapped within or attached to collagen delivery systems play an important role in determining the efficacy of drug delivery system. Since drug release can be influenced drastically by the approach taken to associate the drug with collagen matrix, it is important to understand the current strategies of attaching drug to collagen. An informed decision made in selection of strategy for drug attachment to collagen will endow us with a much better tool to engineer drug delivery system with improved tunability, and cell-instructive capacity.

Current strategies of drug incorporation can be separated into three distinct strategies (Figure 6): i) physical entrapment of drug, ii) affinity binding based drug retention, and iii) chemical or covalent immobilization of the drug into the collagen matrix.

Physical admixing involves direct entrapment of drug within matrix or encapsulation of drug, and relies on diffusion to facilitate drug release into the surrounding tissue. Chemical immobilization usually involves covalent binding through the use of chemical crosslinkers and the drug is primarily released through degradation. Affinity binding involves affinity based interaction between the drug and collagen substrate and drug might be released by both diffusion and degradation.
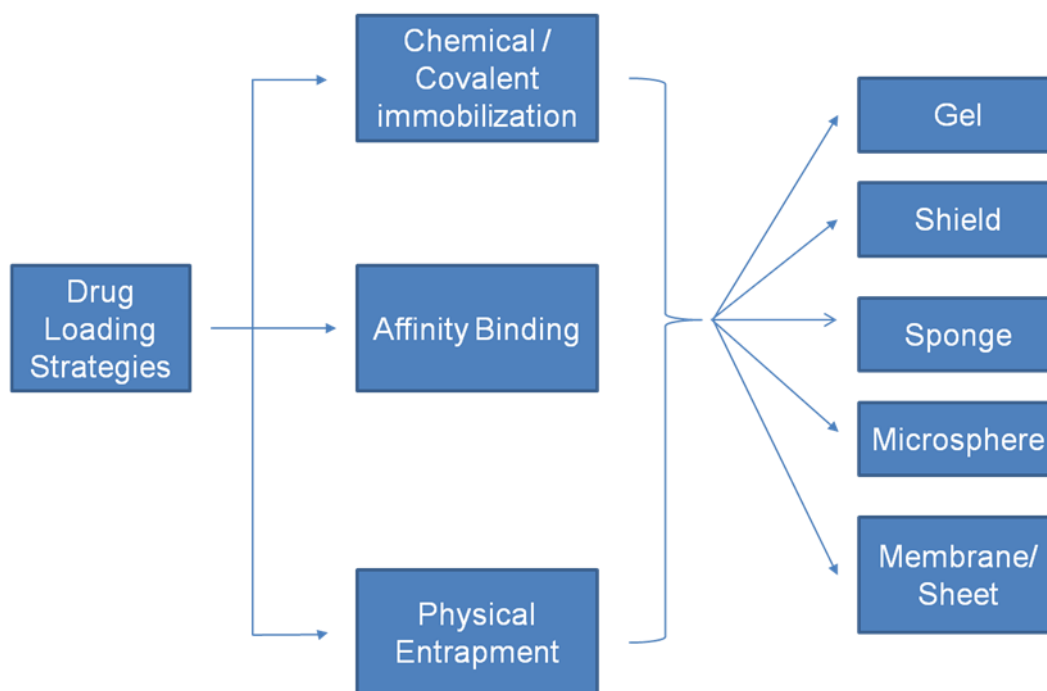
Figure 4: Schematics of strategies of drug incorporation in collagen based drug delivery systems.

i) Physical admixing/entrapment/adsorption of drug into collagen: Physical admixing involves dissolving or suspending the drug within a polymer reservoir to form a porous device. It is the most common strategy used for local drug delivery due to its simplicity and cost effectiveness [89]. Rate of drug release is controlled by diffusion dominated mechanisms observed initially, followed by further release as reservoir degrades by surface or bulk erosion [90]. Fabrication methods for entrapping drug involve lyophilization (freeze drying), particulate leaching, phase emulsion (microspheres) and in-situ polymerization (gels). Many of these methods start with slurries of shredded collagen or whole collagen tissue fragments that are exogenously cross-linked, and combined with drug at certain ratios before subjecting to lyophilization [91]. Sometimes, the drug is added after lyophilization as in cases of collagen sponge. During lyophilization, the pore-sizes that are formed within the matrices are often bigger than the size of the drug, resulting in diffusion dominated release. However, there is little control over pore size during lyophilization, which limits the ability to tune drug entrapment and release. Moreover, harsh condition of processing in physical entrapment method (e.g. homogenization used during emulsion method of formulating microspheres) can affect

the bioactivity of encapsulated molecules by inactivating active sites or denaturing the drug [92].

ii) Affinity based immobilization of drugs into collagen: Rather than simply admixing a drug in collagen, site-specific tethering of drug to the collagen gives an option of extending drug release by modifying the interaction between the drug and matrix. Affinity can be described as the tendency for one molecule to bind to another. Affinity based systems utilize the molecular interaction between the therapeutic agent and the delivery vehicle. The strength of the interaction depends on the variety of molecular forces: charge, hydrophobicity, hydrogen bonding, and van der Waals forces [93]. This non-covalent physical adsorption technique involves adsorption of drugs onto surfaces typically exploiting direct charge–charge or secondary drug-matrix affinity interactions, or indirect interaction via intermediate proteins or other biological molecules (e.g., heparin [94], fibronectin [95]). Such interactions have been employed to deliver basic fibroblast growth factor (bFGF) and vascular endothelial growth factor (VEGF) through engineered biomimetic collagen matrices, showing controlled diffusion and matrix degradation to induce angiogenesis [94, 96-99].

iii) Chemical / covalent immobilization of drug on collagen: Immobilization of the drug within collagen matrix can also be achieved by its covalent conjugation to collagen. Covalent binding of drugs to collagen matrices can sustain drug release for longer time period and offer control over amount and spatial distribution of drug in collagen matrices. Drugs can be conjugated to collagen matrices via functional groups, which are incorporated by co-polymerization or through chemical treatment. For example, to overcome rapid diffusion and clearance from the implant site and to increase its conformational stability, recombinant transforming growth factor $\beta2$ (TGF-$\beta2$) was covalently bound to injectable bovine dermal fibrillar collagen (FC), using a difunctional polyethylene glycol (PEG) linker to create FC-PEG-TGF-$\beta2$ sequences throughout the matrix [100]. The activity of the covalently bound TGF-$\beta2$ was compared to admixed TGF-$\beta2$, and results showed that covalent binding of TGF-$\beta2$ to collagen resulted in a significantly larger and longer-lasting TGF-$\beta2$ response than that observed with admixed formulations of collagen and TGF-$\beta2$. It should be noted however, that despite advantages offered by this method of drug incorporation, it is difficult to selectively

assign specificity of the coupling site on conjugated drug as binding interactions are specific to each drug and difficult to predict. Also, biomolecules may lose their bioactivity if screening or damage of the active pockets occurs during the immobilization [61].

The ultimate success of any of the above method of drug loading, whether physical entrapment, affinity based retention, or covalent immobilization, is dependent on the preservation of collagen's native physiological properties. Physical entrapment and affinity based molecular retention methods are often confounded by the weak mechanical properties of conventional collagen formulations. As mentioned earlier, materials formed without any cross-linking are characterized as mechanically unstable, too soft to handle, and unable to resist cell-induced contractions [4, 75-77] thus failing to support cell ingrowth and migration required for tissue regeneration. On the other hand, exogenous crosslinking [4, 10, 12, 13, 86, 101, 102] or chemical immobilization based approaches can lead to detrimental effects on cells and tissues [78], such as cytotoxicity [6, 79] or tissue calcification [80-82] and partial denaturation of collagen itself [86] [8]. Consequently, current collagen based products suffer from problems related to mechanical integrity, inability to give controlled release and inflammation based tissue response. This limits the clinical success of collagen for tissue engineering and molecular delivery applications [72],[103],[104].

1.1.5 An approach inspired by *in-vivo* collagen synthesis and self-assembly

It is realized that for promoting healing of chronic wound, there is a need for design and development of a multifunctional collagen based platform that supports recreation of natural type I collagen fibril scaffold while fostering rapid and functional neovascularization and tissue regeneration at the site of implantation. Since the wound healing period can vary according to wound type, age and many other factors including infection, sex hormones, stress, diabetes, obesity, and medications [105], it is important that such a multifunctional platform supports a broad range of customizable spatiotemporal release profiles of biomolecules, through a loading strategy that does not compromise physiologically relevant properties of native collagen. As such, we decided

to take the inspiration from *in-vivo* collagen synthesis and self-assembly in the development of such multifunctional tissue engineering and drug delivery platform.

In vivo, type I collagen constitutes a major structural and mechanical component of connective tissues and organs, accounting for more than 90% of the ECM in skin, bone and tendon of vertebrates [106] and approximately 30% of total body protein [2, 4]. Its ability to form polymerizable, porous collagen-fibril matrix that can degrade into physiologically non-toxic products make it an excellent biocompatible material with low immunogenicity. Additionally, its versatility and ability to be processed on an aqueous basis make it a viable candidate for formulating drug delivery systems [107]. Being a natural polymer, collagen also provides advantages related to its inherent cell-signaling potential which is facilitated by adhesion domains that engage in integrin-mediated cell binding [108]. These biophysical properties of collagen are summed up below in Figure 5.
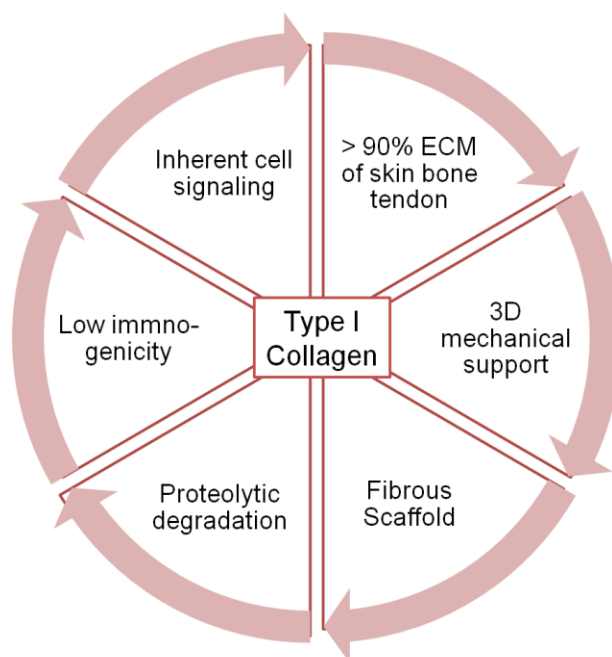
Figure 5: Schematics showing biophysical properties of type I collagen that add to its advantages for forming a tissue engineering and drug delivery platform.

The unique properties exhibited by type I collagen that are mentioned above are due to its complex, unique hierarchical structure [109-113] developed during *in vivo* biosynthesis and self-assembly. The basic building block of this hierarchical structure is a collagen

molecule consisting of three peptide chains (two α1 (I) and one α2 (I) chain). Collagen molecule comprises a central helical domain flanked on each end by non-helical telopeptide domains [71, 114] as shown in Figure 6A. The 300 nm-long helical domain consists of Gly-X-Y repeats where the X and Y positions are often occupied by proline and hydroxyproline. These collagen molecules, also known as tropocollagen, are the fundamental building blocks of type I collagen. Tropocollagen molecules self-assemble in a hierarchical fashion as shown in Figure 6B, to form tissue-specific networks of fibrils that then combine to form suprafibrillar and tissue level structures [14].
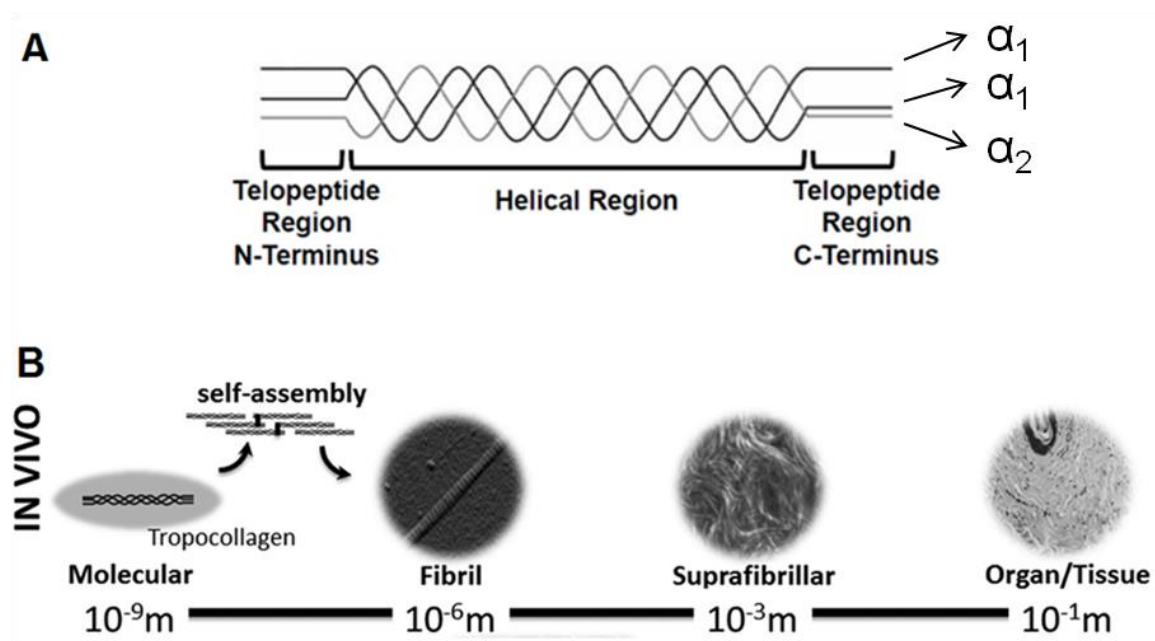
Figure 6: A) Schematic of type I collagen molecular structure. Figure shows three polypeptide chains intertwined to create a right-handed helical structure. The N- and C-termini of the molecular structure contain the non-helical telopeptide regions. (From [115]) B) Hierarchical, multi-scale organization of type I collagen as it occurs *in vivo* (From[116]).

The *in-vivo* biosynthesis of collagen involves ribosomal production of individual tropocollagen alpha (α) chains, followed by hydroxylation of specific proline and lysine residues which contribute to triple helix stabilization and molecular cross-linking respectively [14]. Processed polypeptide chains then undergo trimerization to form heterotrimeric procollagen molecules consisting of two α1 (I) and a single α2 (I) chains.

Upon extrusion into the extracellular space, both amino- and carboxy-terminal propeptides are cleaved enzymatically [71], thus rendering the resultant tropocollagen molecule capable of fibril formation [117]. As the prefibrillar aggregates of staggered tropocollagen molecules assemble, lysyl oxidase binds and catalyzes cross-link formation between prefibrillar aggregates of staggered collagen molecules (telocollagen) to create covalently cross-linked dimers or trimers (called oligomers) [118]. These different oligomer precursors direct the progressive molecular packing, fibril assembly, and suprafibrillar network formation that eventually gives rise to tissue-specific form and function [14, 119].

1.1.6 Proposed strategy to design collagen based drug delivery platform

Inspired by the *in-vivo* collagen synthesis and self-assembly, we wanted to create a designer collagen biograft material that would provide a strong structural support, and promote rapid neovascularization and tissue regeneration through tunable molecular release. We decided to achieve this goal through a combination of improved collagen formulation, and by strategic use of physical or affinity based retention of molecules in collagen. The unique type I collagen building blocks we employed in the design of such multifunctional platform, were **oligomers**, and monomers such as **telocollagens** and **atelocollagens** (Figure 7) that have been developed in Voytik-Harbin laboratory previously. These unique collagen building blocks of oligomer, telocollagen and atelocollagen are extracted from porcine skin type I collagen (PSC), and have been previously proven to predictably and reproducibly control the relevant fibril- and matrix-level properties such as matrix pore size, permeability and diffusivity, stiffness, and cell surface-receptor mediated signaling [14, 120, 121].

These collagen building blocks differ in their intermolecular cross-link content, composition and cross-link chemistries [14, 120]. While the **oligomers** comprise small aggregates of collagen molecules (e.g., trimers), which retain collagen's tissue-specific, covalent intermolecular cross-links, **telocollagens** are individual collagen molecules, which lack these intermolecular covalent cross-links. The telocollagen and oligomer formulations possess intact telopeptide regions and contain reactive aldehydes building blocks generated from acid-labile, intermediate cross-links [14]. Upon *in-vivo*

polymerization, the process through which collagen fibrils assemble to form a gelled polymeric network, these reactive aldehydes spontaneously reform covalent, intermediate cross-links as part of the fibril-forming process. Pepsin-solubilized (telopeptide-deficient) **atelocollagen** formulations are created when collagen is treated with proteolytic enzymes that remove the terminal telopeptide regions. As both the amino (N)- and carboxyl (C)-telopeptides play important roles in cross-linking and fibril formation, their complete removal results in an amorphous arrangement of collagen molecules and a consequent loss of the banded-fibril pattern in the reconstituted product [122].
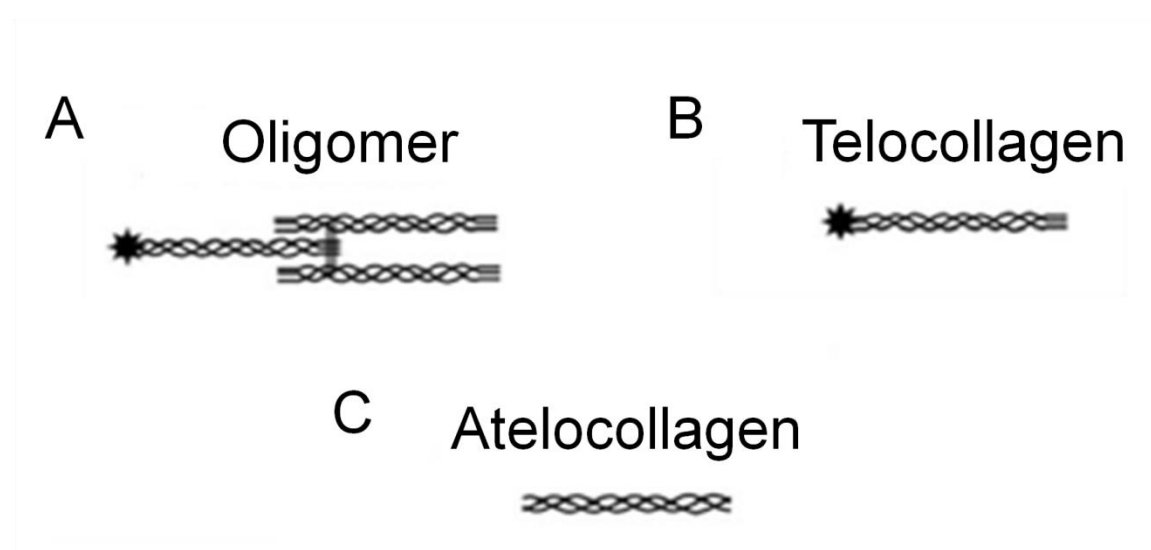
Figure 7: Collagen polymer building blocks as defined based on cross-link type. (A) Oligomer, (B) Telocollagen (C) Atelocollagen. Stars and gray bars represent reactive aldehydes and stable, mature covalent cross-links, respectively.

The matrices formed from these building blocks have previously shown superior mechano-biological properties compared to commercially available collagen formulations under the same polymerization conditions [120]. The microstructural and mechanical properties given by these isolated unique building blocks are different from that obtained from collagen formulations in other categories. The relationship between matrix stiffness and fibril density, as exhibited by the building blocks was found to be important in regulating the cell behavior and vessel morphogenesis [14]. PSC showed decreased polymerization times, enhanced mechanical integrity and a larger dynamic stiffness range than the other collagen formulations [14, 120]. It then became evident that

fundamental differences existed between the porcine skin collagen and conventional collagens on the molecular level, and these are most likely due to intermolecular cross-linking and ability of to self-assemble as demonstrated by porcine skin collagen building blocks [14, 120, 123]. We decided to capitalize on these inherent strengths of collagen building-blocks for controlling molecular release.

This work deals with application of these unique collagen building blocks towards tunable molecular release through i) control of the fibril microstructure and proteolytic degradability of collagen at molecular level, and ii) use of affinity binding based approach that can prolong retention of molecules in collagen. Strategically, we employed heparin that has binding affinity for oligomer as well as VEGF, for loading of the VEGF189 molecules in oligomeric collagen, and tested its applicability towards enhancing neovascularization *in vivo* using a well-established chicken egg chorioallantoic membrane (CAM) assay.

1.2   Organization of thesis

This dissertation aims to demonstrate how specific molecular and fibril level design features of collagen, along with affinity binding properties, can be used to tune the molecular release from collagen biografts for applications such as improving local vascularization and tissue regeneration in engineered collagen constructs.

In Chapter 2, we address our specific aim 1 of designing self-assembling collagen-based drug delivery system of low and high fibril-density, and defining how its specific molecular and fibril level features can modulate molecular release. We used FITC-dextrans of various sizes ranging from 10kDa to 2000 kDa as a drug analogue in this aim. After matrix self-assembly and polymerization, we compared the FITC-dextran release from various collagen matrices in absence, and presence of collagenase. Weibull function was fit to the empirical data to decipher associated release mechanisms. Through this study, we first established use of oligomer as a robust drug delivery system compared to commercial telocollagen-based drug delivery system. Next, we showed how molecular release can be tuned by altering collagen molecular composition and fibril density. Lastly, we showed how varying levels of collagenase could affect molecular release from the low and high fibril density implants.

In CHAPTER 3, we addressed specific aim 3 of demonstrating application of low and high fibril-density collagen graft materials towards controlled VEGF delivery for enhancing local neovascularization in an *in-vivo* chorioallantoic membrane model. To improve the local retention of VEGF in collagen, we exploited heparin binding affinity towards collagen and VEGF189. The implants were evaluated for their ability to provide enhanced neovascularization in an accelerated time frame of 3 days.

In CHAPTER 4, we summarize our findings while outlining the scope of future work.

CHAPTER 2.   DESIGN AND MODULATION OF COLLAGEN FIBRIL BIOGRAFTS FOR TUNABLE MOLECULAR RELEASE

2.1   Introduction

Type I collagen represents an important candidate biopolymer when considering the design of multifunctional tissue implants. Being a natural biomaterial, it forms major structural and mechanical component of the majority of connective tissues and organs in our body. It accounts for more than 90% of the extracellular matrix (ECM) of vertebrates [106] and approximately 30% of total body protein [2, 4]. Its hierarchical structure, self-assembly and intermolecular cross-links ubiquitously preserved across species [70], and its ability to form porous collagen-fibril matrices with cell signaling potential make it an excellent material for creating multifunctional drug delivery platforms for *in-vivo* implantation.

The hierarchical organization of collagen during its *in-vivo* synthesis involves binding of lysyl oxidase enzyme to catalyze cross-link formation between prefibrillar aggregates of staggered collagen molecules (monomers) to create covalently cross-linked oligomers (e.g., at least two collagen molecules joined by a covalent cross-link) [14, 124, 125]. These different oligomer precursors (dimers or trimers) in turn, direct the progressive molecular packing and assembly of collagen that eventually gives rise to tissue-specific fibril microstructure and matrix physical properties with exceptional cell signaling potential, facilitated by adhesion domains that engage in integrin-mediated cell binding. The porous microstructure and unique biochemical composition makes collagen a viable candidate for drug delivery [4, 5, 65-67, 70, 71] with most applications explored in ophthalmologic [126-135] dental [136], [137], wound healing [138-140] [141] [142, 143] [144] [145] [146], and bone regeneration [147-150] fields.

Despite this, only a handful of collagen drug delivery systems are commercially available [5] [72, 151],[103],[104] [152].   Major shortcomings in conventionally available collagens include poor molecular characterization; low mechanical integrity and stability; rapid proteolytic degradation; limited design control; and deleterious tissue responses associated with chemical modifications [4],[9],[10, 12, 13, 86, 101, 102].   Implants

formed from conventional formulations are unable to form suprafibrillar structural assemblies as observed in vivo, instead exhibiting amorphous microstructures [72, 73] with low tearing strength [153], poor mechanical integrity [154] [155], and an uncontrolled molecular release [72] [156] [77] [156] [157] [158] [159]. Strategies to overcome these limitations include utilizing exogenous cross-linking, chemical modification, or mixing with other natural/synthetic polymers (Appendix 2). However these strategies have been associated with several limitations, including but not limited to detrimental effects on cells and tissues [78], such as cytotoxicity [6, 79], tissue calcification [80-82], and partial denaturation of collagen [86] [8] or biomolecule [160].

Here we address these shortcomings through the development of self-assembling, collagen-fibril biograft materials that feature integrated tissue engineering and molecular delivery design. More specifically, collagen polymers specified by their intermolecular crosslink composition and self-assembly capacity [14, 120, 121] were used to customize and design materials in terms of 1) collagen fibril microstructure and mechanical properties and 2) proteolytic degradability. While these features were found to define tissue formation and cell-instructive properties previously, here we exploited them to define local molecular release profiles. The objective of the proposed work was to develop a tunable, multifunctional, collagen-based platform that supports a broad range of customizable spatiotemporal molecular release profiles, including burst and sustained. The unique feature of this technology is that it capitalizes on the differential self-assembly of collagen and avoids use of exogenous crosslinking or chemical modifications.

2.2 Methods

2.2.1 Preparation of soluble collagen formulations

All laboratory-produced self-assembling type I collagen formulations (oligomer, telocollagen, and atelocollagen) were derived from the dermis of market weight pigs. Collagen oligomers were prepared as described previously [120]; telocollagen was prepared by extracting porcine dermis with 0.5 M acetic acid followed by salt precipitation [115, 121]; and atelocollagen was prepared via complete pepsin digestion

[161]. All collagens were then dialyzed exhaustively against 0.1 M acetic acid and lyophilized. Prior to use, lyophilized collagens were dissolved in 0.01 N hydrochloric acid (HCl) and rendered aseptic by overnight exposure to chloroform at 4°C. Collagen concentration was determined using a Sirius Red (Direct Red 80) assay [162]. Laboratory-produced collagens were standardized based upon purity as well as polymerization capacity, as described in ASTM F3089-14[163]. Polymerization capacity, as a functional performance criterion, is defined as the relationship between shear storage modulus (G') of polymerized matrices and collagen content of the polymerization reaction [14, 120]. Commercial monomeric collagen, namely type I collagen acid solubilized from rat tails, was purchased from Corning (Catalogue Number 354249; Corning, NY, USA) and is referenced as rat tail collagen (RTC). All collagen solutions were diluted with 0.01 N HCl to achieve desired concentrations and neutralized with 10X phosphate buffered saline (PBS) and 0.1 N sodium hydroxide (NaOH) to achieve pH 7.4 [120]. Neutralized solutions were kept on ice prior to induction of polymerization by warming to 37°C.

2.2.2 Polymerization kinetics and capacity of oligomer collagen in absence and presence of FITC-dextran

Oligomer collagen polymerization kinetics and capacity were measured in absence and presence of 10 kDa or 2000 kDa FITC-dextrans (Invitrogen, Eugene, OR) using an AR2000 rheometer (TA Instruments, New Castle, DE,) equipped with a stainless-steel 40 mm-diameter parallel plate geometry [14, 120]. Oligomer solutions (3 mg/ml) were prepared in the presence and absence of relatively high concentrations of FITC-dextran (1 mg/ml in 10X PBS), neutralized, and pipetted onto the Peltier plate. Upon lowering the geometry, the Peltier plate was maintained at 4 °C for 5 minutes and then increased to 37°C for 15 minutes to induce collagen polymerization. Time-dependent changes in shear storage modulus (G') were measured at 1% controlled oscillatory strain. Each matrix formulation was tested in triplicate (n=3).

2.2.3 Collagen-fibril materials containing FITC-dextran

Collagen fibril matrices were self-assembled to entrap and deliver various sizes of FITC-dextrans. We formulated matrices at both low fibril-density (3 mg/ml) and high fibril-density (20 and 40 mg/ml) using the following procedures.

2.2.3.1 Low-density collagen-fibril matrices

Oligomer solutions (3 mg/ml) were polymerized in the presence and absence of 10 kDa, 40 kDa, or 2000 kDa FITC-dextran (0.5 mg/ml) as described above. For some experiments, mixed oligomer: atelocollagen matrix formulations were prepared by combining neutralized oligomer (3 mg/ml) and atelocollagen (3 mg/ml) solutions at various ratios between 0:100 and 100:0. The neutralized collagen solutions with and without FITC-dextran were kept on ice prior to the induction of polymerization. Collagen solutions were then pipetted into 48-well tissue culture plates (Corning, NY) at 250 μL per well. Due to the viscosity of the collagen solutions, positive displacement pipettes (Microman, Gilson, Middleton, WI) were used. The collagen solutions were allowed to polymerize for 30 min at 37°C in a humidified incubator.

2.2.3.2 High-density collagen-fibril matrices

High-density oligomer matrices were created using confined compression as described previously [164]. Briefly, 10.4 ml and 20.8 ml neutralized collagen oligomer (4.05 mg/ml) containing 0.25 mg/ml of 10 kDa or 2000 kDa FITC-dextran were prepared, pipetted into molds (2 cm width by 4 cm length), and polymerized overnight at 37°C. Polymerized matrices were then densified using a porous polyethylene platen (50 μm pore size) at 6 mm/min to final thickness of 0.26 cm, yielding matrices of 20 mg/ml and 40 mg/ml. Disks (1.1 cm diameter) were punched from the compressed materials and placed in 48-well tissue culture plates for comparison with non-densified, 3 mg/ml oligomeric collagen of identical dimensions. Each experimental group was prepared in triplicate (n=3).

2.2.4 Characterization of 3D collagen-fibril matrices

Both low and high fibril-density collagen fibril matrices were characterized in terms of their microstructure and proteolytic degradability, as described below.

2.2.4.1 Micro-structural analysis

Collagen fibril microstructure was visualized via cryogenic scanning electron microscopy (cryo-SEM) using an Everhart-Thronley detector adapted to a FEI NOVA nanoSEM 200 (FEI, Hillsboro, OR). Collagen materials were quick frozen by submersion into critical point liquid nitrogen, transferred to a CT1000 cold stage attachment (Oxford Instruments North America, Inc., Concord, MA), and sublimated under vacuum for 15 minutes before platinum sputter coating and imaging. Each experimental group was prepared in duplicate (n=2).

2.2.4.2 Sensitivity to proteolytic degradation

To test sensitivity of self-assembled collagen-fibril materials to collagenase degradation, rheologic testing was conducted. Solutions of 3 mg/ml neutralized oligomer, telocollagen, or atelocollagen were polymerized on the rheometer plate in adherence to the 40 mm-diameter parallel plate geometry for 30 minutes as described previously [14, 120]. Polymerized collagen materials were then exposed to 1.8 ml collagenase from Clostridium Histolyticum (type IV, Worthington Biochemical Corporation, Lakewood, NJ) reconstituted at 5000 U/ml, confined in a silicone ring. Time-dependent changes in the tangent of phase shift delta (tan δ) were monitored in oscillatory shear using a time sweep conducted at 1% controlled strain. Total degradation time was defined as time required for inflection of tan δ to an absolute value great than or equal to 1, indicative of matrix to liquid phase transition. Each material formulation was tested in triplicate (n=3).

2.2.5 Molecular Release from Collagen-fibril Matrices

2.2.5.1 Predicting sampling interval

Sampling time intervals for measuring molecular release kinetics from collagen materials were determined using an established mathematical model for monolithic matrices [165]. This model, based on Fick's second law of diffusion, assumes a slab matrix geometry

with homogeneous initial drug distribution and an associated supernatant "sink". Short-time equation (Eq. 1) was used for predicting first 60% of release, and long-time equation (Eq. 2) was used to predict last 40% release [165].

Short-time equation:

$$\frac{M_t}{M_\infty} = 4 \left(\frac{Dt}{\pi L^2} \right)^{\frac{1}{2}} \tag{1}$$

Long-time equation:

$$\frac{M_t}{M_\infty} = 1 - \frac{8}{\pi^2} \exp\left(-\frac{\pi^2 Dt}{L^2} \right) \tag{2}$$

Here, M_t and M_∞ denote cumulative amounts of molecules released at time t and at infinite time respectively; D is the molecular diffusion coefficient within the system; and L represents matrix thickness. Matrix thickness values were 0.26 cm as defined by our experimental system. Diffusion coefficient values for 10 kDa, 40 kDa, and 2 MDa FITC-dextrans were substituted as 1.09 E-10, 4.8 E-11, and 1.76 E-11 (m^2/sec) respectively based upon published experimentally determined values for 3 mg/ml oligomer collagen matrices [121].

2.2.5.2 Measuring release kinetics

For measurement of release kinetics, polymerized collagen-fibril matrices were exposed to 750 μl of either PBS (1X, pH 7.4) or collagenase from Clostridium Histolyticum (type IV, Worthington Biochemical Corporation) prepared at desired enzyme strength in PBS (1X, pH 7.4). At each sampling time, the supernatant was completely removed and replaced with 750 μl of fresh buffer. Supernatant fluorescence was measured using a spectrofluorometer (Molecular Devices Spectramax M5, Sunnyvale, CA) at excitation and emission wavelengths of 493 and 530 nm, respectively. This process was repeated until supernatant fluorescence for each well matched baseline fluorescence (PBS plus/minus collagenase, no FITC-dextran), indicating complete FITC-dextran release. All fluorescence values were normalized to maximum total fluorescence intensity and %

cumulative release was plotted against time. Each formulation was tested in triplicate (n=3).

2.2.5.3 Quantification of release kinetics and definition of molecular release mechanism

FITC-dextran release from various collagen-fibril matrices was quantified using the Weibull function [166] given in equation (3):

$$\frac{M_t}{M_\infty} = 1 - \exp(-at^b) \tag{3}$$

Here, M_t is the molecular mass released at time t, M_∞ is the molecular mass released at infinite time (assumed equal to the amount of drug added), a denotes a scale parameter that describes the time dependence, and b describes the shape of the dissolution curve progression [167]. Here, to compensate for the sensitivity of Weibull function to minor deviations when $Mt/M\infty$ % is close to 0 and 100, a weighting procedure was employed using $(-\log(1-M_t/M_\infty)*(1 - M_t/M_\infty)^2$ as recommended by Jacobsen [168] and Langenbucher [169]. Values of shape parameter b were used as an indicator of specific molecular release mechanisms, as suggested by Papadopoulou and co-workers [170]. Time required to reach 50% of cumulative release ("T_{50} %") was calculated from the Weibull fit using Matlab (The MathWorks, Inc., Natick, MA).

2.2.6 Statistical analysis

The dependence of molecular release parameters as a function of FITC-dextran size and matrix composition was determined using ANOVA followed by a post-hoc Tukey test with a 95% confidence interval. A two-sample Student's T-Test with a confidence interval of 95% was used to compare molecular release parameters from matrices in the presence and absence of collagenase. These statistical analyses were performed in Minitab 16.0 (Minitab Inc., State College, PA). Interaction and contour graphs for relationships between fibril density and collagenase level affecting T_{50}% of release, were plotted in Minitab 16.0. The statistically-significant contribution of each factor, specifically fibril density, collagenase level, and factor interaction, was determined using two-way mixed model of ANOVA, through Proc MIXED procedure in Statistical Analysis Software (SAS Institute, Cary, NC).

2.3   Results

2.3.1   Admixed FITC-dextran did not affect oligomer self-assembly capacity

We and others have documented that collagen fibril self-assembly or fibrillogenesis is dependent upon a number of polymerization parameters, including buffer composition, pH and ionic strength, presence of copolymers (e.g., other collagen types) or accessory molecules (e.g., proteoglycans), collagen molecule integrity (e.g., presence or absence of telopeptides), as well as the presence of cells [14, 120, 162, 171-176]. Here, the effect of FITC-dextran molecules on oligomer self-assembly, was determined by polymerizing oligomer solutions (3 mg/ml) in the presence or absence of 10 kDa or 2000 kDa FITC-dextran, each admixed at a relatively high concentration of 1 mg/ml. As shown in Table 3, values for polymerization half time ($P_{50}\%$) and matrix shear storage modulus (G', Pa) were statistically similar for oligomer prepared with and without FITC-dextran, indicating no significant effect of these molecules on oligomer self-assembly capacity (p=.592, n=3).

Table 3: Collagen polymerization properties

Composition	$P_{50}\%$ (min)	G' (Pa)
Oligomer	0.62 ± 0.03 [A]	689.93 ± 52.46 [A]
Oligomer + 10 kDa	0.57 ± 0.06 [A]	641.69 ± 52.69 [A]
Oligomer + 2000 kDa	0.62 ± 0.04 [A]	667.50 ± 60.13 [A]

2.3.2   Prediction of diffusion-based release from oligomer collagen suggested size-dependent release of FITC-dextran molecules

Sampling intervals for drug release must be carefully timed to accurately capture and depict material-based molecular release profiles. Sampling intervals for FITC-dextran release from oligomer matrices were predicted using an established mathematical model for monolithic materials [165] and experimentally determined FITC-dextran diffusion coefficients[177]. As expected, the predicted time for diffusion-based release showed the

tendency of larger molecules to be retained for longer times in oligomer matrices compared to small molecules (Figure 8). Resultant time periods were also used to determine supernatant collection time points for *in-vitro* molecular release studies.

A

B

FITC-dextran (kDa)	$T_{50}\%$ (hrs)
10	0.87
40	1.93
2000	5.27
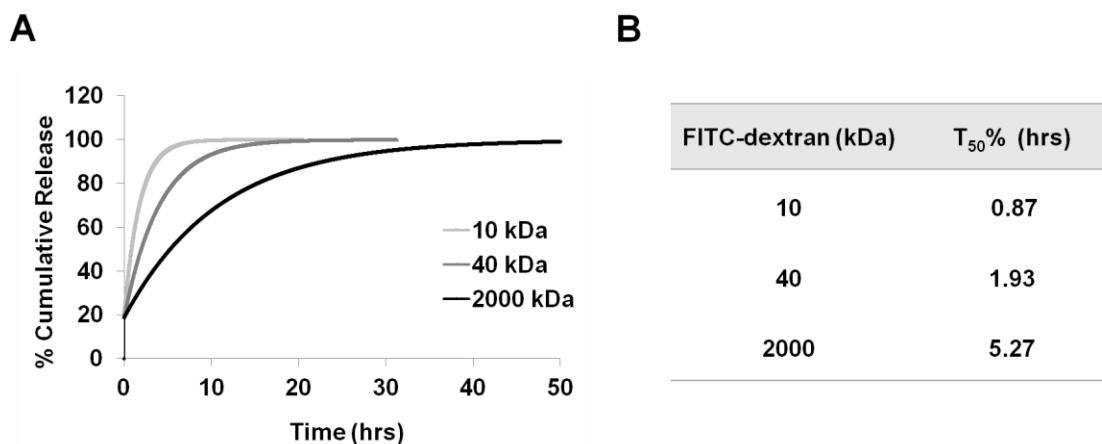
Figure 8: Small-sized molecule release is predicted to be faster than that of large sized molecules in 3 mg/ml collagen. Predicted size-dependent FITC-dextran release profiles from 3 mg/ml oligomer matrices (A) and associated $T_{50}\%$ values (B) calculated using diffusion-based models as described in the Methods section.

2.3.3 Comparison of ultrastructure and molecular release properties of collagen-fibril matrices formed from lab produced oligomer solution vs. commercial RTC solution

Matrices formed from conventional soluble collagen monomer formulations (telocollagen and atelocollagen) have three notable shortcomings, namely high lot-to-lot variability, poor structural integrity and high sensitivity to proteolytic degradation [164, 178]. As such, controlled molecular release using these materials has proven challenging [157]. Oligomer collagen, with its uncommon molecular composition, has previously been shown to possess low intra-hide and inter-hide variability [120], increased intermolecular crosslinking [14, 121], improved mechanical integrity [116], shape retention, and resistance to cell-induced contraction compared to their monomer counterparts [125, 177].

To compare the molecular release from oligomer and RTC matrices in both absence and presence of collagenase, 3 mg/ml oligomer and RTC collagen solutions containing 0.5 mg/ml of 10, 40, and 2000 kDa FITC-dextrans were polymerized to form 3D matrices, and then exposed to 1X PBS buffer with or without 125 U/ml collagenase.

Visualization of self-assembled collagen-fibril ultrastructure with cryo-SEM (Figure 9A) showed that oligomer fibrils were more uniform in size with a greater mean diameter compared to RTC. These differences in microstructure and mechanical integrity between oligomer and RTC matrices might have contributed to the differences in proteolytic resistance of the two matrices, where RTC matrices showed dramatically reduced resistance to proteolytic degradation resulting in rapid molecular release, compared to the oligomer matrices.

2.3.3.1 In absence of collagenase, oligomer matrices but not RTC matrices display size-dependent molecular release

When 3 mg/ml oligomer fibril-matrices containing various sizes of FITC-dextrans were exposed to 1X PBS buffer without collagenase, distinct molecular size-dependent release profiles were obtained as shown in Figure 9B. 10 kDa FITC-dextran was retained for the shortest time with $T_{50}\%$ of 11.40±1.25 hrs (mean±SD), followed by 40 kDa and 2000 KDa with values of 15.21±1.48 hrs, and 23.44±2.95 hrs respectively. While the release of 2000 kDa FITC-dextran was significantly slower than that of the smaller molecules (p=.001, n=3), there was no significant difference in release kinetics for 10kDa and 40kDa. Release mechanisms, as determined using Weibull fits, were diffusion-based for all molecules tested (Figure 9B). However, 10 kDa FITC-dextran was classified as diffusion through a disordered substrate, while 40 kDa and 2000 kDa FITC-dextrans represented diffusion through a normal Euclidian substrate. These results were encouraging given that oligomer materials were prepared at relatively low collagen-fibril densities, approximately 0.5% fibril dry weight [116].

A
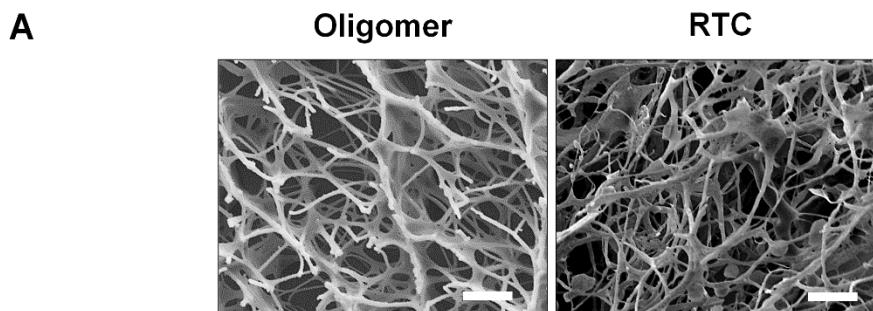
Oligomer   RTC

B

Oligomer (No Collagenase)
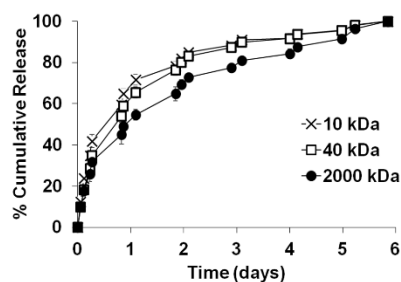
	Weibull Parameters			
FITC-dextran (kDa)	$T_{50}\%$ (hr)	b	R^2	Release Mechanism
10	11.40 ± 1.25 [B]	0.64	0.98	Diffusion; disordered substrate
40	15.21 ± 1.48 [B]	0.73	0.98	Diffusion; normal Euclidian substrate
2000	23.44 ± 2.95 [A]	0.75	0.95	Diffusion; normal Euclidian substrate

RTC (No Collagenase)
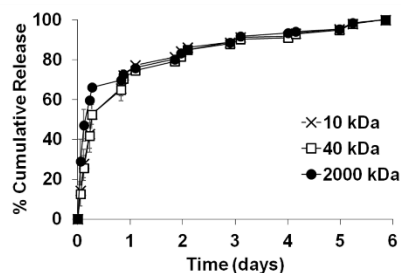
	Weibull Parameters			
FITC-dextran (kDa)	$T_{50}\%$ (hr)	b	R^2	Release Mechanism
10	7.10 ± 2.18 [x]	0.51	0.96	Diffusion; disordered substrate
40	8.08 ± 2.91 [x]	0.52	0.96	Diffusion; disordered substrate
2000	4.14 ± 0.26 [x]	0.41	0.93	Diffusion; disordered substrate

C

Oligomer (Collagenase)
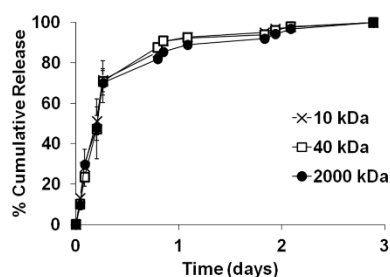
	Weibull Parameters			
FITC-dextran (kDa)	$T_{50}\%$ (hr)	b	R^2	Release Mechanism
10	3.15 ± 0.79 [A]	0.59	0.94	Diffusion; disordered substrate
40	3.49 ± 0.67 [A]	0.56	0.90	Diffusion; disordered substrate
2000	3.32 ± 0.66 [A]	0.53	0.93	Diffusion; disordered substrate

RTC (Collagenase)
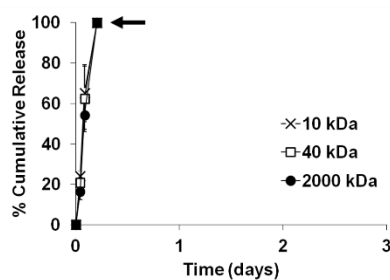
	Weibull Parameters			
FITC-dextran (kDa)	$T_{50}\%$ (hr)	b	R^2	Release Mechanism
10	1.66 ± 0.24 [x]	1.94	0.56	Complex
40	1.76 ± 0.28 [x]	2.11	0.46	Complex
2000	1.91 ± 0.19 [x]	2.03	0.80	Complex

Figure 9: Matrices prepared with self-assembling collagen oligomers show different fibril ultrastructures and molecular release profiles than commercial RTC matrices. (A) Fibril ultrastructure of collagen-fibril matrices (3 mg/ml) prepared by polymerization of oligomer or RTC, as visualized by cryo-SEM. Scale bar represents 4 μm. FITC-dextrans (10 kDa (´), 40 kDa (□), or 2000 kDa (●)) were admixed within 3 mg/ml oligomer and RTC solutions and, upon polymerization, time-dependent release from matrices was monitored spectrofluorometrically in absence (B) and presence (C) of 125 U/ml collagenase. Black arrow in release profiles from RTC (C) marks complete degradation of matrix. Tables indicate Weibull-fit based T50% (mean±SD), parameter "b", and release mechanisms based on the value of "b". Letters in T50% column indicate statistically different experimental groups as determined by Tukey-Kramer range test (n=3, p<0.05)

In contrast, conventional RTC matrices prepared at the same collagen concentration did not show size-dependent molecular release (Figure 9B). T_{50}% values ranged from 4.14±0.21 hrs for 2000 kDa molecules to 7.10±2.18 hrs for 10 kDa and were all statistically similar. Moreover, the Weibull-based release mechanism, diffusion through disordered substrate, was the same across the molecular size range tested. When compared with oligomer, RTC matrices had significantly (p<0.05) lower T_{50}% values for all FITC-dextran sizes.

Thus, the molecule size-dependent release profiles and associated distinctive release mechanisms observed through mechanically and microstructurally integrated oligomer matrices, but not RTC matrices, confirmed the viability of oligomer collagen-fibril matrices as a drug delivery system with improved control over molecular release compared to a conventional collagen-based drug delivery.

2.3.3.2 In presence of collagenase, oligomer matrices but not RTC matrices exhibit sustained release

Typically, rapid proteolytic degradation-based release from conventional collagen materials is prevented via exogenous crosslinking or chemical modification methods [4, 104, 159]. However, such methods have detrimental effects on cells and tissues [6, 78-82], and on collagen itself [8, 86]. Here completely avoiding the need for exogenous crosslinking or chemical modification, we attempted to control proteolytic degradation based release using oligomer fibril matrices that possess enhanced interfibril associations [179].

Molecular release was measured in presence of 125 U/ml collagenase from both 3 mg/ml oligomer and RTC matrices containing 0.5 mg/ml FITC-dextran (10, 40 and 2000 kDa). Oligomer matrices exhibited significantly greater $T_{50}\%$ for all FITC-dextrans, compared to the RTC matrices (Figure 9C). Notably, oligomer matrices lasted for approximately 3 days at the high concentration of collagenase while RTC degraded in mere 4.8 hrs, pointing to remarkable proteolytic resistance of oligomer matrices.

Weibull-fits indicated that the release mechanisms through oligomer changed from diffusion through normal Euclidian substrate in absence of collagenase to diffusion through disordered substrate in presence of collagenase. However, degradation based release dominated RTC matrices, resulting in complex mechanism of release, where the rate of release initially increases nonlinearly up to the inflection point and thereafter decreases asymptotically [170]. This should be interpreted with caution though, since the rapid degradation of RTC matrices dramatically reduced the sampling availability and the quality of Weibull fits for RTC matrices, compared to the increased sampling and robust Weibull fits observed with oligomer matrices.

Collectively, these results in presence of collagenase highlighted the ability of oligomer matrices to resist proteolytic degradation and exhibit significantly sustained molecular release, compared to the conventional RTC matrices.

2.3.4 Matrices composed from oligomer and atelocollagen exhibit significantly different ultrastructure and release kinetics

Collagen polymer precursors oligomer, telocollagen, and atelocollagen differ in their intermolecular crosslink composition and self-assembly capacity, giving rise to different fibril densities [180] and matrix physico-mechanical properties [14, 15, 120]. Since these parameters are known to affect mass transport[181], here we hypothesized that the molecular release kinetics can be altered by changing the collagen compositional precursors.

Ultrastructural differences between matrices prepared from oligomer, telocollagen, and atelocollagen were visualized via cryo-SEM. While oligomer matrices displayed highly branched, dense, and mechanically integrated fibrillar networks, atelocollagen matrices were characterized with sparse, thin fibrils with minimal branching (Figure 10A). Telocollagen matrices showed an intermediate fibril branching and entangled fibrils.

Influence of different precursors (3 mg/ml oligomer, telocollagen, and atelocollagen) on release of 10 kDa and 2000 kDa FITC-dextran (0.5 mg/ml) was observed in both absence (Figure 10 B) and presence of 125 U/ml collagenase (Figure 10 C). Release profiles for atelocollagen differed significantly from oligomer and telocollagen (p<.001; n=3) For instance, the T_{50}% exhibited by atelocollagen matrices for 10 kDa was 0.49±0.09 hrs, significantly lower (p<0.001, n=3) than that for oligomer (11.40±1.25 hrs) and telocollagen (10.50±1.22 hrs) matrices. Similarly, atelocollagen exhibited significantly lower T_{50}% in case of 2000 kDa FITC-dextran compared to oligomer and telocollagen matrices. Oligomer and telocollagen values were however not significantly different. Furthermore, Weibull fitting indicated that the release mechanisms were different through atelocollagen matrices when compared to telocollagen and oligomer matrices, in both absence (Figure 10 B) and presence (Figure 10 C) of collagenase. The molecular release was accelerated from all matrices in presence of collagenase, elucidating role of proteolytic degradation in release.

A

Atelocollagen	Telocollagen	Oligomer

B
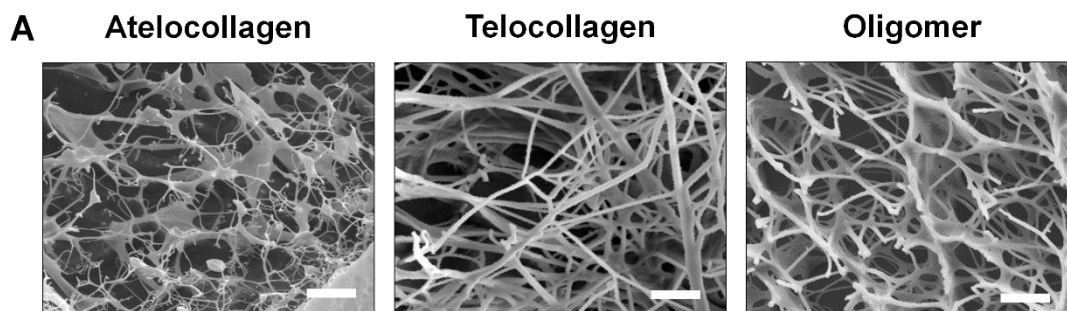
10 kDa (No Collagenase)
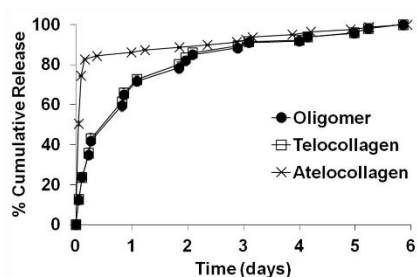
Weibull Parameters				
Matrix	$T_{50}\%$ (hr)	b	R^2	Release Mechanism
Oligomer	11.40 ± 1.25 [A]	0.64	0.98	Diffusion; disordered substrate
Telocollagen	10.50 ± 1.22 [A]	0.62	0.98	Diffusion; disordered substrate
Atelocollagen	0.49 ± 0.09 [B]	0.21	0.83	Diffusion; highly disordered substrate

2000 kDa (No Collagenase)
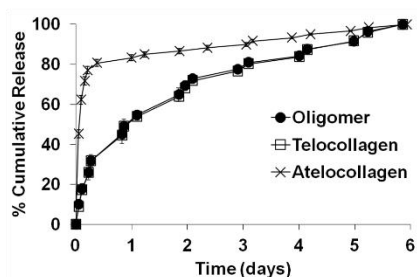
Weibull Parameters				
Matrix	$T_{50}\%$ (hr)	b	R^2	Release Mechanism
Oligomer	23.44 ± 2.95 [X]	0.75	0.95	Diffusion; normal Euclidian substrate
Telocollagen	24.42 ± 0.22 [X]	0.77	0.96	Diffusion; normal Euclidian substrate
Atelocollagen	0.13 ± 0.02 [y]	0.25	0.90	Diffusion; highly disordered substrate

C

10 kDa (Collagenase)
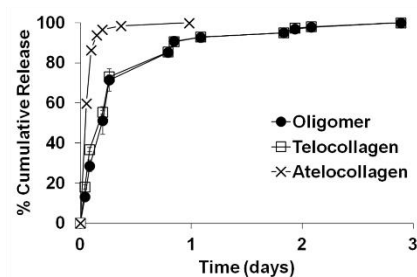
Weibull Parameters				
Matrix	$T_{50}\%$ (hr)	b	R^2	Release Mechanism
Oligomer	3.15 ± 0.79 [A]	0.59	0.94	Diffusion ; disordered substrate
Telocollagen	2.79 ± 0.81 [A]	0.56	0.93	Diffusion; disordered substrate
Atelocollagen	0.73 ± 0.15 [B]	0.81	0.88	Diffusion + Degradation

2000 kDa (Collagenase)
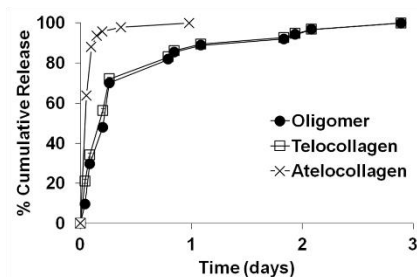
Weibull Parameters				
Matrix	$T_{50}\%$ (hr)	b	R^2	Release Mechanism
Oligomer	3.32 ± 0.66 [x]	0.53	0.93	Diffusion; disordered substrate
Telocollagen	2.76 ± 0.39 [x]	0.51	0.95	Diffusion; disordered substrate
Atelocollagen	0.58 ± 0.09 [y]	0.66	0.88	Diffusion; disordered substrate

Figure 10: Molecular release profiles of self-assembled collagen-fibril matrices are dependent upon collagen polymer composition. (A) Fibril ultrastructure of collagen-fibril matrices (3 mg/ml) prepared by polymerization of atelocollagen, telocollagen, and oligomer as visualized using cryo-SEM. Scale bar represents 4 μm. FITC-dextrans (10 kDa or 2000 kDa) were admixed within 3 mg/ml atelocollagen (×), telocollagen (□), and oligomer (●) solutions, and upon polymerization, time-dependent release was monitored spectrofluorometrically in absence (B) and presence (C) of 125 U/ml collagenase. Associated tables indicate Weibull-fit based $T_{50}\%$ (mean±SD), parameter "b", and release mechanisms interpreted based on the value of "b". Letters in $T_{50}\%$ column indicate statistically different experimental groups as determined by Tukey-Kramer range test (n=3, p<0.05).

The proteolytic degradation was observed to be different for matrices formed form different precursors, as determined by exposing each of the matrices to 5000 U/ml collagenase on rheometer. Time sweep tracking transition of matrix from solid to liquid phase then indicated that the degradation time for each type of matrix was significantly different (p<0.001; n=3), as shown in Table 4. Atelocollagen matrices degraded fastest, followed by telocollagen and then oligomer matrices.

Collectively, these results highlighted the slowest and fastest release kinetics displayed by oligomer and atelocollagen precursor based matrices, identifying them as viable candidates for further tuning of molecular release from collagen.

Table 4: Matrix degradation time

Matrix	Time (min)
Oligomer	219.5 ± 10.9 [A]
Telocollagen	186.7 ± 19.7 [B]
Atelocollagen	138.0 ± 1.0 [C]

2.3.5 Tuning molecular release from collagen-fibril matrices

The structure, density, and integrity of fibrillar and nonfibrillar ECM components are major factors in regulation of interstitial transportation and mediation of cellular responses during physiological and pathological states in human body [182]. Here we wanted to capture these features to modulate molecular release from collagen-based materials. As such, we chose to systematically alter collagen fibril microstructure and proteolytic degradation through 1) change in compositional ratio of oligomer and atelocollagen precursors in the matrix, and 2) change in the polymerized oligomer fibril-matrix density. While first strategy enabled tuning release through changes to collagen made before polymerization, second strategy enabled to do so after polymerization of collagen.

2.3.5.1 Oligomer and atelocollagen mixed matrices enable tuning polymerization kinetics, ultrastructure, and molecular release kinetics

Whittington et al. [121, 180] previously showed that by varying oligomer to telocollagen ratio, matrix mechanical properties as well as cell growth and differentiation can be guided. Park et al. further elucidated effect of modulating collagen precursor ratios on mass transport properties of collagen through computational modeling[181]. Here, we aimed at determining the effect of modulating collagen precursors, specifically 3 mg/ml oligomer and atelocollagen, on molecular release kinetics of both small and large sized FITC-dextran. Therefore, neutralized oligomer and atelocollagen solutions (3 mg/ml) were mixed in ratios 0:100, 25:75, 50:50, 75:25, and 100:0 respectively and its effects were assessed on the collagen polymerization kinetics, viscoelasticity, and molecular release kinetics.

Mixing resulted in matrices with significantly different polymerization kinetics and stiffness ($p<.05$, n=3; Figure 11). Matrix stiffness and polymerization rate correlated positively with increase in oligomer content. All matrices except 100% atelocollagen polymerized within 5 minutes. Cryo-SEM was performed to determine the effect of mixing oligomer and atelocollagen precursors on collagen fibril ultrastructure (Figure 12A). The 100% oligomer matrices demonstrate increased fibril thickness, density, and interconnectivity when compared to 100% atelocollagen matrices. Matrices containing

equal proportions of oligomer and atelocollagen showed intermediate fibril density and interconnectivity.
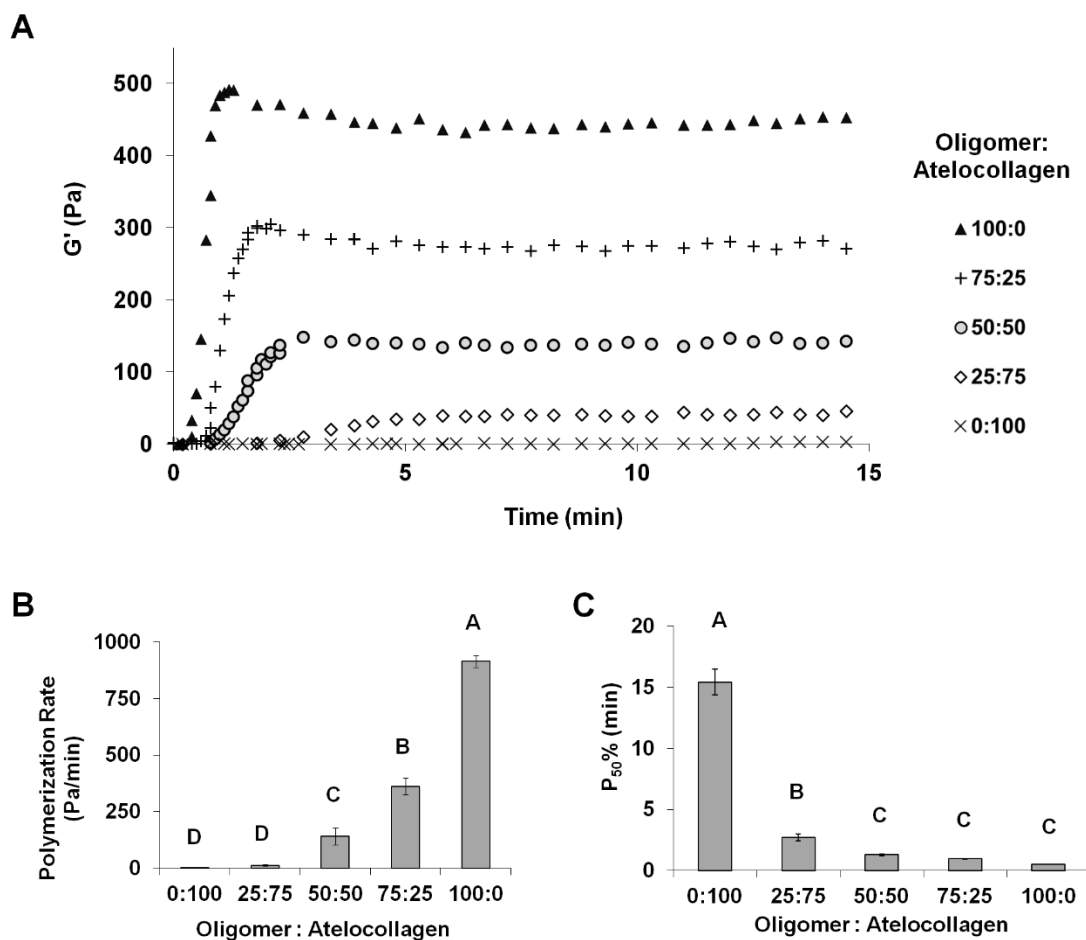
Figure 11: Collagen polymerization kinetics are dependent upon the oligomer: atelocollagen ratio. Time-dependent changes in shear-storage modulus were monitored as collagen formulations transitioned from solution to matrix following an increase in temperature from 4°C to 37°C. (A) Time-dependent changes in shear storage modulation during polymerization were used to quantify (B) polymerization rate (mean±SD) and (C) polymerization half-times (P50%; mean±SD). Each sample was tested in triplicate

To determine the effect of mixed matrices on molecular release kinetics, neutralized collagen solutions (3 mg/ml) containing either 10 kDa or 2000 kDa FITC-dextran were prepared from oligomer and atelocollagen, then mixed in ratios of 0:100, 5:95, 10:90, 50:50, 75:25, and 100:0 respectively. Upon polymerization, matrices were exposed to 1X PBS buffer with no collagenase or 10 U/ml collagenase.

A

Oligomer:Atelocollagen

100:0 **50:50** **0:100**

B

No Collagenase

10 kDa **2000 kDa**

Collagenase

10 kDa **2000 kDa**

Oligomer:
Atelocollagen

- 0:100
- 5:95
- 10:90
- 50:50
- 75:25
- 100:0
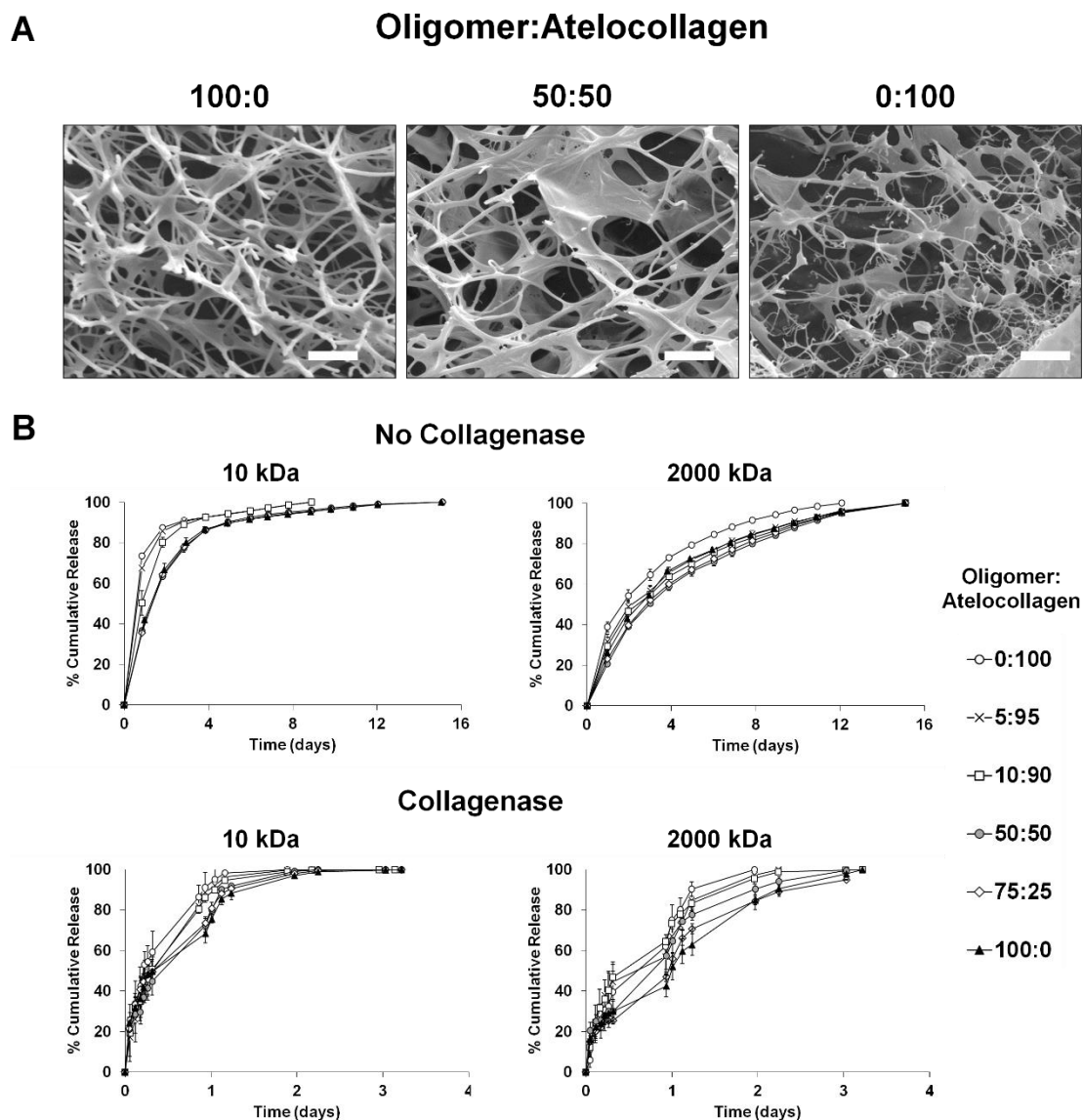
Figure 12: Collagen-fibril matrix molecular release can be tuned by varying the oligomer:atelocollagen ratio. (A) Fibril ultrastructure of collagen matrices (3 mg/ml) prepared by polymerization of oligomer and atelocollagen mixed at different ratios as visualized by cryo-SEM. Scale bar represents 4 μm. FITC-dextrans (10 kDa and 2000 kDa) were admixed within oligomer:atelocollagen solutions prepared at 0:100 (o), 5:95 (×), 10:90 (□), 50:50(●), 75:25(◊), and 100:0 (▲) ratios and, upon polymerization, time-dependent release of FITC-dextrans was monitored spectrofluorometrically in the absence (B) and presence (C) of 10 U/ml collagenase.

In the absence of collagenase (Figure 12B), mixed matrices exhibited different release profiles, for both 10 kDa and 2000 kDa FITC-dextrans. Release was prolonged with increase in oligomer proportion in the mixed matrices. 2000 kDa FITC-dextran was retained for a longer time than 10 kDa FITC-dextran, indicating molecular size dependent release characteristic of mixed matrices. Further, the presence of collagenase highlighted the distinction between release profiles of various mixed matrices (Figure 12C), with a more pronounced effect on 2000 kDa FITC-dextran. The exaggerated differences in release profiles observed in the presence of collagenase might be attributed to the differences in proteolytic degradability associated with each collagen matrix component seen earlier (Table 4).

Collectively, this method of changing collagen matrix composition through varying oligomer and atelocollagen ratio shed light on its effectiveness on tuning molecular release of both small and large sized molecules, through modulation of microstructure and proteolytic degradation.

2.3.5.2 Oligomer densification tunes matrix ultrastructure and molecular release

Previously, using the method of confined compression, Blum et al. prepared high fibril density oligomer matrices that possessed higher-order interfibril associations, and mechanical properties of soft connective tissues [116]. Due to the smaller matrix pore sizes [183] and increased resistance to proteolytic degradation [116] associated with these high fibril-density collagen matrices, we hypothesized that confined compression can be used to extend drug release from collagen fibril matrices. To test this hypothesis, polymerized 4.05 mg/ml oligomer matrices containing 0.25 mg/ml FITC-dextran (10 kDa or 2000 kDa) were subjected confined compression [164], yielding 20 and 40 mg/ml densified matrices.

The effect of densification on matrix ultrastructure was revealed by cryo-SEM (Figure 13A). Densified matrices exhibited enhanced fibril density and higher-order interfibril associations, in agreement with Blum et al. [164].

The effect of densification on molecular release from collagen-fibril matrices was determined by exposing matrices to 1X PBS buffer containing either no collagenase (Figure 13B) or 10 U/ml collagenase (Figure 13C). Significantly prolonged the release

was observed from 20 and 40 mg/ml matrices, compared to 3 mg/ml matrices ($p<0.001$, n=6). For 10 kDa FITC-dextran release, while the 40 mg/ml matrices gave a T_{50}% value of 14.02 ± 2.16 hrs, 20 mg/ml matrices closely followed with a value of 13.61 ± 1.10 hrs. However, low fibril-density (3 mg/ml) matrices exhibited lowest value of 1.7 ± 0.41 hrs. This distinction between molecular release properties of high fibril-density and low fibril-density matrices was maintained for 2000 kDa FITC-dextran release as well, since the T_{50}% of 20 and 40 mg/ml matrices (229.42 ± 10.22 hrs and 339.85 ± 3.56 hrs) were significantly longer than that for 3 mg/ml matrices (36.18 ± 4.84 hrs). These higher values of T_{50}% exhibited by high fibril density matrices were most striking, especially in the absence of any exogenous modification of collagen. Thus, 20 mg/ml and 40 mg/ml matrices provided a remarkable extension of 2000 kDa FITC-dextran release for up to 44 and 55 days respectively, which is well above the release period of uncrosslinked/unmodified conventional collagens [4, 5, 66]. Exposure of low and high fibril density matrices to 10 U/ml collagenase further elucidated the role of proteolytic degradation in molecular release. Degradation accelerated release of 10 kDa (Figure 13C) as well as 2000 kDa (Figure 13D) FITC-dextran. It also amplified the distinctness of release profiles given by low and high fibril-density matrices. While 3 mg/ml matrices showed rapid release of 10 kDa FITC-dextran (T_{50}% 1.03 ± 0.49 hrs), 20 and 40 mg/ml matrices showed significantly extended ($p<.001$, n=6) release (T_{50}% 8.72 ± 1.94 hrs and 11.98 ± 1.70 hrs respectively). This distinctness of molecular release between low and high fibril density matrices was maintained in case of 2000 kDa FITC-dextran, with 3 mg/ml matrices showing lowest T_{50}% (4.64 ± 1.20 hrs), followed by 20 mg/ml (39.68 ± 7.55 hrs) and 40 mg/ml (69.20 ± 10.15 hrs) matrices. These results point to enhanced collagenase resistance of high fibril density matrices that must have contributed to the longer retention of molecules compared to that by the low fibril density matrices. Weibull fits showed diffusion-based release mechanisms for both 10 and 2000 kDa FITC-dextrans in absence of collagenase, but complex release mechanisms in presence of collagenase. Additionally, increased value of parameter "b" obtained for high fibril-density (20 and 40 mg/ml) matrices reflected the decrease in disorder of the system at high fibril density compared to low fibril-density [170].

For 10 kDa, Weibull fits indicated both diffusion- and proteolytic degradation-based molecular release mechanisms for 20 and 40 mg/ml matrices. The 3 mg/ml matrices exhibited diffusion through disordered substrate, as expected from previous results. For 2000 kDa, 20 and 40 mg/ml matrices showed complex release mechanisms while 3 mg/ml matrices exhibited diffusion through a disordered substrate. Release mechanisms differed with collagen-fibril density in the presence of collagenase.

A

Oligomer (mg/ml)

3 **20** **40**

B

10 kDa (No Collagenase)

% Cumulative Release vs Time (days)
- ✳ 3 mg/ml
- ☐ 20 mg/ml
- ● 40 mg/ml

Weibull Parameters				
Oligomer (mg/ml)	$T_{50}\%$ (hr)	b	R^2	Release Mechanism
3	1.70 ± 0.41 [B]	0.48	0.95	Diffusion; disordered substrate
20	13.61 ± 1.10 [A]	0.75	0.98	Diffusion; normal Euclidian substrate
40	14.02 ± 2.16 [A]	0.77	0.98	Diffusion; normal Euclidian substrate

2000 kDa (No Collagenase)

% Cumulative Release vs Time (days)
- ✳ 3 mg/ml
- ☐ 20 mg/ml
- ● 40 mg/ml

Weibull Parameters				
Oligomer (mg/ml)	$T_{50}\%$ (hr)	b	R^2	Release Mechanism
3	36.18 ± 4.84 [z]	0.82	0.91	Diffusion; normal Euclidian substrate
20	229.42 ± 10.22 [y]	0.93	0.98	Diffusion; normal Euclidian substrate
40	339.85 ± 3.56 [x]	0.98	0.97	First order release

C

10 kDa (Collagenase)

% Cumulative Release vs Time (days)
- ✳ 3 mg/ml
- ☐ 20 mg/ml
- ● 40 mg/ml

Weibull Parameters				
Oligomer (mg/ml)	$T_{50}\%$ (hr)	b	R^2	Release Mechanism
3	1.03 ± 0.49 [C]	0.55	0.76	Diffusion; disordered substrate
20	8.72 ± 1.94 [B]	0.91	0.93	Diffusion + Degradation
40	11.98 ± 1.70 [A]	0.87	0.94	Diffusion + Degradation

2000 kDa (Collagenase)

% Cumulative Release vs Time (days)
- ✳ 3 mg/ml
- ☐ 20 mg/ml
- ● 40 mg/ml

Weibull Parameters				
Oligomer (mg/ml)	$T_{50}\%$ (hr)	b	R^2	Release Mechanism
3	4.64 ± 1.20 [z]	0.55	0.91	Diffusion; disordered substrate
20	39.68 ± 7.55 [y]	1.33	0.92	Complex
40	69.20 ± 10.15 [x]	1.64	0.91	Complex

Figure 13: Increasing fibril density of oligomer matrices prolongs molecular release. A) Fibril ultrastructure of 3 mg/ml, 20 mg/ml and 40 mg/ml oligomer matrices as visualized using cryo-SEM. Scale bar represents 4 μm. Time-dependent release profiles of 10 kDa and 2000 kDa FITC-dextran from 3 mg/ml (×), 20 mg/ml (□), and 40 mg/ml (●) oligomer matrices were monitored spectrofluorometrically in the absence (B) and presence (C) of 10 U/ml collagenase. Associated tables indicate Weibull-fit based $T_{50}\%$ (mean±SD), parameter "b", and the release mechanisms interpreted based on the value of "b". Letters in $T_{50}\%$ column indicate statistically different experimental groups as determined by Tukey-Kramer range test (N=3, p<0.05)

2.3.6 Oligomer fibril density modulates molecular release at various collagenase levels

Tunablity in proteolytic degradation based molecular release is highly desirable in applications such as wound healing, where different levels of collagenase exist [184]. In wounds with high protease level, normal wound repair process is obstructed, and together with altered cytokine expressions, matrix repair and degradation rate is affected [23, 185, 186]. In such situations, densified oligomer-fibril matrices could accelerate wound healing, due to their high mechanical strength, resistance to proteolytic degradation, high cell signaling capacity [116], and ability to provide sustained molecular release. On the other hand, faster molecular release from low fibril-density matrices may be beneficial in acute wounds where protease levels are low and wounds heal faster. However, even in each type of wound, collagenase levels are affected by the pathophysiological states, *in-vivo* locations, as well as by the age of the wound [187-189]. Therefore, it is important to characterize the tunability in molecular release of collagen fibril matrices under varying collagenase levels [190] [191].

To capture this scenario of varying collagenase concentrations, molecular release from different fibril density matrices (3 mg/ml, 20 mg/ml and 40 mg/ml) was determined in the absence (0 U/ml), or presence of low (10 U/ml) and high (100 U/ml) collagenase levels. These levels were chosen as representatives of collagenase in physiologically normal state, acute wound and chronic wound conditions respectively [184, 187, 192]. This study was focused on molecular release of small sized FITC-dextran (10 kDa) only, since large molecular release is easier to control [4, 5, 193].

Results show that an increase in fibril density of oligomer matrices affects the $T_{50}\%$ values positively, while the increase in collagenase level affects these values

negatively (Figure 14A). An interaction exists between fibril density and collagenase levels (Figure 14B). Mixed ANOVA further confirmed that both the collagenase level, fibril density, and their interaction affected $T_{50}\%$ significantly ($p<0.001$, $n=6$). The molecular release from 40 mg/ml matrices was most sustained, followed by 20 mg/ml and 3 mg/ml matrices at all collagenase levels (Figure 15). Contour graph of $T_{50}\%$ plotted as a function of collagenase level and fibril density (Figure 14) further elucidated that matrix fibril density played a greater role in tuning the $T_{50}\%$ than the collagenase level.

These results highlight the ability of oligomer fibril matrices to modulate molecular release in presence of varying levels of collagenase, based on the alteration of their fibril density. This is a significant achievement for high fibril-density oligomer matrices, considering the absence of any exogenous crosslinkers or chemical modifiers that are typically applied to control molecular release from conventional collagen matrices.

A

Weibull Parameters

Oligomer (mg/ml)	Collagenase (U/ml)	$T_{50}\%$ (hr)	b	R^2	Release Mechanism
3	0	1.7 ± 0.41	0.48	0.95	Diffusion; disordered substrate
	10	1.09 ± 0.49	0.55	0.76	Diffusion; disordered substrate
	100	1.13 ± 0.02	1.45	0.99	Complex
20	0	13.61 ± 1.10	0.75	0.98	Diffusion; normal Euclidian substrate
	10	8.72 ± 1.94	0.91	0.93	Diffusion + Degradation
	100	3.95 ± 0.43	0.91	0.96	Diffusion + Degradation
40	0	14.02 ± 2.16	0.75	0.98	Diffusion; normal Euclidian substrate
	10	12.19 ± 1.81	0.87	0.94	Diffusion + Degradation
	100	6.41 ± 1.02	1.05	0.94	First order release

Figure 14: Oligomer matrix molecular release is dependent upon fibril density and collagenase level. 10 kDa FITC-dextran was admixed within 3 mg/ml, 20 mg/ml, and 40 mg/ml oligomer matrices and release kinetics were monitored spectrofluorometrically in the presence of 100 U/ml, 10 U/ml, and 0 U/ml collagenase. A) Table indicates Weibull-fit based $T_{50}\%$ (mean±SD), parameter "b", and related release mechanisms. Letters in $T_{50}\%$ column indicate statistically different experimental groups as determined by Tukey-Kramer range test (n=3, p<0.05). B) Interaction plot for different fibril density oligomers at various levels of collagenase. C) Corresponding contour plot showing the influence of various levels of oligomer fibril density and collagenase on $T_{50}\%$ of release for 10 kDa FITC-dextran.
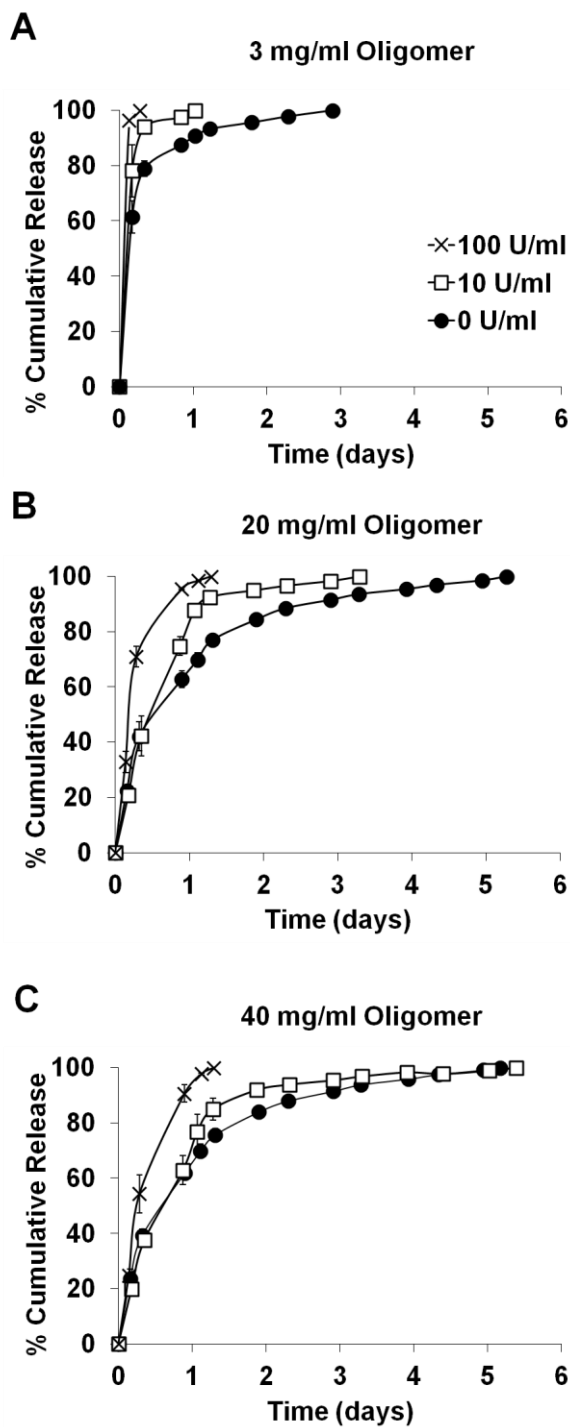
Figure 15: Oligomer matrix molecular release is dependent upon collagenase level. Time-dependent release profiles for 10 kDa FITC-dextran admixed within 3 mg/ml, 20 mg/ml, and 40 mg/ml oligomer matrices were monitored spectrofluorometrically in the presence of 100 U/ml (×), 10 U/ml (□), and 0 U/ml (●) collagenase.

2.4   Discussion

Many complex biological tissues in the human body, including collagen-based tissues, display some remarkable features in common, including molecular self-assembly, hierarchical organization at the atomistic, molecular, and macro scales, as well as multifunctionality [194]. It is the microstructure and proteolytic degradability of the formed tissue that then plays an important role in regulating the mass transport through body. Therefore to control molecular transport through collagen based matrices *in vitro*, it is important to mimic collagen self-assembly, and provide control over the microstructure and proteolytic degradability of resultant matrices.   However, the conventional monomeric collagen (telocollagenic and atelocollagenic) formulations fail to capture the self-assembly characteristic of collagen. Unlike oligomers, these conventional monomeric formulations do not retain their tissue-specific, covalent intermolecular cross-links [125]. As a result, the matrices formed from conventional collagen formulations display weaker mechanical integrity and rapid proteolytic degradation. Consequently, they fail to retain molecules/drugs for longer time and cannot be tuned to match their release rates to desired need.

To address this gap, we decided to employ a collagen polymer engineering approach that is inspired by the *in-vivo* collagen-fibril assembly. By incorporating collagen natural intermolecular cross-link chemistries through oligomer building blocks [14] we created self-assembled collagen fibril matrices that retained their multiscale structure and biological signaling properties. This work explores the viability of these self-assembled collagen fibril matrices in serving as multi-functional platforms for delivery of a wide range of sizes of molecules. Through systematic variation of collagen polymer composition and fibril density, we demonstrated the capability of these matrices to tune molecular release based on modulation of microstructure and proteolytic degradability features of matrix as the two main regulators of molecular transport. Notably, this tunability in molecular release under both proteolytic and non-proteolytic conditions, is achieved without using any exogenous crosslinking or chemical modification.

In order to design and validate the potential of oligomers to formulate a multi-functional drug delivery system, we admixed oligomeric collagen with FITC-dextrans of sizes 10

kDa, 40 kDa and 2000 kDa and polymerized them to form 3D collagen-fibril matrices of 3mg/ml density. FITC-dextrans molecule sizes were chosen to span a range of therapeutic molecules including growth factors, antibodies, antibacterial agents, viruses, nanoparticles, and plasmids[195].

An important aspect of our experimental procedure was to emulate the *in-vivo* molecular release kinetics. Literature indicates that molecular release *in vivo* occurs by a combination of diffusion and enzymatic breakdown of the collagen matrix [196]. In pathological diseases such as cancer [197, 198] and chronic foot ulcers [188] well as during normal tissue homeostasis, [199], proteolytic degradation of collagen is caused by members of matrix metalloproteinase (MMP) family. To capture these *in-vivo* behaviors, we measured the release kinetics of FITC-dextran infused oligomeric matrices under two scenarios: 1) in absence of collagenase (diffusion only); or 2) in presence of collagenase (diffusion+degradation). The *in-vitro* model system we adopted for measuring release is a well-established model that has been used in the past by several researchers for quantifying molecular release from various collagen-based drug delivery systems[137, 200-206]. In this model, the drug-containing collagen matrices are typically submerged in a small volume of PBS buffer (typically 400 to 2500 µL) with or without collagenase, the system is subjected to gentle shaking and the buffer volume is replaced periodically in the given release study period, to quantify drug elution at various time points. In our system, we chose 750 µL buffer volume for submerging collagen matrices as this volume was within the range of previously reported buffer volumes [137, 200-206] and could fit in a 48 well tissue-culture plate. We then subjected the entire plate to gentle shaking conditions and periodically replaced buffer with fresh volume, that allowed us to quantify release kinetics based off of fluorescence of FITC-dextrans eluted at a given time point.

Along with quantifying molecular release kinetics, the understanding of release mechanisms involved in the release process is crucial when designing a controlled release system[207]. For understanding and elucidating the mechanisms of drug release, empirical modeling of drug release has been found to play an important role [208-210]. Characterizing molecular release from polymer matrices have been accomplished through use of various empirical models, including the well-known Higuchi, and Peppas and Weibull models [211-218]. The basic mathematical expressions used to describe the

release kinetics and discern the release mechanisms are elegantly described in the articles on Higuchi law [219] and the Peppas equation or the so-called power law ([220-222]). Despite their wide use, [170, 216-218, 223], both Higuchi and power law are short time approximations of complex exact relationships[223, 224], therefore, their use is confined to the description of the first 60% of the release curve[170]. Beyond 60%, the quality of the fit has been observed to be poor. However, Weibull function has been found to be appropriate for fitting the entire set of data while effectively explaining the mechanisms of molecular release [170, 225-228] and has been applied successfully by several researchers for discernment of drug release mechanisms [166, 226-237]. Therefore, in this study, Weibull function was used to fit release data, quantify $T_{50}\%$, and decipher the associated release mechanisms.

2.4.1 Oligomeric collagen enables formation of multi-functional platforms with robust microstructure and extended molecular release characteristics

To avoid the use of external agents, and yet maintain the mechanical integrity of collagen based drug delivery system, we used novel self-assembling oligomeric collagen building blocks that show a unique ability to form hierarchical fibrillar structures similar to those found *in vivo* [115, 177]. These building blocks also possess many critical design features amenable for engineering 3D cellular microenvironments, such as ability provide mechanical support as well as biological cues for cell proliferation [14, 120, 177, 179, 238]. A number of factors such as microstructure, matrix composition, and extent exogenous cross-linking can affect mass transport through collagen-based tissues and matrices [239-241]. Whittington et al. [177] recently showed that the inclusion of intermolecular cross-links as a component of the fundamental collagen building blocks (oligomers) affects molecular diffusion within polymerized matrices by regulating hierarchical assembly and interfibril branch formation. Here we extend upon that work by showing that oligomer collagen matrices affect the molecular release of FITC-dextrans differently than conventional telocollagenic (RTC) matrices, both in the absence and presence of collagenase. In absence of collagenase, large FITC-dextran (2000 kDa) release was significantly extended (p<0.05, n=3) when compared to small FITC-dextrans (10 kDa and 40 kDa) through oligomeric, but not RTC matrices. Release profiles through oligomer matrices were distinct for both smaller and larger molecules, as

expected from predictive models of diffusion-based release (Figure 8). On the other hand, RTC matrices showed lumped release profiles (not distinguished based on sizes of FITC-dextrans). These results demonstrate the ability of oligomeric matrices to exhibit molecular size-dependent release, similar to what is observed in *in-vivo* tissues such as sclera [242] or brain ECM [243]. This is impressive because conventional collagen matrices have not been able to achieve such a size dependent release without exogenous crosslinking or modification with additives [78, 244, 245]. It is now known that cross-linking agents such as glutaraldehyde can exhibit detrimental effects on cells and tissues [78] and non-collagenous additives affect the physiological properties of matrices.

In simultaneous experiments with collagenase (125 U/ml), ability of oligomer fibril matrices to give sustained release (Figure 9C) was highlighted, in contrast to the rapid release displayed by RTC matrices that were completely degraded in just 4.8 hrs. However, at the same high collagenase level, the oligomer matrices persisted for about 3 days, highlighting their enhanced resistance to proteolytic degradation. Notably, this resistance is observed in absence of any exogenous crosslinking, while it is typical to use exogenous crosslinkers in conventional collagen formulations for obtaining sustained molecular release in presence of collagenase[192, 246, 247].

The molecular release differences observed between oligomer and RTC matrices could be attributed to their ultrastructure differences (Figure 9A). Cryo-SEM comparison of 3 mg/ml oligomer matrices with conventional telocollagenic RTC matrices revealed that oligomer matrices had a uniform, interconnected porous nature when compared to the non-uniform fibril ultrastructure and weak mechanical stability of conventional RTC matrices. Oligomer matrices also exhibited superior handling properties compared to RTC matrices during the cryo-SEM sample preparation, as the RTC matrices were observed to be physically breaking apart during the loading of samples on SEM sample stage, while the oligomer matrices remained intact. The low mechanical integrity of RTC matrices has been observed previously [120] and could be due to the poor mechanical stiffness of telocollagenic formulations [238, 248] that the RTC matrices are claimed to be made of [249]. Previous reports have shown that oligomer matrices were significantly stiffer than their telocollagenic counterparts when polymerized at the same collagen concentration, owing to increased interfibril branching [177] [238, 248]. Thus, the altered

packing and alignment of collagen molecules that occurs in the presence of covalently cross-linked molecules (oligomers) during self-assembly may have resulted in increased interfibril branching and distinct hierarchical architecture [120].

The release mechanisms that were inferred from Weibull fit-based parameters indicated differences in release from oligomer and RTC matrices in both absence and presence of collagenase. In the absence of collagenase, release from oligomeric matrices emulated diffusion through normal Euclidian substrate while that through RTC matrices was similar to diffusion through a disordered substrate (Figure 9). Similar differences were observed in presence of collagenase as well, with oligomer showing diffusion through disordered substrate, but RTC matrices showing complex release mechanism. However, the mechanisms in RTC case had to be interpreted carefully, due to the poor Weibull fit (R^2) values observed. These could be attributed to the rapid degradation of RTC matrices causing reduction in sampling availability and thereby affecting the Weibull fitting of the data [250].

In general, RTC matrices exhibited significantly faster diffusion compared to that shown by oligomer matrices. Such a rapid release from conventional non-crosslinked collagens has been previously observed. For example, basic fibroblast growth factor (bFGF) was released from non-crosslinked collagen matrices during the first 6 hours [251]. Similarly, a collagen sponge incubated with rhBMP-2 (~26 kDa) solution released 55% of the protein in 1 h and 100% in 2 days [252].Larger molecule Riboflavin (376.36 g/mol) was also released in a short duration of 16 hours from collagen sponges [253]. Implantation of a gentamicin-impregnated collagen sponge Garamycin in horses resulted in peak concentration of gentamicin within 3 hours [254]. Considering these burst release examples from conventional collagen, the ability of oligomeric collagen to provide both size-dependent and sustained molecular release in both the absence and presence of collagenase appears impressive. These results indicate the potential of these unique building blocks in forming a multifunctional drug delivery platform capable of delivering a wide range of molecules without the need for exogenous agents.

2.4.2 Tuning microstructure and molecular release properties of oligomer fibril matrices

The ability to provide sustained drug release is not adequate for the success of a drug delivery implant *in vivo*. Implants should be tunable in terms of their mechanical, microstructural, and molecular release properties to match tissue regeneration rates, as these rates can vary based on the location of soft tissue damage or its healing stage, as well differences in an individual's age, dietary intake, healing rate, and lifestyle-related factors [255]. Despite wide research and promising results of collagen-based materials in improving therapeutic efficacy and delivery [3, 4, 66], the inability of the collagen based systems to provide tunable release is still a major limitation restricting its clinical utility.

Challenges in tuning molecular release from conventional collagen matrices stem from open weave structure of collagen [4]. This problem is compounded by the poor characterization of conventional formulations in terms of their molecular composition and inability to fully capitalize on the inherent self-assembly or polymerization capacity of collagen leading to weak mechanical integrity and cursory control over physical and molecular release properties [14, 15, 116, 248]. Hence, to tune molecular release from collagen, it has been necessary to rely on methods such as exogenous crosslinking, mixing with another polymer phase, covalent or non-covalent bonding, or sequestration in a secondary matrix as listed in Table 1. However, such steps not only increase the complexity of the system, but also alternative microstructure of collagen [256, 257]. Therefore, a combination of improved collagen formulation and a tuning strategy that does not alter physiologically relevant properties of collagen is desirable to improve tunable molecular delivery from collagen.

Here, we addressed this problem with the use of self-assembling oligomer building blocks that have been shown to retain physiologically relevant crosslinks [14] and have been used to predictably and reproducibly control fibril- and matrix-level physical properties for the creation of 3D *in-vitro* tissue systems [116, 125] while illustrating robust physico-mechanical properties [14, 120, 177, 179, 238]. To tune molecular release using these novel oligomer building blocks, we applied two strategies that can preserve the physiologically relevant microstructure of collagen: 1) modulating the polymer composition through change in compositional building blocks of collagen; and

2) densifying oligomer fibril matrices. While the first strategy offers an option of tuning matrix microstructure, degradation, and release properties before polymerization of collagen, the second strategy offers this tunability after polymerization.

2.4.3 Tunability by altering polymer composition

It has been known that modulation of collagen microstructure and composition affects molecular transport from collagen-based materials [239-241, 258-260]. Literature survey also reveals that collagen precursors (atelocollagen, telocollagen and oligomer) show differences in mechanical [116, 120], physical [14], and biological properties owing to the different interfibril branching capacity of the precursors. Here we wanted to extend upon this work by studying the effect of these precursors on molecular release from collagen. First, we observed microstructural differences between oligomer, telocollagen and atelocollagen (Figure 10A), that could be attributed to the interfibril branching differences observed between these precursors previously. For example, Kreger et al. [120] observed slight decrease in fibril density of atelocollagen based PureCol matrices at 0.5 and 2 mg/ml concentrations, and Whittington et al. observed increased interfibril branches in oligomer when compared to telocollagen (also called monomer) at 1.5 mg/ml collagen concentration [115]. When effect of this changing microstructure between oligomer, telocollagen and atelocollagen was studied on molecular release kinetics, oligomer matrices were found to provide the slowest release kinetics in contrast to the fastest release kinetics provided by atelocollagen matrices, under both absence and presence of collagenase conditions (Figure 10B and C respectively). These differences in molecular release can be attributed to the differences in proteolytic degradation (Table 4) as well as differences in ultrastructure between oligomer and atelocollagen fibril matrices. Telocollagen showed release characteristics slightly faster than oligomer, but they were not statistically significant. As a result, oligomer and atelocollagen precursors displaying slowest and fastest release kinetics were identified as viable candidates for further tuning of molecular release from collagen.

Upon further mixing of oligomer and atelocollagen in different ratios, both matrix microstructure and molecular release were found to be affected (Figure 12). Increases in oligomer percentage was correlated with improved fibril thickness and fibril inter-

connectedness (Figure 12A). Furthermore, increase in oligomer percentage within the mixed matrices led to an increase in matrix stiffness, an increase in polymerization rate, and a decrease in polymerization half time (Figure 11) that is in agreement with previous reports that studied effect of increasing oligomer content in mixed matrices consisting of oligomer and telocollagen [123]. These effects can be attributed to an increase in interfibril branching [179].

Molecular release was also modulated through the mixing of oligomer and atelocollagen in different ratios (Figure 12 B and C). In absence of collagenase, variations in release profiles for both small and large FITC-dextran were obtained - ranging from burst to sustained - by increasing the oligomer percentage within mixed matrices (Figure 12B). This tunability, especially for small molecule 10 kDa, cannot be achieved with the use of conventional collagen formulations in the absence of secondary retention mechanisms [72],[103, 193]. The presence of collagenase further exaggerated this tunability, especially for large molecules (2000 kDa FITC-dextran). This was most likely due to the differences in proteolytic degradation of oligomer and atelocollagenic matrices that contributed to existing differences in diffusional release. In general, molecular release of 2000 kDa FITC-dextran was slower than that of 10 kDa FITC-dextran, which is in agreement with previous reports documenting increased diffusional hindrance for large molecules when compared to small sized molecule [193, 261]. Collectively, these results demonstrate effectiveness of mixing oligomer and atelocollagen precursors in tuning molecular release as well as matrix degradation.

2.4.4 Tunability via densification of oligomer fibril matrices

Increasing fibril density or collagen concentration is another way to controls molecular release as this approach decreases matrix porosity [4, 5]. This strategy has been previously applied to control release of a number of molecules from collagen-based materials. For example, by varying collagen content from 1.5% to 2.0% and 2.5 %, FITC-coupled pexiganan release from collagen was extended from 24 h to 48 h and 72 h respectively [262]. Lauzon et al. observed that modulating the concentration of collagen hydrogels from 1.5 to 4.5 mg/ml affected pBMP-9 interaction with collagen and its molecular release [263]. Fujioka et al. [73, 264, 265]observed sustained release of various

proteins by increasing collagen density using methods such as ethanol immersion and air drying. While these methods were successful in tuning molecular release, an associated concern is decrease in the porosity to an extent that cell migration and proliferation can be hampered [4].   Therefore, it is important to maintain a balance between matrix porosity and collagen concentration.

Another problem associated with densifying collagen matrices is the viscosity of collagen. Practically, due to the high viscosity, formulating collagen solutions at concentrations above 10% has been very difficult [70, 73, 174]. Therefore, alternative methods such as reverse dialysis[266], continuous injection and evaporation [267] and centrifugation followed by polymerization [268] have been attempted to increase the density of collagen. Unfortunately, these methods can require weeks to months to prepare and can result in matrices with varying microstructures[116], and limited cell migration or infiltration into the densified material [269, 270].

To overcome these limitations, and to better approximate the structural hierarchy and mechanical properties of mature tissues, Blum et al. recently used the method of confined compression on oligomeric collagen matrices to yield high fibril density matrices with high cell viability [116]. Due to the success of this technique in maintaining collagen microstructure and physiological relevance (D banding pattern) even at high fibril density, we decided to apply it for molecular release. As such, high density oligomer fibril matrices (20 and 40 mg/ml) containing either 10 or 2000 kDa FITC-dextran were formulated from low fibril density matrices (3 mg/ml) through irreversible removal of the interstitial fluid component in a confined format.

The resultant matrices showed an increase in fibril density (Figure 13A) and mechanical integrity, in agreement with previous reports, where increasing collagen concentration has been correlated with increase in fibril density and a concomitant increase in matrix stiffness [14, 116, 120, 271, 272]. Oligomers, as distinct collagen building blocks form more elastic and stiffer fibrillar and suprafibrillar assemblies by fostering formation of interfibril branches [116] [14] compared to conventional collagens. Since these factors are known to affect molecular transport from collagen, we hypothesized that molecular release can be affected through the use of densified oligomer matrices.

Indeed the densification of matrices from 3 mg/ml to 20 mg/ml and 40 mg/ml significantly extended molecular release profiles and increased retention of both 10 kDa and 2000 kDa FITC-dextrans (Figure 13B & C). In absence of collagenase, release through both low and high fibril density matrices was found to be diffusion-based, as indicated by Weibull-fit based parameters. When matrix density was increased from 3 mg/ml to 20 mg/ml, both 10 kDa and 2000 kDa FITC-dextran release was significantly prolonged. However, upon increase of fibril density from 20 to 40 mg/ml, only 2000 kDa FITC-dextran release was further extended, thus elucidating that both fibril density and molecular size influenced release kinetics.

Further exposure of the collagen matrices to 10 U/ml collagenase amplified the molecular release differences between low and high fibril density matrices. This exaggeration in molecular release differences can be a result of differences in proteolytic degradation of matrices. Such differences in the proteolytic degradation of low and high fibril density oligomer matrices were previously observed by Blum et al. [116]. In line with these results, slowest degradation based molecular release was observed from 40 mg/ml matrices, followed by that through 20 mg/ml and 3 mg/ml matrices. Thus, as fibril density of matrices was decreased, the degradation based molecular release was enhanced. Collectively, these results show that by varying the fibril density of oligomer matrices, we could provide a broad range of tunability for both small and large sized molecular release, both in the absence and presence of collagenase.

2.4.5   Tuning proteolytic degradation based molecular release

Conventional collagen implants with minimal or no crosslinking degrade so quickly that the scaffolds disappear before the host tissue can deposit its own ECM [273]. Therefore, there is a need to control degradation of implants [274] as well as their degradation-based molecular release kinetics. However, collagenase levels vary in normal versus pathophysiological states and also at various locations *in vivo* [187, 188]. Moreover, the level of collagenase varies according to age of the wound [189]. Therefore, it is important for collagen-based implants to be tunable in terms of their molecular release under varying collagenase levels[190] [191].

While many studies have documented controlled degradation of collagen-based materials [275, 276] and drug delivery devices [277-279], these were conducted at only one level of collagenase. Literature about collagen-based drug delivery devices providing controlled degradation at varying collagenase levels [187, 277] is sparse. Moreover, data for enzymatic activity is limited. Therefore, to choose appropriate levels of collagenase in demonstrating tunable proteolytic degradation based molecular release, we reviewed literature describing *in-vivo* concentrations of collagenase [184] [192] [187] and selected collagenase levels of 100 U/ml and 10 U/ml as representative values of matrix metalloproteinase equivalents present in chronic and acute wounds. The collagenase at the levels of 100 U/ml and 10 U/ml was then used to compare molecular release in their presence to that in absence of collagenase (Figure 14). From Figure 14A and C, it can be observed that the low collagenase level and higher fibril density provided maximum molecular retention. This can be attributed to a proportionate decrease in enzymatic breakdown of collagen with decreasing collagenase concentration [192] and enhanced resistance to proteolytic degradation with increased fibril density [116]. Furthermore, the interaction plot Figure 14B showed that collagenase level, fibril density as well as the interaction of collagenase and fibril density with each other had a significant effect on molecular release. To find out which of the two factors- collagenase level or fibril density had a more dominant effect on tuning molecular release, we plotted a contour graph (Figure 14C) where the changing gradient of contour colors from light grey to dark grey indicated increasing $T_{50}\%$ values. The color change was fastest on x axis (fibril density) than on y axis (collagenase level), indicating the dominant role of fibril density parameter in affecting $T_{50}\%$ values, compared to role of collagenase level. Amongst all fibril density matrices, 40 mg/ml matrices exhibited the greatest resistance to collagenase and therefore displayed the most extended release (Figure 15).

Weibull function-based modeling showed the effect of fibril density and collagenase level on the release mechanisms. Interestingly, 40 mg/ml matrices showed different release mechanisms at each collagenase level (Figure 14A), i.e. diffusion with 0 U/ml collagenase, diffusion+degradation in presence of 10 U/ml, and first order release in presence of 100 U/ml. These results offer key information about the behavior of different matrix fibril densities in response to different proteolytic levels, conveying the potential

of oligomeric collagen in providing proteolytic resistance and control over diffusional release, even in the presence of high levels of collagenase.

2.5   Conclusion

There is a significant challenge in the design and manufacture of multifunctional biograft materials from conventional collagen due to their poor mechanical properties, rapid proteolytic degradation, and cursory control over physical properties and molecular release profiles.

This work attempts to address these limitations by the application of novel self-assembling collagen-fibril biograft materials. More specifically, collagen polymers specified by their intermolecular crosslink composition and self-assembly capacity were used to customize and design materials in terms of 1) collagen fibril microstructure and mechanical properties, and 2) proteolytic degradability, collectively defining overall local molecular release profiles. Results showed that by altering collagen fibril-level features that dictate matrix-level microstructure and degradation properties, collagen-based platforms were successfully formed for tunable delivery of both small and large sized molecules.

With its uniform, highly branched and porous microstructure, coupled with its high mechanical integrity and high tunability, we believe the self-assembling collagen-based matrices have a clear advantage over conventional collagens, increasing their potential to transition into clinically successful drug delivery products.

CHAPTER 3.   APPLICATION OF COLLAGEN FIBRIL BIOGRAFTS FOR ENHANCING LOCAL VASCULARIZATION IN AN *IN-VIVO* CHICK CHORIOALLONTOIC MEMBRANE (CAM) MODEL

3.1   Introduction

As a result of their difficult-to-heal nature, complex and chronic wounds, such as skin ulcers, are increasingly impacting the health and life-style of our society and remain a major clinical challenge. At present, 6.5 million people are affected by chronic wounds in the United Stated alone [17] with an estimated 25 billion dollars spent annually to treat these patients. This societal and economic burden continues to escalate largely owing to increasing health care costs, an aging population, and a higher incidence of diabetes and obesity [19].

Chronic wounds fail to heal because of an imbalance between extracellular matrix (ECM) deposition and degradation, impaired cell recruitment, and lack of essential neovascularization [28]. Normal healing of acute wounds represents a multi-step process beginning with hemostasis and inflammation during the acute stages of healing, followed by phases of robust cellular proliferation, ECM deposition, matrix remodeling, and ultimately scar formation [17, 24]. However, in chronic wounds, the dynamic spatio-temporal interaction between endothelial cells, angiogenesis factors, and surrounding ECM proteins is impaired [280], causing the wound to be in a permanent inflammatory state [16] and display increased proteolytic activity contributed by excessive production of matrix metalloproteinases (MMPs) [25, 26]. MMPs in turn break down components of the ECM and inhibit growth factors that are essential for tissue synthesis and regeneration [27]. Therefore, promoting recreation of the natural type I collagen fibril scaffold while fostering rapid and functional neovascularization and tissue regeneration at wound site, is pivotal to restoration of healing of chronic wounds.

As such, many efforts have been lately focused on the design and development of collagen based biomaterials that can provide the structural and mechanical support for the cellular infiltration and growth, while promoting the neovascularization at the wound site. A number of advanced wound dressings, and skin substitutes have been introduced in the

wound care market during the last decades [32, 34-39, 281]. However, no general satisfactory clinical solution has been achieved to date [32, 282] because of undesirable outcomes of these products, including inflammation mediated healing leading to scar formation rather than tissue regeneration, slow neovascularization and cellularization and a need for multiple applications that adds to patient discomfort, pain and healthcare cost. Therefore, there is an acute need to overcome these problems through improved design of multifunctional collagen biografts.

An alternative of combining growth factors into collagen could potentially address the issue of slow vascularization and tissue regeneration through collagen based products, [59-61], since growth factors play important regulatory role in tissue repair and regeneration in wounds (e.g. granulocyte-macrophage colony stimulating factor (GM-CSF), platelet derived growth factor (PDGF), vascular endothelial growth factor (VEGF), and basic fibroblast growth factor (bFGF)) [283]. Among the various growth factors, VEGF is one of the most potent proangiogenic growth factors that significantly impacts wound vascularization [284]. VEGF is a 45 kDa heterodimeric heparin-binding protein, acting as a potent mitogen (ED~50: 2-10 PM) for micro and macrovascular endothelial cells derived from arteries, veins and lymphatics, inducing their proliferation, migration and tube formation [285]. VEGF level rises in normal wound repair, leading to a vigorous angiogenic response, however, in chronic, nonhealing wounds, active VEGF falls to abnormally low level, due to possible degradation of VEGF by the excessively high protease activity in chronic wounds [286]. Poor vascularization which is a hallmark on chronic wounds such as diabetic foot ulcers, can therefore benefit by the use of VEGF delivery [287].

Lately, the important role of ECM in coordinating VEGF signaling in wounds *in-vivo* has come to light [61, 92]. ECM localizes VEGF via heparin and heparan sulphate proteoglycan (HSPG) molecules [282, 288]. Heparin or HSPGs have highly negative charge (approximately 75) due to the prevalence of sulfate and carboxylate groups, that endows heparin with an ability to electrostatically bind to many basic biomolecules, including proteins, growth factors, proteases and chemokines [289]. The binding of VEGF to heparin occurs through such electrostatic interaction (affinity binding) [290]. Heparin then facilitates binding of VEGF to its two receptors Flt-1/VEGFR1 and Flk-

1/VEGFR2 through binding and stable complex formation with neuropilin (NRP)-1 coreceptor, resulting in phosphorylation and further signaling activity of VEGF [291], such as providing essential stimulatory cues to initiate vascular branching [292] as well as endothelial tip cell filopodia emission [293]. Heparin binding thus regulates the physiological effect of VEGF on endothelial cells [294-296]. Heparin plays another important role of enabling the ECM to act storage depot of growth factors. Because of affinity of heparin for type I collagen in ECM, heparin retains VEGF in ECM, protects it from proteolytic degradation [297-300], and allows prolonged presentation of VEGF to cells [301, 302].

Inspired by this role of ECM, heparin and VEGF in providing coordinated biochemical and biomechanical cues for in vivo vascularization, and due to well documented affinity of heparin for VEGF and ECM [303-306], many systems have incorporated heparin based interactions in collagen for loading of VEGF [64, 98, 307-311] previously. However, these systems consisted of monomeric collagen formulations that were chemically crosslinked for retention of heparin. As a result of chemical crosslinking, VEGF had to be loaded in the last step of formulation, so that chemicals used for croslsinking would not destroy the bioactivity of VEGF. VEGF was then loaded typically either through immersion of the formulated matrices into VEGF solution or through impregnation of VEGF in the matrices, both of which can lead to low VEGF loading efficiency. Furthermore, VEGF used in these formulations is VEGF 165 that binds to heparin through positively charged lysine and arginine residues encoded by exon 7 of VEGF gene [312]. However, it is also known that VEGF 189 isoform contains in addition to the amino acids encoded by exon 7, 24 amino-acids that are derived from exon 6, constituting yet another heparin binding domain [313]. As a result, VEGF 189 shows stronger affinity for heparin due to presence of two heparin binding domains [314, 315] and these binding sites are reported to be distinct from VEGF's receptor-binding domain [316].

Considering the stronger affinity of VEGF189 for heparin, and binding affinity of heparin for type I collagen self-assembling molecules, we decided to engineer a unique self-assembling collagen based biograft system that can act as a storage depot for VEGF189 and promote vascularization of the implant in an accelerated manner (Figure

16).   A key element of our design approach is the application of type I collagen oligomers, which represent a soluble collagen formulation capable of self-assembling into collagen-fibril matrices with higher-order interfibril associations. As such, the supramolecular assembly of oligomers supports the creation of collagen–fibril matrices with a broad range of structural and mechanical properties (specified by fibril density and matrix stiffness) beyond those that can be achieved with conventional collagen monomers, such as atelocollagen, and telocollagen [14, 120, 121]. Heparin was added to oligomer molecules in selective quantities that did not alter the oligomer molecule self-assembly and viscoelastic properties and VEGF189 was added in quantity lower than heparin. Through single step admixing, the collagen containing heparin and VEGF 189 was self-assembled. This process relied on simple affinity based retention of heparin and VEGF in the polymerized collagen system, without the use of any exogenous chemical crosslinking, which is in stark contrast to current approaches that rely on chemical crosslinking based immobilization of heparin or VEGF in the collagen scaffolds [64, 98, 251, 310, 317, 318].

 Thus, the design of collagen implants in our study differs from previous systems in the following aspects: 1) Application of oligomeric collagen as opposed to monomeric collagen formulations; 2) Use of lower quantities of heparin that do not alter collagen polymerization properties; 3) Use of VEGF189 instead of VEGF165 due to its stronger heparin binding affinity; and 4) pure affinity-based retention of heparin in collagen as opposed to chemical immobilization.

We hypothesized in this study, that through affinity based binding of heparin and VEGF in self-assembling oligomer implants, the vascularization as well as cellularization potential of collagen scaffolds can be improved for tissue engineering and tissue regeneration applications. To test this hypothesis, we designed low and high fibril density oligomer implants with and without heparin and VEGF molecules, and evaluated their functionality in enhancing local vascularization using an established in-vivo chorioallantoic membrane (CAM) model.
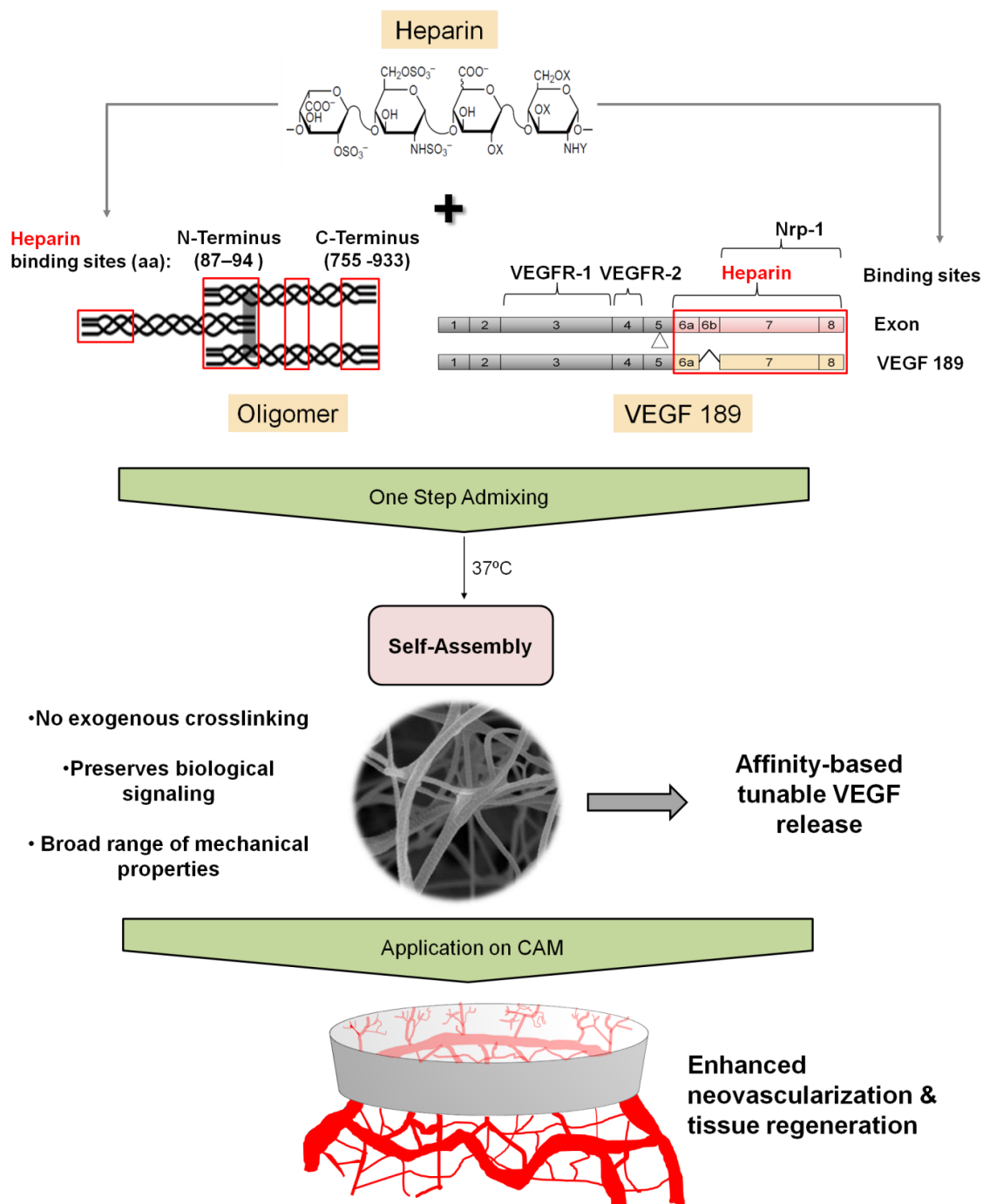
Figure 16: Graphical representation of design strategy used in this study. Affinity of heparin for collagen and VEGF189 was exploited to retain VEGF in self-assembled oligomer matrices. Chicken egg chorioallantoic membrane (CAM) assay was used to test the functionality of implants.

3.2   Methods

3.2.1   Preparation of soluble collagen formulations

Oligomeric self-assembling type I collagen was derived from market weight pig dermis, as described previously [120]. Extracted collagen was lyophilized for storage and dissolved in 0.01 N hydrochloric acid (HCl) for use. Oligomer collagen solution was rendered aseptic by exposure to chloroform overnight at 4°C and was standardized based upon purity as well as polymerization potential, as described in ASTM 3089-14 [163]. Here, polymerization potential is defined as the relationship between the shear storage modulus (G') of the polymerized matrices and the collagen content of the polymerization reaction [14, 120]. The oligomer collagen solution was diluted with 0.01 N HCl to achieve desired concentrations and neutralized with 10X phosphate buffered saline (PBS) and 0.1 N sodium hydroxide (NaOH) to achieve pH 7.4 [120]. Neutralized solutions were kept on ice prior to induction of polymerization by warming to 37°C.

3.2.2   Polymerization kinetics and viscoelastic properties of collagen

Oligomer collagen polymerization kinetics and viscoelastic properties were measured in the presence of 0, 0.5, 1, 5, 10 or 100 µg/ml heparin sodium salt (H3149, Sigma Aldrich, St. Louis, MO, USA), using an AR2000 rheometer (TA Instruments, New Castle, DE) equipped with stainless-steel 40 mm-diameter parallel plate geometry [14, 120]. Oligomer solutions (3 mg/ml) with or without heparin were neutralized and pipetted onto the Peltier plate. Upon lowering the geometry, the Peltier plate temperature was maintained at 4° C for 5 minutes and then increased to 37° C for 15 minutes to induce oligomer polymerization. Time-dependent changes in shear storage modulus (G') were measured at 1% controlled oscillatory strain. Each matrix formulation was tested five times (N=5).

3.2.3   Formation of heparinized oligomer implants with and without VEGF

3.2.3.1   Low fibril-density implants

In total, 4 implant groups were prepared with 3 mg/ml oligomer collagen, namely i) Coll (Oligomer collagen alone); ii) Coll + VEGF (Oligomer collagen + 0.5 µg/ml VEGF189); iii) Coll + Hep (Oligomer collagen + 1 µg/ml Heparin); iv) Coll + Hep +

VEGF (Oligomer collagen + 1 μg/ml Heparin + 0.5 μg/ml VEGF189). Heparin and/or recombinant human VEGF 189 (Abcam, Cambridge, MA) were solubilized in 10X PBS in desired quantities and admixed with oligomer. Solutions were then pipetted into 48-well tissue culture plates (Corning, Corning, NY) at 0.25 ml per well, followed by induction of polymerization by warming at 37°C overnight. In some instances, implants were washed in sterile 1X PBS by gentle rotation on microplate shaker (ThermoFisher Scientific, Waltham, MA) for 24 hrs. All references of admixing VEGF 189 in this work are henceforward referred to as simply "VEGF" addition.

3.2.3.2 High fibril-density implants

High-density oligomer implants were created using confined compression as described previously [116]. Briefly, neutralized oligomer of concentration 4.56 mg/ml (with or without 1 μg/ml heparin and 0.5 μg/ml VEGF) was prepared on ice, and pipetted into 48-well tissue culture plate at 1.1 ml per well. The plate was incubated overnight at 37°C to induce polymerization of oligomer. Polymerized matrices were then densified 4.4 X, using a porous polyethylene platen (50 μm pore size) at 6 mm/min to final thickness of 0.26 cm, yielding 0.25 cm^3 densified collagen implants at 20 mg/ml concentration. Based on the addition of heparin and VEGF, the resultant 20 mg/ml, high-density implants were classified into 4 groups, similar to those in low-density implants. Washing of select implants was conducted as described for low-density implants.

3.2.4 Characterization

3.2.4.1 Assessing spatial distribution and retention of heparin in oligomer

To visualize heparin localization within matrices, fluorescein conjugated heparin (FITC-heparin, H7482, Fisher Scientific, Carlsbad, CA) was dissolved in 10X PBS and used to neutralize 3 mg/ml oligomer collagen. FITC-heparin containing oligomer solutions were then pipetted on Lab-Tek chambered cover glass slides (Nunc, Thermo Fisher Scientific, Rochester, NY) and polymerized overnight in a 37°C incubator. Samples were washed for 24 h with 1X PBS and compared with unwashed samples for FITC-heparin retention. Confocal microscopy was performed on implants using an Olympus Fluoview FV1000 confocal system adapted to an Olympus IX81 inverted

microscope (Olympus, Tokyo, Japan). Image Z-stacks (10 μm depth; 0.5 μm step size) from at least three random locations within each matrix were taken with a 60X water immersion objective at 4X digital zoom using 488 nm excitation and 510-530 emission.

3.2.4.2 Quantifying heparin retention in collagen

The amount of heparin in collagen implants was quantified using the 1,9-dimethylmethylene blue (DMMB) assay [319] adapted for microplate reading [320]. Heparinized oligomer constructs were prepared as described above. All 3 mg/ml washed and unwashed collagen implants were digested with an equal volume (250 μL) of a digestion buffer consisting of 1 mg/ml papain, 6.9 μg/ml of sodium phosphate monobasic, 0.326 μg/ml of N-acetyl cysteine, and 0.76 μg/ml of EDTA tetrasodium salt (Sigma-Aldrich, St. Louis, MO) dissolved in H_2O. Digestion was performed at 65°C for 24 hrs. DMMB dye was added to papain-digested samples and absorbance measured at 525nm and 595nm wavelengths using a spectrophotometer (Molecular Devices Spectramax M5, Sunnyvale, CA). Sample heparin concentrations were then determined from a standard curve generated with known heparin concentrations [321]. All standard solutions and samples were prepared in triplicate and assayed three times (N=3, n=3).

3.2.5 Chicken chorioallantoic membrane (CAM) vascularization assay

The CAM assay was performed as described elsewhere [322, 323]. Briefly, fertilized White Leghorn chicken eggs (Poultry Unit, Purdue University Animal Science Research Center) were horizontally positioned and incubated at 38 °C under 58% $\pm$ 2% relative humidity in an egg incubator equipped with a turner which automatically rotated the eggs 5 times/day until day 7 [324]. On day 8, a window of approximately 2.5 cm diameter was created using a Dremel tool (Dremel, Racine, WI) equipped with a cutting disc. The window was sealed with adhesive tape and eggs were returned to the incubator. On day 9, collagen implants were inserted on the CAM of viable eggs. The implant groups consisted of i) CAM alone; ii) CAM with washed 10 mm diameter paper disc (Sigma-Aldrich, St. Louis, MO); iii) Absorbable collagen dressing Helicote (Integra Life Sciences, Plainsbboro, NJ) - referred to in this work as Integra collagen; and iv) 3 mg/ml oligomer. CAM was digitally photographed on day 9 and day 12 after completion of the

assay. In another set of experiment, washed low density (3 mg/ml) and high density (20 mg/ml) implants (Coll; Coll + VEGF; Coll + Hep; and Coll + Hep + VEGF) were inserted on CAM to determine effect of heparin and VEGF189 infused oligomer implants on vascularization. Post 3 days of implantation, on embryonic day 12, all CAM samples were photographed and fixed in situ using 4% paraformaldehyde as per to protocol [325]. Each experimental group was assigned at least 6 viable eggs (N=6-8). The timeline of CAM assay is shown in Figure 17.
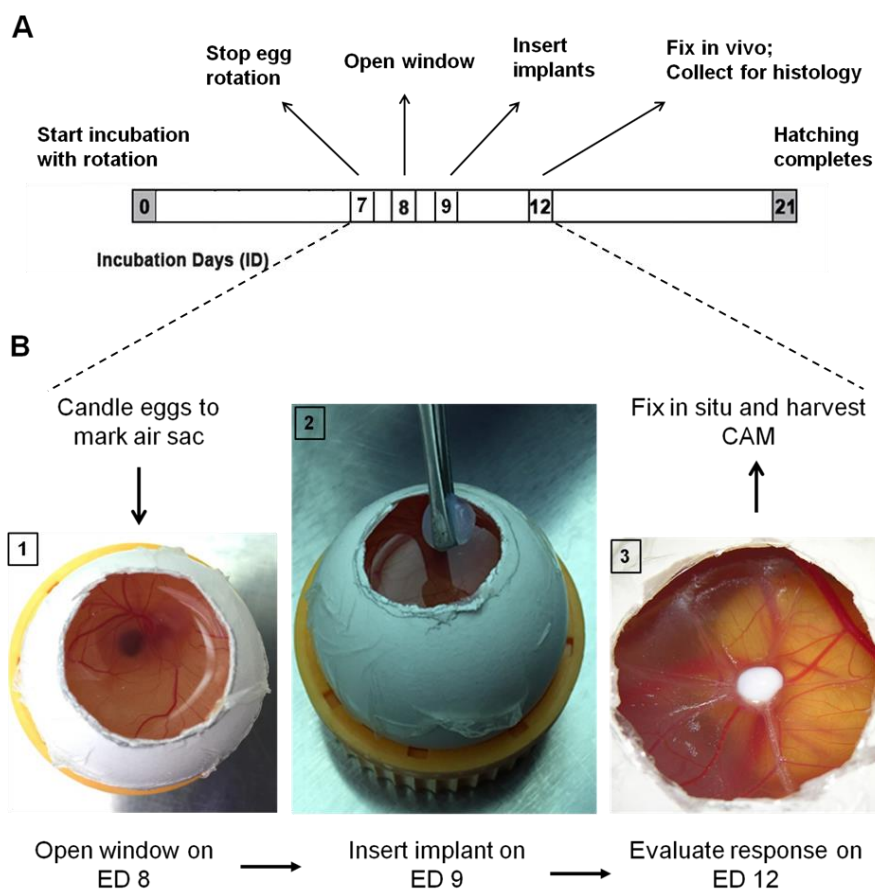
Figure 17: The schematics of CAM assay timeline (A). The pictorial visualization of assay steps between embryonic day (ED) 9 and 12 is shown in part B. Image 1 in part B shows a window cut open in egg on ED8, image 2 shows implantation of 3 mg/ml oligomer implant on ED9, and image 3 shows the status of implant on ED12.

3.2.6 Scoring vascular response and contraction of implants used in CAM assay

The vascularization response was determined using two scoring schemes to compare photographs from day 12 to those from day 9. A "vascular score" was determined by

scoring the vessel density and distribution (5 = strong, 1 = weak) around the collagen implants on CAM [326], by observing top view as shown in Figure 18. Similarly, vessel tortuosity and abnormality in CAM was scored on a scale of 1 to 5 (5= irregular/tortuous/brush like, 1 = normal), based on observation of irregular vessels or fine brush-like vessels on CAM. Percent contraction of implant area (mm^2) was also quantified based on the differences between implant area observed on day of insertion (day 9) and day of CAM harvest (day 12 or 18).

A   **Score from top view**

Evaluate Histology

B

1   2   3

4   5   **Vascular score**
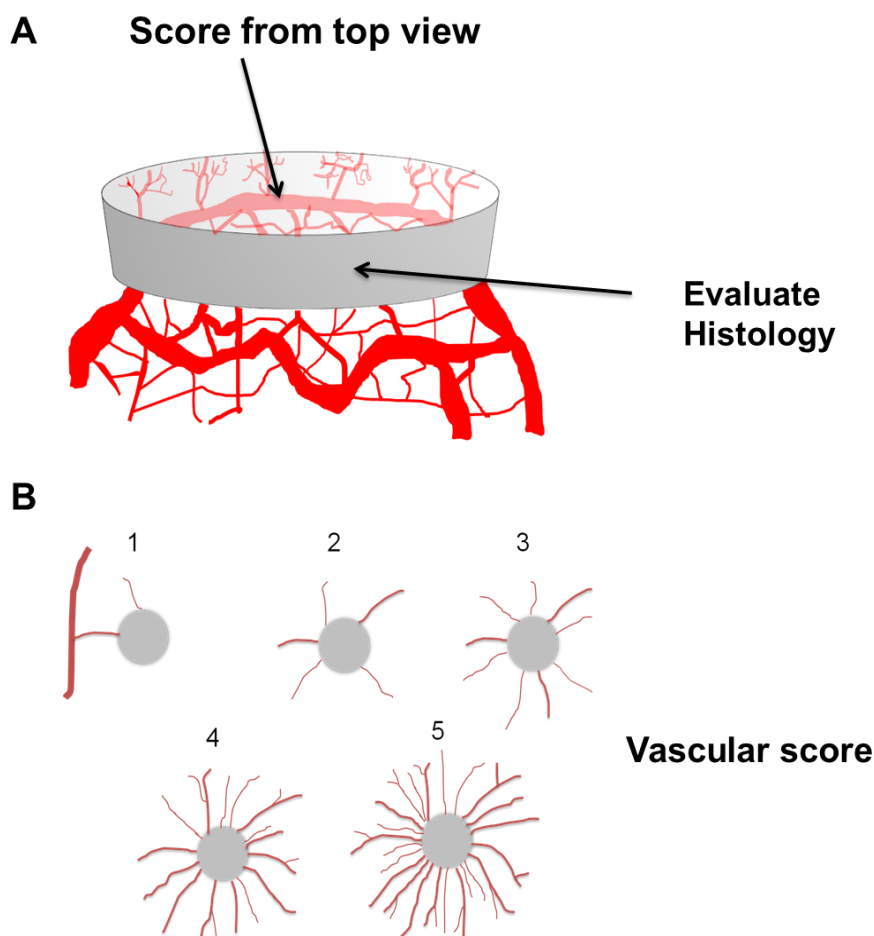
Figure 18: Implant evaluation for vascular response. (A) Implants were evaluated for their vascularization ability by scoring CAM vessel response from top view, before performing histological staining. (B) Drawings representing examples of different vascular responses in CAM assay. A ranking method from 1-5 was used for semi-quantitative scoring of vessel density and distribution of CAM around the implanted inserts.

3.2.7 Histology

The fixed, excised CAM tissue samples were analyzed with the help of Purdue Histology Research Lab. Samples were routinely processed, sectioned and stained for Hematoxylin and Eosin. All samples were sectioned at 5um thickness using a rotary microtome. Slides were imaged with a Nikon Eclipse E200 optical microscope using 40, and 4X objective to visualize CAM cells and capillaries invading the implants.

3.2.8 Statistical Analysis

The differences between all experimental groups were determined using ANOVA followed by a post-hoc Tukey test with a 95% confidence interval, except for identifying difference between heparin content in washed versus unwashed matrices. For that purpose, a two-sample Student's T-Test with a confidence interval of 95% was used. For all tests, $p < 0.05$ was considered significant. All the groups were analyzed using Minitab 16.0 statistical software (Minitab Inc., State College, PA).

3.3 Results

3.3.1 Upto 1 μg/ml heparin does not affect oligomer polymerization kinetics and viscoelastic properties

Previous studies have shown that heparin affects self-assembly or polymerization of conventional monomer formulations (telocollagen and atelocollagen), altering matrix consistency and viscoelastic properties [327]. Here we determined the effect of heparin on oligomer collagen polymerization and viscoelastic properties and defined heparin levels that do not alter matrix physico-mechanical properties. Based on the oscillatory shear based tracking of rate of change of the storage modulus (G') of oligomer containing different amounts of heparin (Figure 19A), we found that the polymerization kinetics of 3 mg/ml oligomer was statistically similar for heparin concentrations up to 10 μg/ml (Figure 19B). At 100 μg/ml a significant decrease in polymerization half time was observed (Figure 19B). Evaluation of heparin addition on matrix viscoelastic properties (Figure 19B) showed that addition of 0.5 and 1 μg/ml had no significant effect; however, addition of heparin at 5, 10, and 100 μg/ml resulted in a significant lower G' (p<0.05,

N=5). Collectively, these results confirmed that addition of upto 1 μg/ml heparin does not alter oligomer polymerization and viscoelastic properties.

A)

B)

Heparin (μg/ml)	P_{50}% (min)	G' (Pa)
0	0.59 ± 0.02 [B]	784.40 ± 55.41 [A]
0.5	0.55 ± 0.10 [B]	750.98 ± 56.33 [A]
1	0.56 ± 0.05 [B]	750.50 ± 19.70 [A]
5	0.63 ± 0.03 [B]	594.30 ± 55.76 [B]
10	0.67 ± 0.06 [B]	516.58 ± 38.21 [B]
100	1.15 ± 0.10 [A]	71.28 ± 8.88 [C]
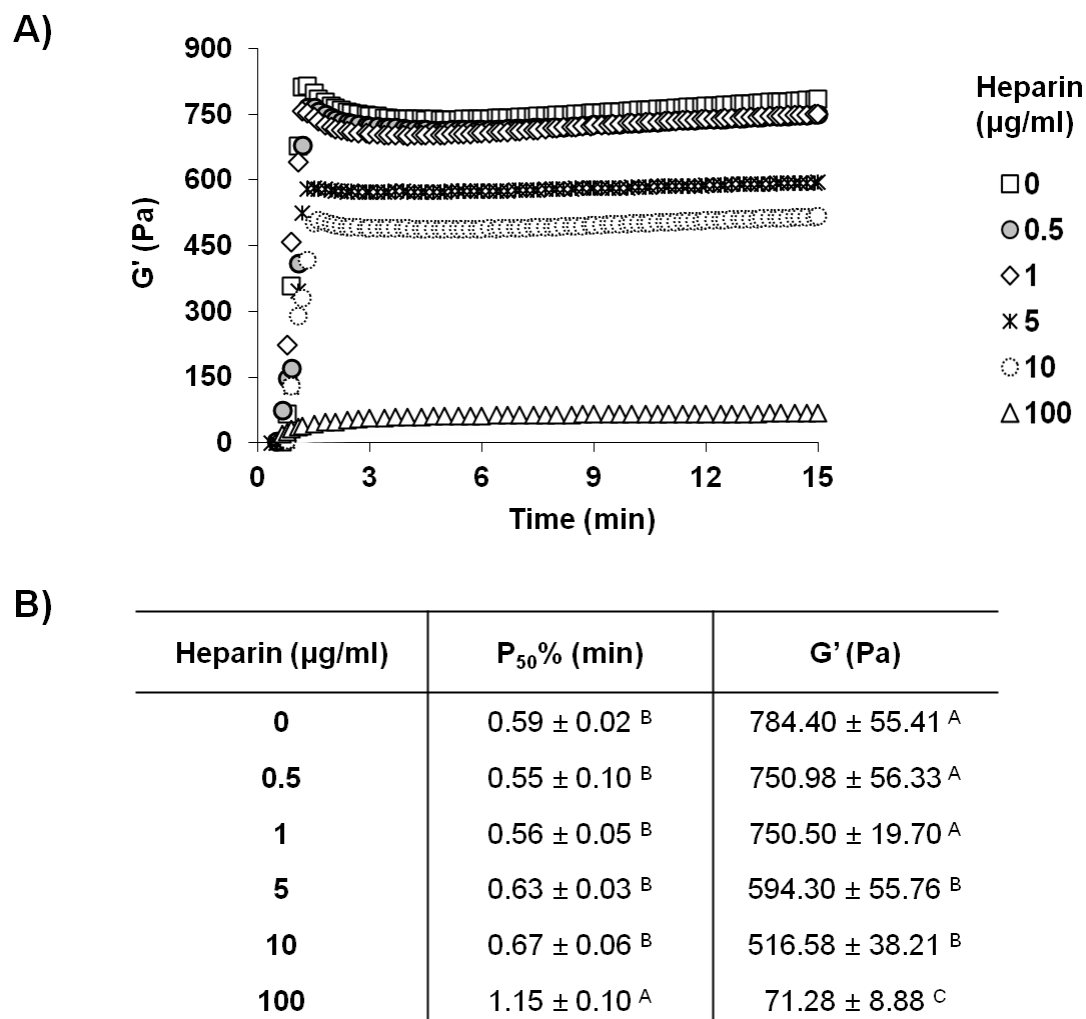
Figure 19: Effect of heparin on oligomer matrix polymerization kinetics and viscoelastic properties. (A) Time-dependent changes in shear-storage modulus of 3 mg/ml oligomer with 0, 0.5, 1, 5, 10 and 100 μg/ml of heparin. At t=0, temperature was raised to 37°C to induce matrix self-assembly. (B) Polymerization half-times represented by P_{50}% (mean±SD), and shear storage modulus (G', Pa) after 15 minutes of polymerization (mean±SD), were quantified from the curves in (A). Each sample was tested five times (N=5). Letters in P_{50}% and G' column in (B) indicate statistically different experimental groups as determined by Tukey-Kramer range test (N=5, p<0.05).

3.3.2 Heparin colocalizes with oligomer fibrils and is retained after washing

Heparin is known to bind to type I collagen monomer formulations with high affinity [328-330] and its effect on collagen fibril size and self-assembly has been studied

extensively in the past [327, 330-333]. Here, heparin localization and retention within self-assembled oligomer matrices was measured using confocal microscopy and established DMMB assay.
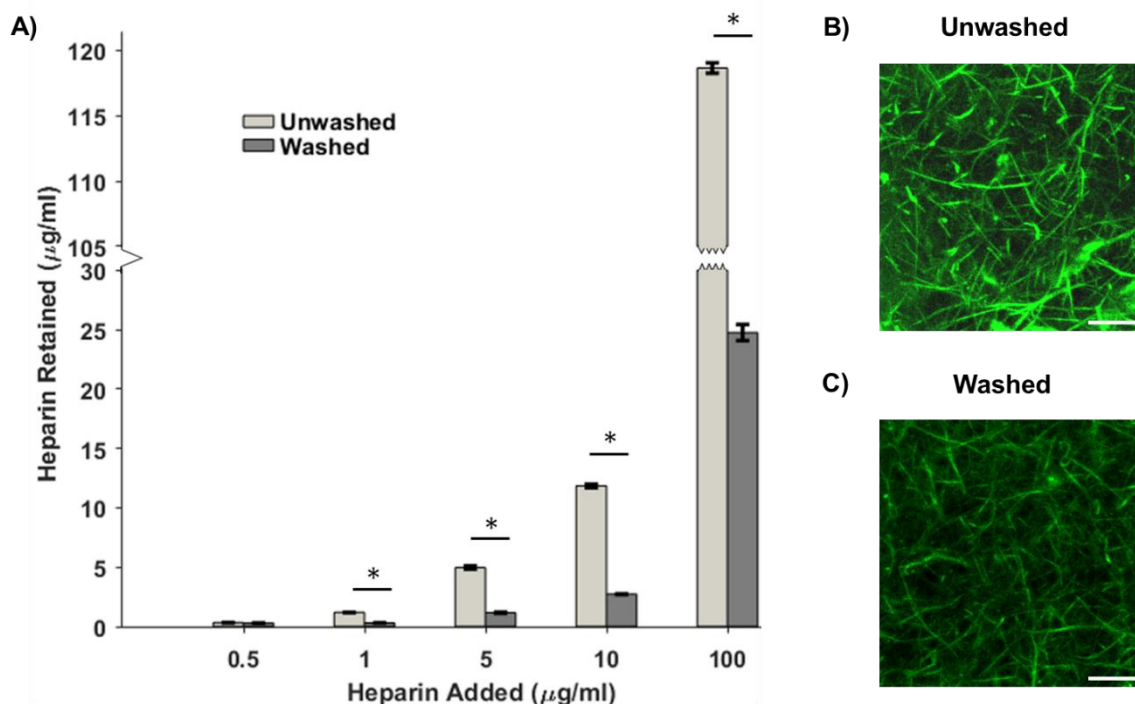
Figure 20: Heparin in oligomer matrix is retained after washing. The amount of heparin retention was confirmed by 1, 9- dimethylmethylene blue (DMMB) assay (A). Asterisk (*) indicates significant difference based on two sample student's T test (N=3, n=3, p<0.05). Fluorescein conjugated heparin (FITC-heparin,) was loaded in oligomer matrices at 100 μg/ml concentration to visualize heparin localization within matrices. Image Z-stacks (10 μm depth; 0.5 μm step size) were taken with a 60X water immersion objective at 4X digital zoom using 488 nm excitation and 510-530 emission. FITC-Heparin was observed to be colocalizing in oligomer fibril matrix (3 mg/ml) (B) and was found to be retained in matrix after 24 h washing (C). Scale bar in (B) and (C) represents 10 μM.

DMMB results indicated that the concentration of heparin detected in unwashed oligomer matrices with 0.5, 1, 5, 10 and 100 μg /ml heparin was 0.33, 1.19, 4.97, 11.84, 117.61 μg /ml respectively, and that in washed matrices was 0.29, 0.31, 1.17, 2.72, 24.74 μg /ml respectively (Figure 20, A). The increased amount of heparin retention with increased heparin addition in oligomer matrices is in agreement with previous studies [327, 332]. It was evident that while the washing step eliminated superficially attached heparin at all concentrations (except for 0.5 μg /ml), at least 21% or higher amount of

heparin was retained in all matrices. The exact percentage of heparin retained in washed oligomer matrices containing 0.5, 1, 5, 10 and 100 µg /ml was 88.75%, 25.75%, 23.60%, 22.96%, and 21.03% respectively.

Corroborating results obtained using confocal imaging suggested that retained heparin was associated and co-localized with formed collagen fibrils. (Figure 20, B and C).

3.3.3 Oligomer implants but not Integra collagen or paper disc exhibit enhanced vascularization response in CAM after 3 days of implantation

To determine the capability of oligomer implants in inducing vascularization *in vivo*, we implanted non-heparinized 3 mg/ml oligomer implants in CAM model between embryonic day 9 and 12 and compared its evoked vascular response on CAM with that of the CAM inserted without any sample, or with samples of paper disc, and commercial Integra collagen sponge.

The visual appearance of these implants in their hydrated state before implanting on CAM is shown in Figure 21. The paper disc, and the 3 mg/ml oligomer implants (Figure 21, A and C respectively) were observed to maintain shape integrity upon hydration, however,   however, the Integra collagen implants (Figure 21B) could be easily deformed into any shape upon hydration.
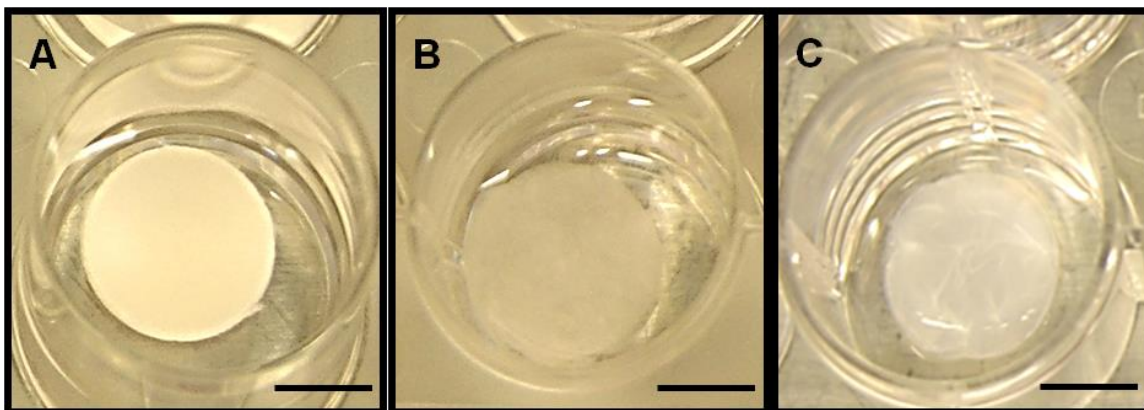
Figure 21: Visual appearance of implants used in testing vascular response in CAM assay. Samples include A) Paper disc B) Integra collagen C) 3 mg/ml (low-density) oligomer. Scale bar represents 5 mm length.

After implantation of oligomer, paper discs and Integra collagen samples for 3 days on CAM, the blood vessel density and distribution of CAM surrounding the implants was

scored using a semi-quantitative ranking system [326], as indicated in Figure 18 B. CAM without any inserted sample served as a control (Figure 22, A). It was observed that compared to the vascular response induced on CAM by the paper disc (Figure 22, B) or the Integra collagen sponge (Figure 22, C), 3 mg/ml oligomer implants showed enhanced vascular response to the implant (Figure 22, D). Among all the implant groups tested, the 3 mg/ml oligomer implants ranked significantly higher in their vascular score ($p < 0.05$, N=6). The Integra collagen showed no significant difference in their vascular score compared to paper disc (Figure 22 E).
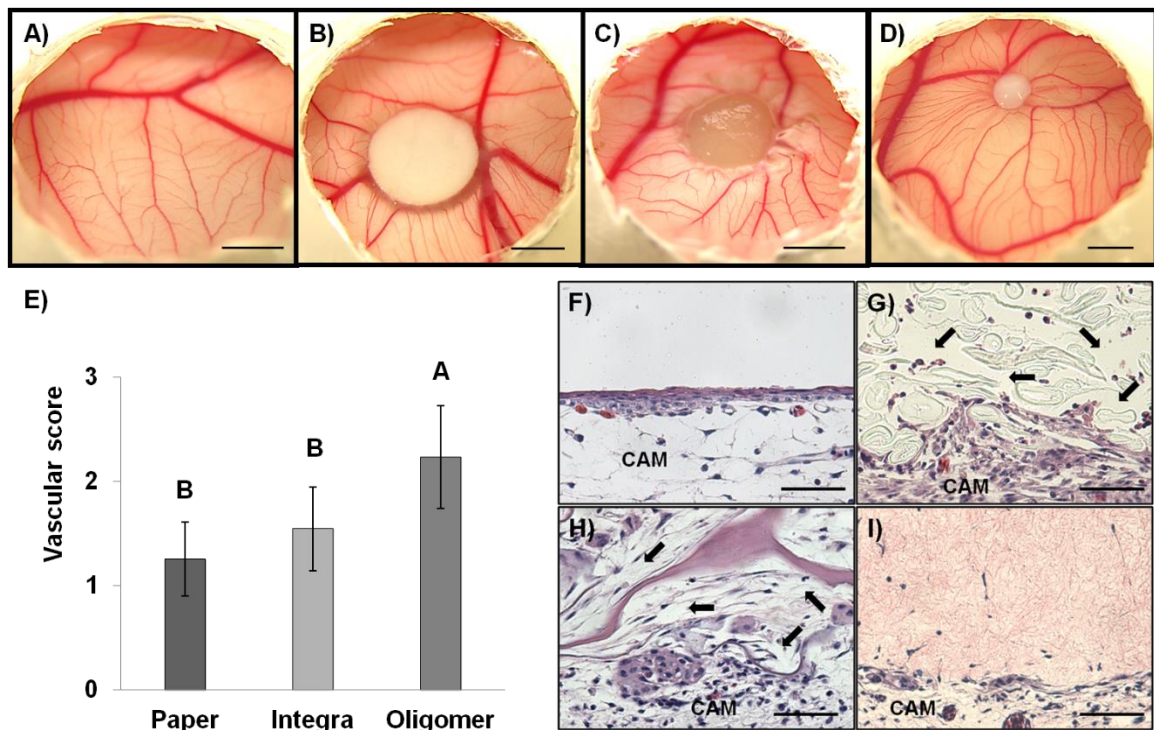
Figure 22: 3 mg/ml oligomer implants promoted enhanced vascular response of the CAM around constructs compared to paper disc and Integra collagen samples. CAM was implanted with various test sample groups represented by (A) No sample, (B) paper disc, and (C) Integra collagen and (D) 3 mg/ml oligomer implant. Images were taken with digital camera and represent top view of implants in situ. Scale bar= 5 mm. (E) Vascular score calculated from top view images. Letters represent statistically different groups determined by Tukey-Kramer range test (N=6-8, $p < 0.05$). H&E staining was performed on transverse histological sections of CAM implanted with F) no sample G) paper disc H) Integra collagen I) 3 mg/ml oligomer. Black arrows in G) and H) indicate empty spaces observed within the samples. Cells from CAM were found to infiltrate the implanted Integra collagen H) and 3 mg/ml oligomer I). Scale bar represents 50 μM.

Interestingly, both Integra collagen and oligomer implants contracted significantly compared to the paper disc samples by day 3 of implantation. We suspected that this contraction in part could have been contributed by cell infiltration as suggested by Kilarski et al. [334]. To determine whether Integra and oligomer collagen samples indeed supported cell infiltration, we performed histology on transverse sections of the CAM implanted with Integra and oligomer collagen samples, after their in situ fixation.

Results of the H&E staining of transverse histological cross-sections of implants on CAM are shown in Figure 22 (F-I). Both the oligomer (Figure 22I) and Integra collagen (Figure 22H) were observed to be infiltrated by cells from the CAM. However, the Integra collagen showed highly porous structure indicated by black arrows in Figure 22H. Paper disc also showed large empty spaces, however CAM cells failed to invade them (Figure 22G). These results also showed that the oligomer matrices were in close contact with the CAM tissue, pointing tissue integrity, as opposed to the non-intact and highly porous paper disc and Integra collagen samples on CAM tissue. Collectively, these results showed that oligomer implants enhanced vascular response of CAM around the constructs while maintaining cell infiltration within the constructs.

3.3.4 CAM vascular response around the implants is affected by contents and density of oligomer fibril implants

After observing that 3 mg/ml oligomer alone induced a vascular response on CAM, we decided to test if the functionality of oligomer implants in inducing vascularization on CAM can be further enhanced through incorporation of heparin and VEGF. Heparin and VEGF incorporation was also performed in high fibril density implants, since high fibril density implants have been shown to add tunability and scalability in design of self-assembled collagen constructs, recapitulating the multi-scale structural and functional properties of soft tissues *in vivo* [116].

Therefore, we prepared 4 groups from both low fibril density and high fibril density matrices for implantation on CAM, namely - i) Coll group, ii) Coll + VEGF group, iii) Coll + Hep group, and iv) Coll + Hep + VEGF group. All groups were washed with 1X PBS for 24 h in order to remove any unbound heparin and VEGF from oligomer matrix. Our hypothesis was that the heparinized oligomer implants would retain VEGF longer

due to affinity of VEGF for heparin, and as a result, induce more robust vascularization *in vivo*.

After 3 days of implantation, results showed that densified 20 mg/ml constructs occupied larger area on CAM (Figure 24 A-D) compared to the low fibril density 3 mg/ml implants (Figure 23A-D), indicating the successful resistance to contraction as quantified in Table 5. Both low and high fibril density oligomer implants containing heparin and VEGF together (Coll + Hep + VEGF group) exhibited a strong vascular response in the form of a spoke wheel pattern (Figure 23 D and Figure 24 D), which can be attributed to the successful retention of VEGF in the implant. Oligomer implants with heparin alone (Coll + Hep group) showed a weaker vascularization response (Figure 23 C and Figure 24 C), with thinner vessels drawn towards the construct. The oligomer alone (Coll group) showed only slight vascular response (Figure 23 A and Figure 24 A), while oligomer with VEGF (Coll + VEGF) showed vascular response which was found to be abnormal due to tortuous, fine-brush like or irregular appearance of the vessels (Figure 23 B and Figure 24 B).

Semi-quantitative scoring of CAM vascular response indicated that heparinized oligomer implants induced higher vascularization than non-heparinized implants, in both the cases of 3 and 20 mg/ml oligomer (Figure 23 E and Figure 24 E). Addition of VEGF to heparinized oligomer implants further enhanced the vascularization capacity in 3 mg/ml implants, but addition of VEGF to non-heparinized implants triggered an abnormal vascular response showing tortuous and/or fine brush-like vessel formation, resulting in high tortuosity score in both low and high fibril density oligomer implants (Figure 23 F and Figure 24 F). This result highlighted the effectiveness of heparin in retaining VEGF within the oligomer implant, leading to enhanced vascular response on CAM, as opposed to tortuous vascular response observed with VEGF loaded implants that did not contain heparin.
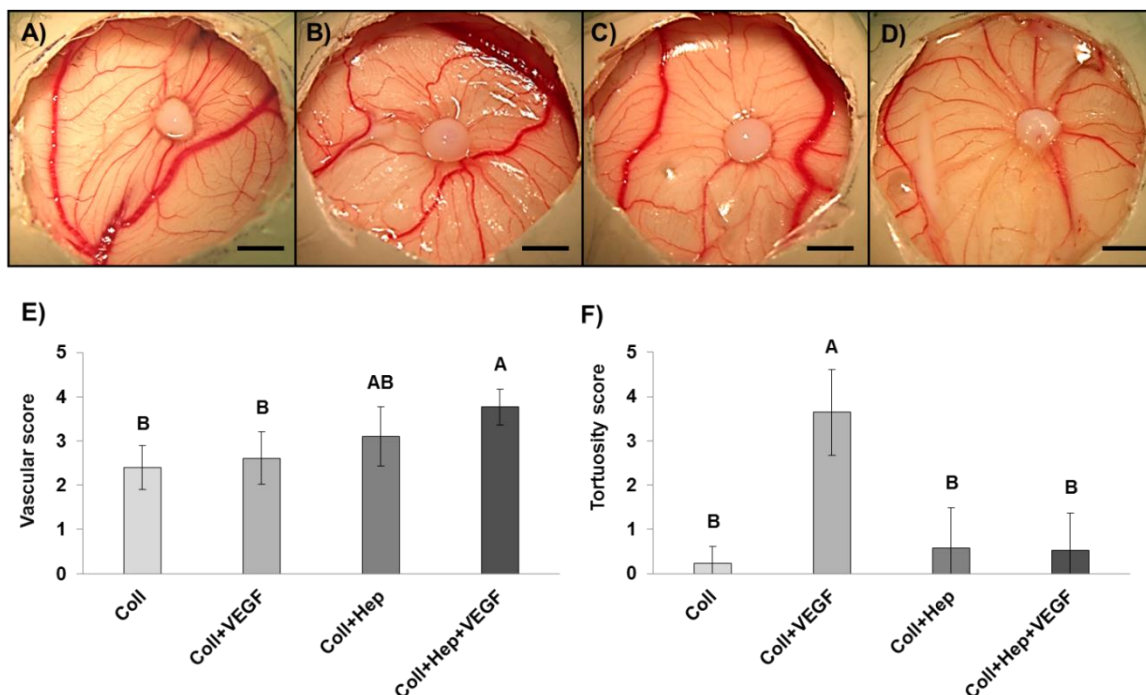
Figure 23: Heparinization improved vascular response of CAM to low fibril-density oligomer implants. (A-D) Top view of implants imaged in situ using digital camera. CAM was implanted with 3 mg/ml collagen consisting of oligomer alone (A), oligomer + 0.5 µg/ml VEGF (B), oligomer + 1 µg/ml heparin (C), and oligomer + 1 µg/ml heparin + 0.5 µg/ml VEGF (D). Tortuous vessels were observed in VEGF loaded implants without heparin (B), while VEGF-loaded implants with heparin showed a clear spoke-wheel pattern of vascular response (D). Vascular score (E) and tortuosity score (F) calculated from top view of implants. Scale bar represents 5 mm. Letters represent statistically different groups determined by Tukey-Kramer range test (N=6-8, $p<0.05$).
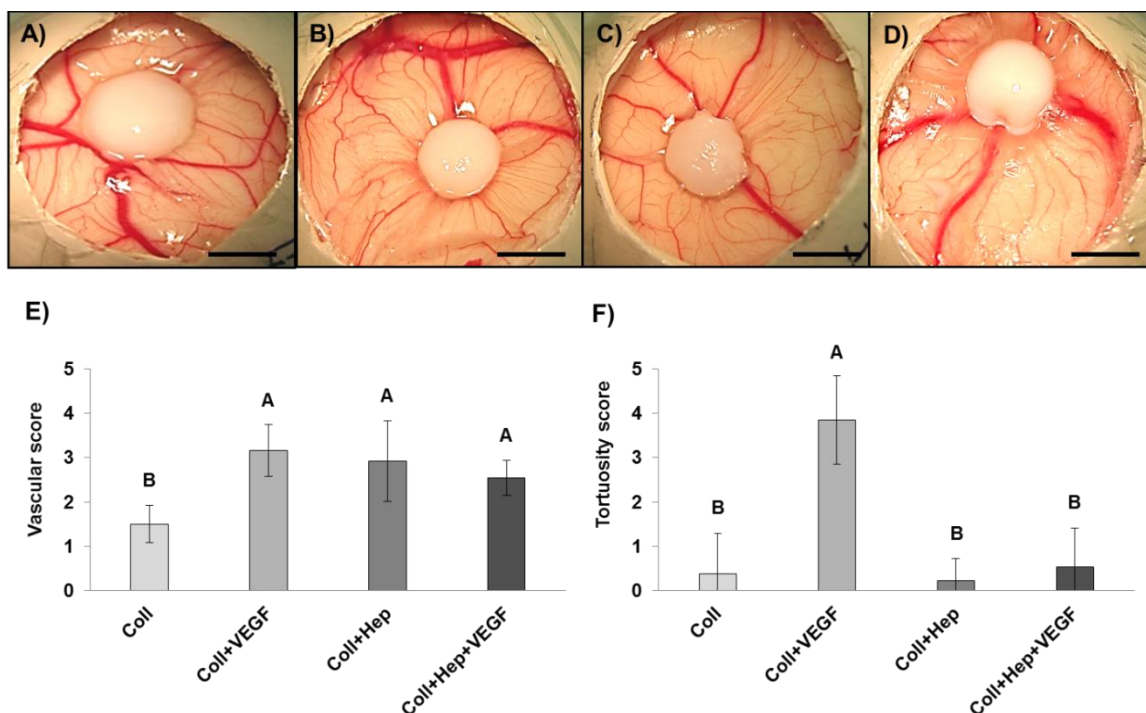
Figure 24: Heparinization of high fibril-density oligomer implants improved vascular response of CAM while preventing abnormal vessel formation. CAM was implanted with 20 mg/ml collagen consisting of oligomer alone (A), oligomer + 0.5 μg/ml VEGF (B), oligomer + 1 μg/ml heparin (C), and oligomer + 1 μg/ml heparin + 0.5 μg/ml VEGF (D). (A-D) top view of implants imaged in situ using digital camera. VEGF loaded implants without heparin (B) induced tortuous vessel response, while VEGF loaded implants with heparin induced normal and enhanced local neovascularization (D). Scale bar= 5 mm. (E) Vascular and (F) tortuosity score calculated from top view. Letters represent statistically different groups determined by Tukey-Kramer range test (N=6-8, p<0.05).

The abnormal vascular response on CAM could have been likely a result of free, passive diffusion of VEGF out of the oligomer. To confirm this speculation, we implanted 3 mg/ml oligomer implants containing VEGF alone (Coll + VEGF) on CAM immediately after overnight polymerization without involving any washing step, and expected to see a heightened tortuous response on CAM after 3 days of implantation. Results of this study showed an increased chaotic, tortuous and fine brush like vessel response on CAM (Figure 25 A). Further to confirm that this response was due to free diffusion of VEGF alone was and that oligomer in conjunction with VEGF was not causing the abnormality, we applied a paper disc soaked in VEGF on top of CAM, and post 3 day implantation, found many major tortuous vessels on CAM (Figure 25 B).
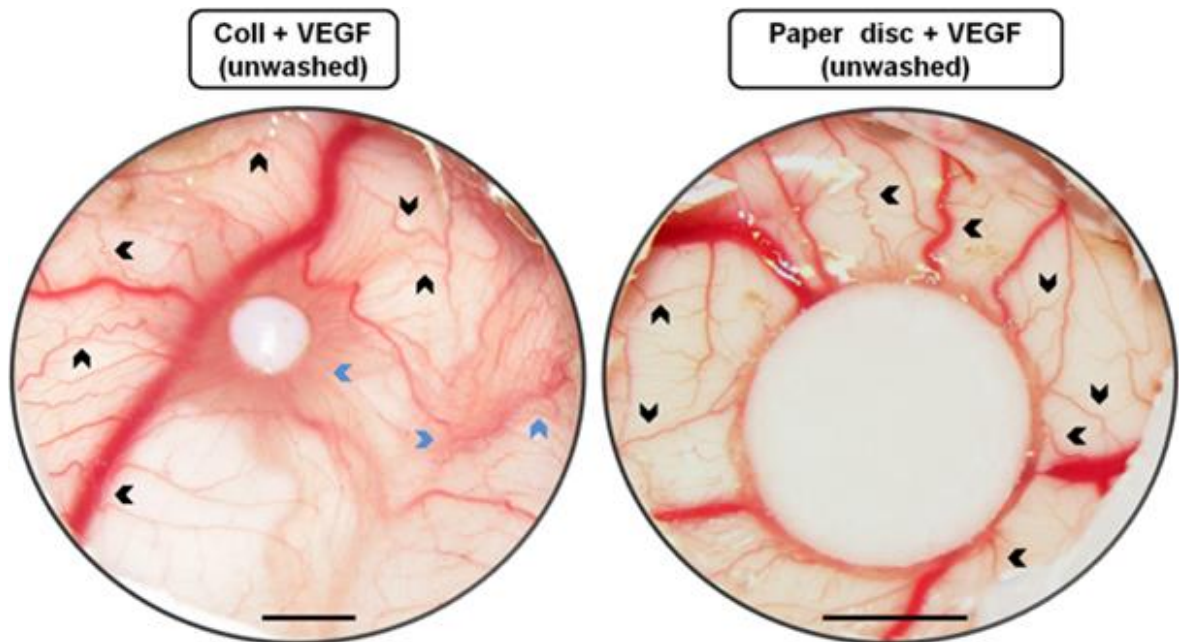
Figure 25: Uncontrolled release of VEGF results in tortuous / abnormal vascular response on CAM. Black arrows indicate tortuous vessels while blue arrows indicate fine brush like vessels and abnormality. Scale bar represents 5 mm

3.3.5 Collagen implant composition and fibril density modulate cell infiltration and capillary formation within the implants

The evaluation of CAM vasculature from top view of the various low (Figure 23) and high (Figure 24) fibril density implants informed us about the vascularization induced by the implants around, but not within the constructs. Therefore, to evaluate the vascular ingrowth within the low and high fibril density implants, we applied standard histological analysis (H&E staining of tissue slices) capturing the cellular interaction between CAM and the implant at their interface.

Results showed that both 3 mg/ml (Figure 26 A) and 20 mg/ml (Figure 26 E) oligomer fibril implants supported some cell infiltration from CAM, however, the ingrowing cells did not appear to be organized or aligned in a particular direction. The addition of VEGF alone in oligomer implants did not seem to increase cell infiltration in low fibril density (Figure 26 C) or high fibril density (Figure 26 G) implants, although it seemed to have promoted higher vascularization on the surface of the CAM. In contrast, addition of heparin alone to the oligomer resulted in enhanced cell infiltration with invading cells aligned perpendicular to the CAM (Figure 26 B- low fibril density implants, and Figure

26 F - high fibril density implants). Finally, the implants containing both heparin and VEGF exhibited a dramatic increase in the cell infiltration while maintaining cell alignment (Figure 26 D - low fibril density implants and Figure 26 H - high fibril density implants). This group also showed remodeling of the collagen and most importantly, exhibited functional capillary formation inside the implants. The functionality of the capillaries inside both the 3 mg/ml (Figure 26 D) and 20 mg/ml (Figure 26 H) implants was evident from the nucleated red blood cells found inside the lumens of these capillaries. The 20 mg/ml Coll + Hep + VEGF implants showed higher cell infiltration and cell alignment into the collagen implant compared to the 3 mg/ml implant (Figure 26 H versus Figure 26 D), which could be on account of higher VEGF retention due to increased fibril density. Collectively these histology-based results indicated that the response of CAM vasculature both around and inside the implants was dependent on presence of heparin and VEGF, as well as the fibril density of implants.

3.3.6 Summary of implant contraction, cellular infiltration and capillary formation

Table 5 summarizes the contraction, cellular infiltration and capillary formation results for all collagen implants tested in this study. Interestingly, the 20 mg/ml oligomer collagen implants showed the least contraction, and it was not significantly different from the contraction showed by Integra collagen. Integra implants showed cell infiltration but not capillary formation. In general, the 20 mg/ml oligomer implants showed improved mechanical integrity and resistance to contraction, compared to the 3 mg/ml oligomer implants.

Cellularization and capillary formation was highest in the Coll+Hep+VEGF group of both the 3 and 30 mg/ml 20 implants. The Coll + Hep group showed the second highest cellular infiltration and capillary formation in both 3 and 20 mg/ml implant groups. The cellular infiltration shown by Coll and Coll +VEGF group was lowest. It was evident that the heparinized implants with VEGF promoted higher cellular infiltration inside implants than the non-heparinized implants.
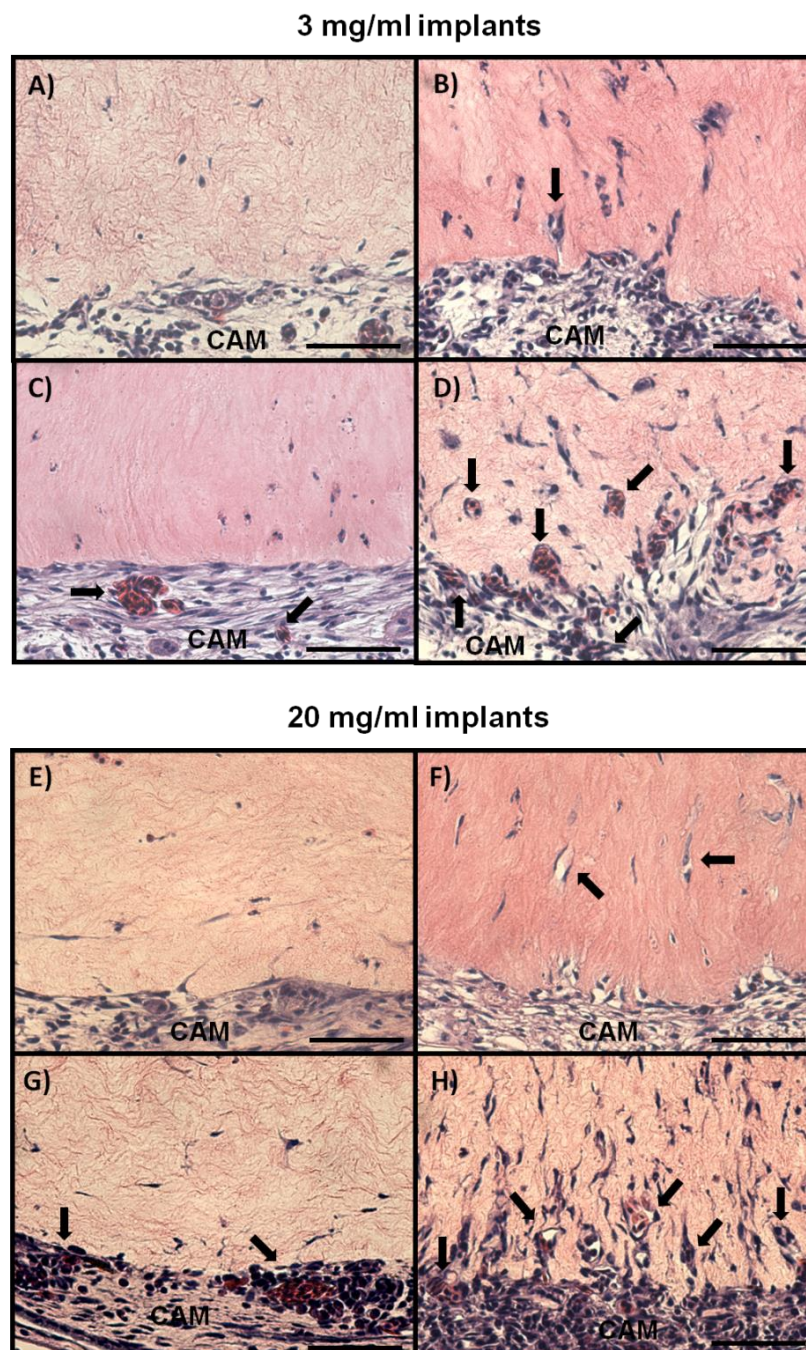
Figure 26: Response of CAM cell invasion and vascularization varies according to contents and density of oligomer implants. H&E staining of histological transverse section of CAM implanted with 3 mg/ml (A-D) and 20 mg/ml (E-H) oligomer implants. Samples consisted of oligomer alone (A&E), oligomer + 1 μg/ml heparin (B&F), oligomer + 0.5 μg/ml VEGF (C&G), and oligomer + 1 μg/ml heparin + 0.5 μg/ml VEGF (D&H). Heparinized VEGF-containing implants (D&H) promoted highest cellular infiltration and capillary formation inside the implants while non-heparinized VEGF-containing implants promoted capillary formation on CAM outside the implant periphery (C&G). Black arrows indicate capillary formation. Scale bar represents 50 μM.

Table 5: Comparison of contraction, cellular infiltration and capillary formation inside different collagen samples

Sample	Final Area (mm^2) Mean ± Std. Dev.	% Contraction Mean ± Std. Dev.	Cellular invasion inside collagen	Capillary formation inside collagen
Control				
1. Integra	39.06 ± 13.75 ^{A}	50.27 ± 17.51 ^{D}	++	-
3 mg/ml Implants				
1. Oligomer	15.78 ± 5.73 ^{C}	83.39 ± 6.03 ^{A}	+	-
2. Oligomer + Heparin	18.08 ± 8.08 ^{BC}	80.97 ± 8.50 ^{AB}	+++	+
3. Oligomer + VEGF189	20.35 ± 5.38 ^{BC}	78.59 ± 5.66 ^{ABC}	++	-
4. Oligomer + Heparin + VEGF189	15.91 ± 7.19 ^{C}	83.26 ± 7.56 ^{AB}	++++	+++
5. Oligomer + VEGF189 (unwashed)	19.30 ± 5.52 ^{BC}	72.56 ± 12.64 ^{ABC}	+	-
20 mg/ml Implants				
1. Oligomer	45.38 ± 9.42 ^{A}	52.24 ± 9.91 ^{D}	+	-
2. Oligomer + Heparin	38.66 ± 9.64 ^{A}	59.31 ± 10.15 ^{CD}	+++	+
3. Oligomer + VEGF189	43.80 ± 10.79 ^{A}	53.91 ± 11.35 ^{D}	++	-
4. Oligomer + Heparin + VEGF189	32.31 ± 8.71 ^{AB}	66.00 ± 9.16 ^{BCD}	+++++	+++
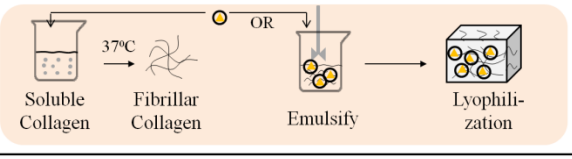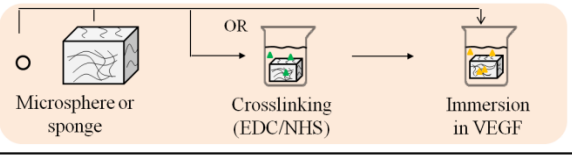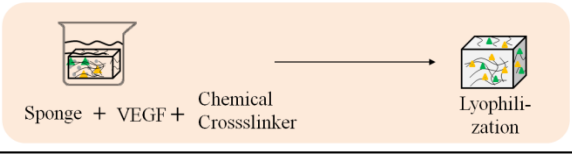
3.4 Discussion

This study makes a contribution to the field of research aimed at enhancing and accelerating the vascularization capabilities of collagen based biomaterials, for potential use as engineered substitutes of tissues grafts. Inspired by the physiological role of heparin in securing binding of VEGF to the ECM, we created self-assembled oligomer matrices infused with heparin and VEGF that showed enhanced vascularization potential. While heparin effects on collagen properties and vascularization has been studied in the past [64, 98, 307-311], these studies involved heparin addition in conventional monomers, not oligomers. Here, we report the use of oligomers for heparin based VEGF retention in collagen implants, and evaluate their functionality for promoting vascularization *in vivo* through a well-established CAM assay. Heparin and VEGF incorporation in the implants was enabled through a single admixing step, and heparin amount was chosen such that it did not alter physiological self-assembly of oligomer. Furthermore, to enhance the mechanical strength and VEGF retention within the implants, we increased the fibril density of the implants and determined its efficacy in promoting microvasculature both around and within the implants. Both low and high fibril density collagen materials maintained their inherent self-assembly, resulting in preservation of native mechanical integrity and biological signaling properties of collagen. Due to the ability of these implants in enhancing local neovascularization and cellularization in an accelerated manner, these implants offer potential use as an ideal platform for integrated tissue engineering and molecular therapy design.

For improving the vascularization ability of collagen scaffolds through VEGF incorporation, a variety of approaches have been adopted in the past, including simple physical entrapment, adsorption, and covalent immobilization as indicated in Table 6, and through affinity based retention approaches shown in Table 7. However, simple physical entrapment (Table 6, approach A) or adsorption (Table 6, approach B) of VEGF in collagen can be ineffective due to its rapid outward diffusion and quick loss of bioactivity [192]. More serious problems such as abnormal, tortuous and leaky vessel formation on account of the uncontrolled release of VEGF can lead to clinical failure of constructs[296]. Therefore, to prevent uncontrolled release of VEGF, covalent immobilization of VEGF has been developed (Table 6, approach C). While chemical

immobilization was able to prevent passive diffusion of VEGF, it comes with a disadvantage that chemical cross-linkers alter the inherent biological signaling capacity of collagen and can result in adverse tissue responses [8, 77]. Moreover, it also presents a danger of damaging the functional group or the screening of active pocket of the VEGF.

Table 6: Selective strategies used for VEGF delivery from collagen based delivery systems

Strategy	Ref.	Limitation
A Physical Encapsulation	[335-337]	Noncollagenous material used for forming micro-particle in (A) causes loss of physio-logical relevance
B Immersion/ Adsorption	[317, 338-342]	
C Covalent Immobilization	[343, 344]	Low VEGF loading efficiency

Long period of vascularization

Chemical crosslinker used in strategy C |
| Legend used in above schematics: ▲ EDC/NHS/ Chemical crosslinker　▲ VEGF　○ Microparticle　◉ VEGF loaded Microparticle | | |

To surpass these limitations, heparin affinity based retention of VEGF in collagen implants has emerged as an attractive option recently (Table 7). However, for heparin incorporation, number of studies (Table 7, A-D) have used chemical crosslinker called EDC (1-ethyl-3-(3-dimethylaminopropyl)carbodiimide) and NHS (N-hydroxysuccinimide) that activates heparin for immobilization in collagen [64, 98, 307-311]. While this cross-linking also serves to improve the mechanical strength and proteolytic resistance of conventional collagen formulations, it alters the native physiological structure of collagen due to chemical cross linkage [345]. As a result, fibrillar mechanics is also affected, and since cell traction forces and adhesive behavior depends on these fibril mechanics, any alteration to this native structure of collagen also

affects cell proliferation and movement [330]. Furthermore, due to EDC/NHS chemical crosslinking step, VEGF has to be loaded to the matrices in a last step, through immersion or impregnation, resulting in low loading efficiency. Moreover, it is currently not possible using EDC chemistry to independently vary implant stiffness vs. the amount of immobilized VEGF [342]. Finally, the heparin quantities used for VEGF retention are also high, and effect of heparin on collagen fibril mechanics is not always given, although it is now known that heparin can alter both microstructure and mechanical properties of collagen [327, 330, 332, 346-348].

We addressed these issues though a design strategy purely relying on affinity based retention of heparin and VEGF as opposed to using exogenous chemical crosslinkers. Exploiting heparin affinity for collagen and VEGF, we created heparin and VEGF infused oligomeric collagen implants (Table 7, Strategy E) that retained their physiologically relevant self-assembly properties as will be seen in following section.
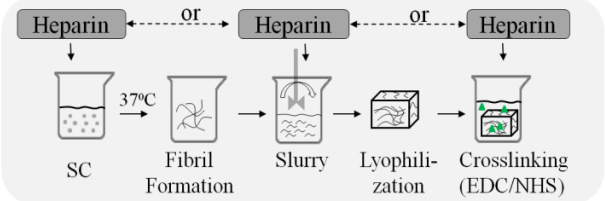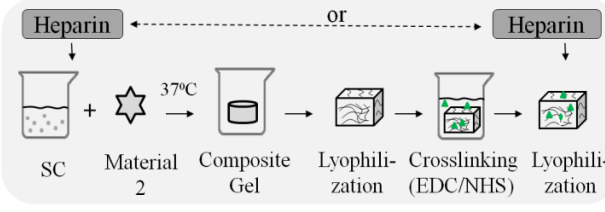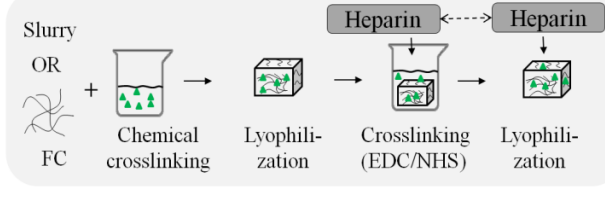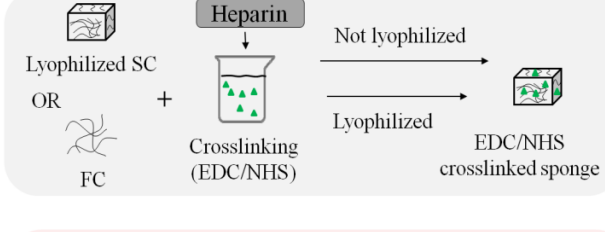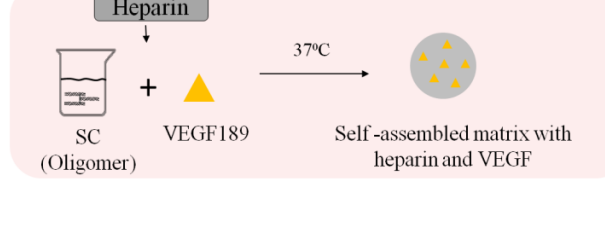
3.4.1 Selecting heparin quantity that does not affect oligomer matrix self-assembly

In vivo, heparin based VEGF retention has been found to increase endothelial cell proliferation, upregulate microvasculature formation, and stimulate blood vessel maturation [64, 96, 349, 350]. However, *in-vitro* addition of heparin has illustrated that these effects are concentration dependent and beneficial effects were found only at low concentrations (0.1-1 µg/ml) of heparin [290, 351], while higher concentrations (10-1000 µg/ml) of heparin progressively inhibited the VEGF binding [291, 352]. These results prompted us to carefully select heparin concentration for admixing to oligomer, so as to obtain beneficial effects of VEGF binding.

Another important consideration in selecting heparin concentration for addition to oligomer was its effect on collagen fibril self-assembly. Heparin is known to bind to type I collagen fibrils with high affinity (Kd= 150 nM) [329]. However, several investigators over the past few decades have reported that the presence of heparin during collagen fibrillogenesis *in vitro* could have a profound concentration dependent effects on fibril size, interconnectivity, diameter, and organization [327, 330, 332, 346-348], that could impact cell growth [332]. Stamov et al. recently reported that these gross physiochemical and morphology changes could be attributed to competitive binding of telopeptides and

heparin to similar regions along the triple-helical main region of intact tropocollagen, leading to inhibition of formation of asymmetric D-staggered fibrils [330].

Table 7: Selective strategies used for VEGF delivery from heparinized collagen materials

Strategy	Ref.	Limitation
A — Heparin or Heparin or Heparin → SC → 37°C Fibril Formation → Slurry → Lyophilization → Crosslinking (EDC/NHS) — VEGF loading	[353, 354]	Collagen self-assembly not capitalized;
B — Heparin or Heparin → SC + Material 2 → 37°C Composite Gel → Lyophilization → Crosslinking (EDC/NHS) → Lyophilization	[355, 356]	Chemical cross-linking used;
C — Slurry OR FC + Chemical crosslinking → Lyophilization → Heparin ↔ Heparin → Crosslinking (EDC/NHS) → Lyophilization	[98, 192, 308-311]	High heparin quantity;
D — Lyophilized SC OR FC + Heparin → Crosslinking (EDC/NHS) → Not lyophilized / Lyophilized → EDC/NHS crosslinked sponge (Affinity-based)	[64, 357]	Low VEGF loading efficiency; Slow vascularization
E — Heparin → SC (Oligomer) + VEGF189 → 37°C → Self-assembled matrix with heparin and VEGF (Affinity-based)	This work	

(center: Immersion or Impregnation)

Legends used in above schematics:

SC = Soluble Collagen
FC = Fibrillar Collagen
▲ EDC/NHS/ Chemical crosslinker
▲ VEGF
Oligomer with natural crosslink

Heparin bears the highest density of negatively charged groups among all other GAGs [358] which can trigger the electrostatic interaction with other macroionic molecules [359]. Heparin–type I collagen interactions likely rely on the basic triple-helical domain present at amino acid positions 87–94 near the N terminus of type I collagen monomer, and at multiple sites within native fibrils [328, 329]. Weak heparin binding sites were also observed near the carboxy terminal region of monomeric tropocollagen between positions 755 and 933 [328, 360]. The regions containing elements of NH2 terminus with affinity for heparin were highly basic, and found near the interface between the overlap and gap region of collagen. However, these regions are also known to be participating in the cross-link formations of collagen [328]. As telopeptides and heparin are prone to bind to similar regions along the triple-helical main region, it has been proposed that heparin binding at this position competitively inhibits the formation of asymmetric D-staggered fibrils [330].

It was noted however, that the profound effects of heparin on the processes of fibril formation, growth and higher-level organizations of collagen matrices were found to be concentration dependent [327, 330, 332, 346-348]. While low concentrations of heparin were reported to be promoting fibril formation, high concentrations inhibited fibril assembly [327, 332, 333, 347]. However, the concentration range of heparin, ratio of collagen and heparin, as well as the investigation techniques varied considerably in these studies, making it difficult to paint a consistent picture of the important parameters of heparin interaction with collagen. Moreover, these studies with heparin were carried out on monomeric collagen formulations, not oligomer formulations. Therefore, before employing the strategy of heparin based VEGF retention in oligomeric collagen, it was extremely important to find the effect of heparin on oligomeric collagen polymerization and viscoelastic properties.

We assessed this effect by adding heparin to 3 mg/ml oligomer solutions in concentration range of 0 to 100 µg/ml through a simple admixing step, allowing electrostatic interaction based binding of heparin to the oligomer molecule, and then assessed the effect of heparin on matrix polymerization kinetics, viscoelastic properties and final stiffness of polymerized oligomer matrices (Figure 19). Results of this study indicated that upto 1 µg/ml addition of heparin to oligomer collagen did not alter its mechanical stiffness,

visco-elastic properties or polymerization kinetics. However, at higher concentrations (5, 10 and 100 μg/ml), the viscoelastic properties and stiffness of matrix decreased significantly. These findings are consistent with previous findings where addition of heparin in pepsin-solubilized bovine dermal collagen resulted in formation of a less cohesive matrix [162, 327, 332].

While it is known that heparin and collagen form stable complexes due to electrostatic interactions between the highly anionic heparin and the positively charged groups of collagen [361, 362], the possibility that not all the added heparin binds to oligomer - was taken into consideration. Some heparin could be merely physically entrapped in polymerizing matrix. Since this free (unbound) heparin in collagen matrix could result in its uncontrolled diffusion out of collagen, it was thought to eliminate any unbound heparin from the collagen matrix using large excess of 1X PBS for 24 h. To quantify the remaining heparin in washed matrices, we performed DMMB assay, exploiting the fact that heparin forms colored complexes with the cationic dye 1, 9-dimethylmethylene blue. All samples were papain digested before the assay to make entire amount of heparin present in matrix accessible for the dye complexation [363].

The DMMB assay confirmed successful elimination of unbound heparin from oligomer matrices, as the quantity of heparin in washed matrices was significantly lower than unwashed matrices at all concentrations tested from 1 to 100 μg/ml (Figure 20 A). At 1 μg/ml heparin addition in oligomer, we found that approximately 26% of added heparin was retained in the washed matrices. Further, confocal microscopy based visualization of FITC-heparin in oligomer matrices confirmed heparin colocalization on oligomer collagen fibrils and its retention after washing for 24 h (Figure 20 B and C). Such a uniform spatial distribution of heparin in collagen and its intercalation in collagen fibrils has been reported in previous studies [330, 348].

The results obtained here are important because they demonstrated for the first time the effect of various concentrations of heparin on polymerization and visco-elastic properties of oligomeric collagen. Based on these results, we selected 1 μg/ml concentration of heparin for further design of VEGF retention system from oligomer, to preserve the oligomer polymerization and viscoelastic properties while enabling VEGF retention.

3.4.2   VEGF loading

Because of the reported strong affinity of VEGF 189 for ECM, and its beneficial role in promoting vascularization *in vivo*, we incorporated VEGF 189 in our design strategy to enhance vascularization potential of oligomer implants. VEGF dose was then carefully chosen because of the evidences that over dosage of VEGF therapy can result in an imbalance in angiogenic signals, leading to dysregulated vasculogenesis [364, 365] and hemangioma-like assemblies [364, 366]. The amount of VEGF 189 used in this study (0.5 μg/ml, or 0.125 μg per implant) was chosen based on previous range of concentrations of VEGF reported in similar assays that showed enhanced vascularization effects *in vivo* either with heparin [64, 98, 307-311] or without heparin [205, 317, 339-344]. For loading of VEGF to oligomeric matrix, we adopted admixing approach again, where 0.5 μg/ml VEGF189 was added along with 1μg/ml heparin in the neutralized oligomer solution and polymer self-assembly was induced at 37°C. Retaining both the heparin and VEGF in collagen matrix was thus achieved through single step.

Since rapid, unregulated exposure of freely diffusible VEGF has been previously reported to cause excessive but abnormal, unstable blood vessel growth [89, 367], we washed all heparin and VEGF-containing oligomer implants for 24 h to remove any unbound heparin and VEGF. The washing step resulted in loss of about 74% of heparin as reflected by the results of DMMB assay for 1 μg/ml heparin-containing matrices. Therefore, we suspected that the final quantity of VEGF remaining in the implants would be very low. To quantify the exact amount retained in samples, we adopted LC-MS/MS technique due to its higher sensitivity than ELISA method (Sensitivity of full MS was 500 fg buspirone on mass spectrometer column with signal to noise ratio of 100:1, while sensitivity of standard Quantikine ELISA kit assay is 9 pg/ml). The samples were enzymatically digested into peptides that were separated by high pressure liquid chromatography (HPLC) and introduced into a mass spectrometer (Q Exactive™ HF Hybrid Quadrupole-Orbitrap MS (Thermo Scientific, Waltham, MA) for fragmentation and sequencing to identify the parent proteins. However, the large presence of collagen in the samples obscured the VEGF detection in samples (data not shown).   To determine whether the VEGF remaining in oligomer implants was able to promote higher vascularization *in vivo*, it was therefore thought to assess the effect of oligomer alone

(without heparin or VEGF) on CAM, followed by its comparison with the VEGF and heparin-infused implants. The results of this study are discussed in the following section.

3.4.3 Evaluation of oligomer implant's vascularization potential in CAM assay

To evaluate the vascularization potential of oligomer matrices in CAM, we implanted oligomer constructs on CAM at embryonic day 9, and after 3 days of incubation, we scored the CAM vessel density and distribution around the implants. The vascular response was also evaluated for occurrence of any tortuous, irregular, or fine, brush like vessels, as it could be an indication of abnormal and leaky vessel formation [89, 368]. Furthermore, to evaluate the vascular ingrowth from CAM into the implants, we performed histology and H&E staining on transversally cut implant samples that allowed us to envision both capillary formation and cellularization in the internal sections of the implants.

3.4.3.1 Validating functionality of oligomer implants on CAM

The first goal was to validate the suitability of oligomer constructs for implantation in CAM, and evaluating their vascularization potential in CAM, as compared to the commercial Integra collagen samples, and paper disc samples. Integra collagen used in this study was an absorbable wound dressing sponge made of collagen obtained from bovine deep flexor (Achilles) tendon, and it was chosen for comparison in this study since it is FDA approved and has been used successfully in clinical trials for treating wounds [369, 370].

Results of 3 day implantation on CAM demonstrated that 3 mg/ml oligomer induced higher vascular response on CAM compared to the Integra collagen implants or paper disc samples (Figure 22). Histology results further provided evidence that oligomer implants supported cell invasion from CAM into the collagen region in just 3 days after implantation. Cell infiltration was also found in Integra samples. However, large empty spaces were characteristic of Integra collagen, as opposed to uniform, dense fibrillar nature of oligomer sample. CAM cells invading the paper disc sample showed apoptic morphology, which can be attributed to the absence of collagen matrix that provides essential mechanical support and biological signaling for cellular growth and

proliferation. The higher induction of vascular response on CAM while maintaining cell infiltration as shown by oligomer implants, established them as suitable material for further vascularization study.

3.4.3.2 Low fibril density heparinized oligomer implants promoted enhanced vascularization in CAM

Having established suitability of oligomer implants in inducing vascularization on CAM, we next evaluated whether heparin and VEGF addition to oligomer implants enhanced its vascularization ability. Results indicated that heparinized oligomer implants containing VEGF induced highest vascular response on CAM among all groups (Figure 23). This enhancing effect of heparin and VEGF has been observed previously, both *in vitro* [309, 355] as well as *in vivo* [98, 310] although the time required for vascular effect was reported to be higher than 3 days. Moreover, these studies incorporated heparin in collagen matrices through EDC/NHS chemical cross-linking for VEGF retention. Here we obtained improved vascularization results through simple admixing of heparin and VEGF in oligomer, in an accelerated period of 3 days.

The non-heparinized oligomer implants containing free VEGF also demonstrated angiogenic activity on CAM, however, the vessels formed around this group of implants were either brush like, or tortuous, indicating an abnormal vessel development. Such abnormal vessel development could be a result of passive, uncontrolled release of VEGF out of the oligomer implants. Similar to these findings, previous reports have indicated formation of chaotic capillary plexus *in vivo* in response to freely diffusible VEGF released from fibrin matrices, while matrix-bound VEGF induced formation of highly organized, functional vessels in CAM [89, 371].

It addition to VEGF loaded implants, heparinized oligomer implants without VEGF (Coll+Hep) also induced a vascular response on CAM, although it was weaker than Coll+Hep+VEGF group. The positive angiogenic effect of heparin by itself on CAM vasculature has been reported previously [372-374]. In the absence of exogenous growth factors, modification of collagen with heparin was found to increase neovascularization, possibly by potentiating endogenous growth factors present *in vivo* [59, 64, 98]. This positive effect of heparin could have been due to its role in protecting cell secreted VEGF from degradation [192], and upregulating VEGF activities by enabling its binding

to the KDR and Flt-1 receptors [375]. Finally, the non-heparinized oligomer implant (Coll), showed a vascular response that was significantly lower than either VEGF or heparin or both VEGF and heparin loaded matrices. Together, these results highlight the potential of heparin in retaining VEGF in oligomer implants and upregulating its activities on CAM. These results also convey the importance of controlled VEGF release essential for formation of normal vasculature on CAM, which was achieved in our system using simple affinity based retention of VEGF.

3.4.3.3 Enhancing CAM vascularization through high fibril density implants

The vascularization potential of low-fibril density oligomer implants can be beneficial in cases such as small injuries or as acute wounds, where the low mechanical properties of the implants could suffice tissue healing for a short period of time. However, in cases such as chronic wounds, where the regeneration of new tissue is difficult due to high level of proteases [189, 376], the implants would be required to last longer to support and accelerate new capillary ingrowth into the implant. For this purpose, oligomer implants of high fibril density can offer a potential solution due to their characteristic higher mechanical strength and resistance to proteolytic degradation [116]. Moreover, the increased fibril-density would have a positive effect on retaining the encapsulated growth factors [4], due to their enhanced fibril density (reduction in pore size) [183]. Therefore, with an objective to provide stronger mechanical support and enhanced VEGF retention, we prepared high fibril-density 20 mg/ml oligomer implants loaded with heparin and VEGF and evaluated their ability to accelerate local vascularization in CAM after 3 days of implantation.

Results of 20 mg/ml implants (Figure 24) were similar to 3 mg/ml implants, where heparinization and VEGF incorporation of the implants led to significantly higher vascularization. VEGF-containing implants without heparin led to brush-like or tortuous/abnormal vessel response again, emphasizing that uncontrolled VEGF release had undesirable consequences on normal vasculature development of CAM. Heparinized implants without VEGF showed a weaker vascular response than with VEGF loading. Oligomer implants without heparin or VEGF incorporation showed significantly lower

vascular response. These results corroborated the advantages of incorporating heparin and VEGF together in oligomer scaffolds, to achieve enhanced neovascularization.

Apart from maintaining their ability to promote vascularization, another remarkable result demonstrated by the 20 mg/ml implants was their ability to retain their shape and exposing large area for growth of CAM vasculature even on day 3 of implantation. In fact, the 20 mg/ml implants retained largest cross-sectional area among all the collagen implants tested in this study (Table 5), which can be a result of the high mechanical integrity of these constructs. Most collagen implants without the aid of exogenous crosslinking suffer from the drawback of low mechanical integrity, rapid degradation and fast diffusion of growth factors [4, 5]. Therefore, considering the lack of exogenous crosslinking in our study, the results obtained here in terms of preservation of mechanical integrity, retention of VEGF and promotion of vascularization on CAM were found to be impressive.

3.4.4   Cellularization of oligomer implants

The induction of high vascular response around both 3 and 20 mg/ml oligomer implants containing heparin and VEGF informed us about the effect of heparin and VEGF delivery from oligomer on CAM vasculature. However, for clinical success of tissue-engineered scaffolds, along with promotion of vascularization around the implant, growth of micro vessels within the implant is crucial to enable survival of cells in the core of the scaffold [296]. CAM assay allows the advantage of envisioning such a microvasculature growth inside scaffolds that can be separated from the surrounding CAM vasculature, as these new micro vessels grow inside the scaffolds against gravity [326, 377, 378]. We evaluated the ability of oligomer implants to draw in such micro vessels, through H&E based staining of transverse histological sections of the implants (Figure 26).

Results revealed that non-heparinized implants supported cellular infiltration, however, these cells were not aligned towards any particular direction. VEGF loaded non-heparinized induced formation of several capillaries on CAM adjacent to the implant periphery, but not within the implant. In contrast, heparinized oligomer implants loaded with VEGF induced formation of several capillaries inside the implants, clearly showing the benefit of adding heparin in upregulating vasculature inside the oligomer implants. As

proposed in previous studies [64, 97, 349, 379], this upregulation of neovasculature inside collagen implants could have on account of the prolongation in VEGF's biological activity [202, 380] and more efficient binding of VEGF to its receptors in presence of heparin [355, 380].

Another outstanding result of implanting heparinized VEGF-containing oligomer on CAM was highest invasion of CAM cells within the implants. These cells also displayed remarkable alignment towards the implant, which could be a result of VEGF signaling gradient present across the boundary of oligomer implant and CAM. Physiologically, such a VEGF gradient in hypoxic or diseased tissues [381], exercising skeletal muscle [381, 382], and wounds [383] has been shown to be responsible for attracting endothelial sprouts towards hypoxic regions. A putative gradient of VEGF formed in collagen implants has also been reported previously to be responsible for cell recruitment in other studies involving VEGF [341] and other growth factor delivery through collagen implants [384]. Therefore, the increased infiltration of CAM cells within heparinized, VEGF-containing oligomer implants obtained here could have been a consequence of presence of such a concentration gradient created across the interface of oligomer implants and CAM.

In the present study, the process of vascularization of heparinized oligomer matrices was seen to be accompanied by a remodeling of the matrix (Figure 26 D and H), and this process is also known to occur in physiological healing of wounds [385]. The physiological remodeling of wound includes degradation of the collagen through matrix metalloproteinases (MMPs) [386] secreted by infiltrating fibroblasts that then deposit newly synthesized collagen [192, 387]. In our CAM study, the cells infiltrating in oligomer matrix could be participating in such activities, subsequently remodeling the collagen matrix they resided in, generating their own micro-environment and, proliferating, differentiating and attracting other cells inside the collagen [384].

While several studies reported that modified collagen implants increased in neovascularization on the CAM surface [64], very few [334] have documented actual neovascularization inside the collagen matrix of the implant. Kilarski et al. [334] reported that neovessels found in their collagen matrix were contained within the expanding CAM tissue that eventually replaced the provisional matrix and there was a

clear demarcation between the ingrowing tissue and the implanted gel, implying that the neovessels entered their collagen gel as a part of ingrowing CAM tissue buds, but not as independent entities. In our model however, we found capillaries both inside the ingrowing CAM tissue as well as inside collagen as separate entities, in addition to the capillaries on CAM tissue on periphery of the implant. Furthermore, such cellularization and neovascularization was obtained in just 3 days, while several collagen implant studies have required several days for cellularization of their constructs in either CAM or rat subcutaneous implantation studies [64, 98, 307-311]. In the light of the current state-of-the-art collagen induced vasculature on CAM, oligomer constructs that demonstrated this distinct microvasculature as well as cellularization inside them appears very promising for promoting tissue regeneration and integration with the host tissue.

3.5   Conclusion

Physiologically, the process of vessel formation takes place in the ECM, that constitutes a dynamic 3D microenvironment of cells, providing the instructive biomechanical and biomolecular signaling required for morphogenesis. The ECM is the natural biological material, which with the help of molecules such as heparin sulphate proteoglycans or heparin, regulates the sprouting of new blood vessels, and their stabilization, leading to restoration of functional blood circulation into ischemic tissues. Inspired by this role of ECM and heparin in spatio-temporal regulation of growth factors *in vivo*, we designed a physiologically relevant collagen implant from self-assembling oligomer molecules that can control the local presentation and release of VEGF at the site of implantation. We leveraged heparin's affinity for oligomeric collagen molecules and VEGF189 for this purpose, enabling a single step local retention of VEGF189 in the oligomer implants for promotion of vascularization.

We then validated the functionality of the oligomer implants in promoting vascularization and cell infiltration *in vivo*, through the use of simple and reproducible CAM assay. When compared and contrasted with paper discs, Integra collagen, and non-heparinized as well as free VEGF loaded implants, we found a clear benefit of heparin addition in oligomer implants that resulted in formation of robust neovascularization in an accelerated time period of 3 days. We also demonstrated that the vasculature response

can be controlled by altering contents (heparin and VEGF loading) as well as the fibril density of oligomer implants. VEGF loaded implants without heparin led to formation of tortuous vessels, corroborating the dangers of uncontrolled VEGF therapy. In contrast, heparinized implants loaded with VEGF demonstrated improved and stable vasculature formation both around and within the implants, signifying the importance of heparin for controlling the VEGF release.

While CAM assay allowed us to evaluate the viability of oligomer implants as angiogenic biomaterial, in a rapid, simple, and low-cost *in-vivo* setting, it should be noted that this model system is an intermediate step between a cell culture and a large animal studies or more complex mammalian model. Therefore, the positive results of enhanced vascularization through heparinization of oligomer implants obtained in this study must be tested in a large animal and mammalian model, and the differences between avian and mammalian biology should be taken into account before applying any conclusions from CAM assay to a mammalian model [388].

Finally, it is worth mentioning that the implants designed in this work were fabricated without the use of exogenous crosslinkers, and the heparin quantity chosen for loading VEGF did not affect oligomer collagen self-assembly. Consequently, the designed implants retain collagen's multi-scale structural features and inherent biological signaling capacity while promoting microvasculature formation inside the implants in an accelerated manner. Accelerated vascularization in turn can shorten the time of cellularization of constructs, decrease the risk of infection, and result in faster tissue integration and regeneration or healing of the affected tissue [389], thus providing an ideal platform for integrated tissue engineering and molecular therapy design.

CHAPTER 4.   CONCLUSION & FUTURE WORK

4.1   Conclusions

There is a significant challenge in the design and manufacture of multifunctional biograft materials capable of providing tunable molecular delivery due to the poor mechanical properties, rapid proteolytic degradation, and inability of collagen formulations to demonstrate physiologically relevant self-assembly. This work attempts to address these limitations with the use of novel self-assembling collagen-fibril biograft materials.

Overall, we achieved a successful design and development of self-assembling, multifunctional 3D collagen-fibril biograft materials with a broad range of tunable physical and molecular delivery properties. More specifically, collagen polymers specified by their intermolecular crosslink composition and self-assembly capacity were used to customize and design materials in terms of 1) collagen fibril microstructure and 2) proteolytic degradability. Furthermore, to increase local retention of biomolecules such as vascular endothelial growth factor (VEGF) in collagen, we successfully employed affinity based strategy that exploited the VEGF-binding and collagen-binding capacity of heparin. The functionality of collagen biograft materials was demonstrated in an *in-vivo* CAM model, where enhanced local retention of VEGF led to increase in neovascularization and cell infiltration of collagen biografts.

Specifically in Chapter 2, we found that when compared with the conventional collagen monomer (e.g., atelocollagen, telocollagen) matrices, oligomer matrices exhibited uniform, highly branched fibril ultrastructure and possessed higher resistance to proteolytic degradation. As a result, oligomer matrices exhibited size-dependent and sustained molecular release while conventional telocollagen matrices showed burst release for small as well as large sizes of FITC-dextrans. Fibril microstructure and proteolytic degradability was also significantly affected by varying the collagen polymer building blocks (e.g. oligomer, telocollagen and atelocollagen) used for self-assembly. Most contrasting release profiles were obtained using oligomer and atelocollagen building blocks, with oligomer showing most sustained release while atelocollagen showing most rapid release in both absence and presence of collagenase. Molecular

release of both small and large molecules was further fine-tuned by combining oligomer and atelocollagen in different percentages. Increase in oligomer percentage extended the molecular release time observed through mixed matrices. An enhancement in molecular retention was further achieved by increasing collagen fibril density that also improved resistance of materials against collagenase. Collectively, through these results, we demonstrated successful development of collagen fibril biografts that could be tuned in terms of their fibril microstructure and proteolytic degradability for providing tunable molecular release of wide range of molecular sizes.

In Chapter 3, we validated the functionality of these collagen biografts for promoting local vascularization and cell infiltration using an established *in-vivo* CAM assay through controlled VEGF delivery. Here, to increase local retention of VEGF in collagen, we employed affinity based strategy that exploited the VEGF-binding and collagen-binding capacity of heparin. Results showed a clear benefit of adding heparin to oligomer matrices, leading to an increased vascular response on CAM and enhanced neovascularization as well as cell infiltration of the implants. We further demonstrated that response was dependent on the absence or presence of heparin and VEGF in oligomer implants and the fibril density of oligomer implants. VEGF loaded implants without heparin led to formation of tortuous vessels, corroborating the potential dangers observed with uncontrolled VEGF therapy by researchers in the past. In contrast, heparinized implants demonstrated stable vasculature response both around and within the implants, signifying the importance of heparin for controlling the VEGF release. Overall, the heparinization prevented uncontrolled VEGF release from collagen and led to a remarkable increase in neovascularization and cellularization of the implants in a short period of 3 days.

Altogether, this work indicates that the collagen polymers specified by their intermolecular crosslink composition and self-assembly capacity can be used effectively to fashion a broad range of multifunctional collagen-fibril biograft materials with tunable physical and molecular delivery properties in absence of excessive processing and exogenous crosslinking. These highly porous collagen materials comprise D-banded fibrils, resembling those found in tissues, and maintain their inherent biological signaling properties. The remarkable ability of these designer implants in supporting enhanced

neovascularization and cellularization of the constructs in an accelerated period indicates their strong potential as an ideal platform for integrated tissue engineering, regeneration and molecular therapy design.

4.2 Future Work

Since the motivation to develop collagen based tissue engineering implants is to address unmet clinical need of soft tissue replacement, the ultimate success in its clinical translation will depend on an interactive, back and forth, "bedside to bench and back again" approach that has recently emerged [390]. For the designer collagen biografts studied in this work to reach patient care in the near future, such an approach is of utmost importance. Many indispensable steps should be met with in this approach, the first and foremost being *in-vivo* trials using small and large animal models to evaluate safety and efficacy of the biografts for desired clinical need.

A specific example of such a clinical need where the collagen biografts developed in this work could be applied, is the treatment of chronic wounds such as diabetic ulcers. As mentioned in first chapter of thesis, diabetic ulcers result in significant morbidity, prolonged hospitalizations, and enormous healthcare costs. Therefore, the efficacy and safety of collagen biografts to heal diabetic ulcers could be shown using non-healing wounds in a diabetes-induced animal model [391]. Among the various animals that can be used for this purpose, such as rabbits, dogs, goats, sheep, or pigs, we propose the pig model studies, because of their known anatomical and physiological similarities to humans[392]. Diabetes can be induced in pigs via streptozotocin injection[391]. Full thickness wounds can then be introduced in pigs to create diabetic ulcers. Collagen biografts will then be implanted on the wounds and untreated wounds will serve as controls.

The pig experiment will be carefully designed to include all variables in the biograft and each variable will be tested separately. As required by law, the animal research protocol would then be submitted to the Institutional Animal Care and Use Committee (IACUC) for approval. The outcome of the pig model study would be immensely valuable in determining the safety and efficacy of the collagen biografts, and would pave the way forward for future clinical translation to address unmet need of treating chronic wounds.

REFERENCES

[1] A. Atala, Tissue engineering and regenerative medicine: concepts for clinical application, Rejuvenation Res, 7 (2004) 15-31.

[2] R. Parenteau-Bareil, R. Gauvin, F. Berthod, Collagen-Based Biomaterials for Tissue Engineering Applications, Materials, 3 (2010) 1863-1887.

[3] C.H. Lee, A. Singla, Y. Lee, Biomedical applications of collagen, International Journal of Pharmaceutics, 221 (2001) 1-22.

[4] W. Friess, Collagen--biomaterial for drug delivery, European journal of pharmaceutics and biopharmaceutics : official journal of Arbeitsgemeinschaft fur Pharmazeutische Verfahrenstechnik e.V, 45 (1998) 113-136.

[5] Z. Ruszczak, W. Friess, Collagen as a carrier for on-site delivery of antibacterial drugs, Advanced drug delivery reviews, 55 (2003) 1679-1698.

[6] E. Khor, Methods for the treatment of collagenous tissues for bioprostheses, Biomaterials, 18 (1997) 95-105.

[7] K. Weadock, R.M. Olson, F.H. Silver, Evaluation of collagen crosslinking techniques, Biomaterials, medical devices, and artificial organs, 11 (1983) 293-318.

[8] K.S. Weadock, E.J. Miller, L.D. Bellincampi, J.P. Zawadsky, M.G. Dunn, Physical crosslinking of collagen fibers: comparison of ultraviolet irradiation and dehydrothermal treatment, Journal of biomedical materials research, 29 (1995) 1373-1379.

[9] R.J. Ruderman, C.W. Wade, W.D. Shepard, F. Leonard, Scanning electron microscopy of surfaces indicing shear hemolysis, Journal of biomedical materials research, 7 (1973) 253-262.

[10] D.T. Cheung, M.E. Nimni, Mechanism of Crosslinking of Proteins by Glutaraldehyde II. Reaction with Monomeric and Polymeric Collagen, Connective Tissue Research, 10 (1982) 201-216.

[11] D.T. Cheung, N. Perelman, E.C. Ko, M.E. Nimni, Mechanism of crosslinking of proteins by glutaraldehyde III. Reaction with collagen in tissues, Connective tissue research, 13 (1985) 109-115.

[12] J.M. Lee, H.H.L. Edwards, C.A. Pereira, S.I. Samii, Crosslinking of tissue-derived biomaterials in 1-ethyl-3-(3-dimethylaminopropyl)-carbodiimide (EDC), Journal of Materials Science: Materials in Medicine, 7 (1996) 531-541.

[13] J.M. Lee, C.A. Pereira, L.W.K. Kan, Effect of Molecular-Structure of Poly(Glycidyl Ether) Reagents on Cross-Linking and Mechanical-Properties of Bovine Pericardial Xenograft Materials, Journal of Biomedical Materials Research, 28 (1994) 981-992.

[14] J.L. Bailey, P.J. Critser, C. Whittington, J.L. Kuske, M.C. Yoder, S.L. Voytik-Harbin, Collagen oligomers modulate physical and biological properties of three-dimensional self-assembled matrices, Biopolymers, 95 (2011) 77-93.

[15] P.J. Critser, S.T. Kreger, S.L. Voytik-Harbin, M.C. Yoder, Collagen matrix physical properties modulate endothelial colony forming cell-derived vessels in vivo, Microvascular research, 80 (2010) 23-30.

[16] T. Wild, A. Rahbarnia, M. Kellner, L. Sobotka, T. Eberlein, Basics in nutrition and wound healing, Nutrition, 26 (2010) 862-866.

[17] A.J. Singer, R.A.F. Clark, Cutaneous Wound Healing, New England Journal of Medicine, 341 (1999) 738-746.

[18] S. Tejiram, S.L. Kavalukas, J.W. Shupp, A. Barbul, 1 - Wound healing A2 - Ågren, Magnus S, in: Wound Healing Biomaterials, Woodhead Publishing, 2016, pp. 3-39.

[19] C.K. Sen, G.M. Gordillo, S. Roy, R. Kirsner, L. Lambert, T.K. Hunt, F. Gottrup, G.C. Gurtner, M.T. Longaker, Human Skin Wounds: A Major and Snowballing Threat to Public Health and the Economy, Wound repair and regeneration : official publication of the Wound Healing Society [and] the European Tissue Repair Society, 17 (2009) 763-771.

[20] A. Alavi, R.G. Sibbald, D. Mayer, L. Goodman, M. Botros, D.G. Armstrong, K. Woo, T. Boeni, E.A. Ayello, R.S. Kirsner, Diabetic foot ulcers: Part I. Pathophysiology and prevention, Journal of the American Academy of Dermatology, 70 (2014) 1.e1-1.e18.

[21] C.f.D.C.a. Prevention, Centers for Disease Control and Prevention. National Diabetes Statistics Report: Estimates of Diabetes and Its Burden in the United States, 2014. , in, Atlanta, GA, 2014.

[22] A. Shearer, P. Scuffham, A. Gordois, A. Oglesby, Predicted Costs and Outcomes From Reduced Vibration Detection in People With Diabetes in the U.S, Diabetes Care, 26 (2003) 2305.

[23] K.G. Harding, H.L. Morris, G.K. Patel, Science, medicine and the future: healing chronic wounds, BMJ, 324 (2002) 160-163.

[24] G.C. Gurtner, S. Werner, Y. Barrandon, M.T. Longaker, Wound repair and regeneration, Nature, 453 (2008) 314-321.

[25] E.A. Rayment, Z. Upton, G.K. Shooter, Increased matrix metalloproteinase-9 (MMP-9) activity observed in chronic wound fluid is related to the clinical severity of the ulcer, British Journal of Dermatology, 158 (2008) 951-961.

[26] D.R. Yager, B.C. Nwomeh, The proteolytic environment of chronic wounds, Wound Repair and Regeneration, 7 (1999) 433-441.

[27] M. Muller, C. Trocme, B. Lardy, F. Morel, S. Halimi, P.Y. Benhamou, Matrix metalloproteinases and diabetic foot ulcers: the ratio of MMP-1 to TIMP-1 is a predictor of wound healing, Diabetic Medicine, 25 (2008) 419-426.

[28] T.N. Demidova-Rice, J.T. Durham, I.M. Herman, Wound Healing Angiogenesis: Innovations and Challenges in Acute and Chronic Wound Healing, Advances in Wound Care, 1 (2012) 17-22.

[29] P.R. Hiebert, D.J. Granville, Granzyme B in injury, inflammation, and repair, Trends in Molecular Medicine, 18 (2012) 732-741.

[30] J.G. Powers, L.M. Morton, T.J. Phillips, Dressings for chronic wounds, Dermatologic Therapy, 26 (2013) 197-206.

[31] J.S. Boateng, K.H. Matthews, H.N.E. Stevens, G.M. Eccleston, Wound Healing Dressings and Drug Delivery Systems: A Review, Journal of Pharmaceutical Sciences, 97 (2008) 2892-2923.

[32] L.I.F. Moura, A.M.A. Dias, E. Carvalho, H.C. de Sousa, Recent advances on the development of wound dressings for diabetic foot ulcer treatment—A review, Acta Biomaterialia, 9 (2013) 7093-7114.

[33] A.S. Halim, T.L. Khoo, S.J. Mohd. Yussof, Biologic and synthetic skin substitutes: An overview, Indian Journal of Plastic Surgery : Official Publication of the Association of Plastic Surgeons of India, 43 (2010) S23-S28.

[34] K.S. Vyas, H.C. Vasconez, Wound Healing: Biologics, Skin Substitutes, Biomembranes and Scaffolds, Healthcare, 2 (2014) 356-400.

[35] L. Yazdanpanah, M. Nasiri, S. Adarvishi, Literature review on the management of diabetic foot ulcer, World Journal of Diabetes, 6 (2015) 37-53.

[36] C. Hrabchak, L. Flynn, K.A. Woodhouse, Biological skin substitutes for wound cover and closure, Expert Rev Med Devices, 3 (2006) 373-385.

[37] Y.M. Bello, A.F. Falabella, W.H. Eaglstein, Tissue-engineered skin. Current status in wound healing, American Journal Of Clinical Dermatology, 2 (2001) 305-313.

[38] R.A. Kamel, J.F. Ong, E. Eriksson, J.P.E. Junker, E.J. Caterson, Tissue Engineering of Skin, Journal of the American College of Surgeons, 217 (2013) 533-555.

[39] T. Biedermann, S. Boettcher-Haberzeth, E. Reichmann, Tissue engineering of skin for wound coverage, Eur J Pediatr Surg, 23 (2013) 375-382.

[40] J.N. Kearney, Clinical evaluation of skin substitutes, Burns, 27 (2001) 545-551.

[41] F.A. Auger, F. Berthod, V. Moulin, R. Pouliot, L. Germain, Tissue-engineered skin substitutes: from in vitro constructs to in vivo applications, Biotechnol Appl Biochem, 39 (2004) 263-275.

[42] M. Balasubramani, T.R. Kumar, M. Babu, Skin substitutes: a review, Burns, 27 (2001) 534-544.

[43] R.J. Snyder, Treatment of nonhealing ulcers with allografts, Clin Dermatol, 23 (2005) 388-395.

[44] I. Jones, L. Currie, R. Martin, A guide to biological skin substitutes, Br J Plast Surg, 55 (2002) 185-193.

[45] P.G. Shakespeare, The role of skin substitutes in the treatment of burn injuries, Clin Dermatol, 23 (2005) 413-418.

[46] H. Cronin, G. Goldstein, Biologic Skin Substitutes and Their Applications in Dermatology, Dermatologic Surgery, 39 (2013) 30-34.

[47] E.N. Mostow, G.D. Haraway, M. Dalsing, J.P. Hodde, D. King, Effectiveness of an extracellular matrix graft (OASIS Wound Matrix) in the treatment of chronic leg ulcers: A randomized clinical trial, Journal of Vascular Surgery, 41 (2005) 837-843.

[48] M. Brown-Etris, W.D. Cutshall, M.C. Hiles, A new biomaterial derived from small intestine submucosa and developed into a wound matrix device, Wounds - A Compendium of Clinical Research and Practice, 14 (2002) 150-166.

[49] R.A. Santucci, T.D. Barber, Resorbable extracellular matrix grafts in urologic reconstruction, Int Braz J Urol, 31 (2005) 192-203.

[50] J.A. Niezgoda, C.C. Van Gils, R.G. Frykberg, J.P. Hodde, Randomized clinical trial comparing OASIS Wound Matrix to Regranex Gel for diabetic ulcers, Adv Skin Wound Care, 18 (2005) 258-266.

[51] I. Yannas, J. Burke, D. Orgill, E. Skrabut, Wound tissue can utilize a polymeric template to synthesize a functional extension of skin, Science, 215 (1982) 174-176.

[52] J.F. Burke, I.V. Yannas, W.C. Quinby, C.C. Bondoc, W.K. Jung, Successful use of a physiologically acceptable artificial skin in the treatment of extensive burn injury, Annals of Surgery, 194 (1981) 413-428.

[53] H. Debels, M. Hamdi, K. Abberton, W. Morrison, Dermal Matrices and Bioengineered Skin Substitutes: A Critical Review of Current Options, Plastic and Reconstructive Surgery Global Open, 3 (2015) e284.

[54] J.T. Schulz, 3rd, R.G. Tompkins, J.F. Burke, Artificial skin, Annu Rev Med, 51 (2000) 231-244.

[55] K.H. Lee, Tissue-engineered human living skin substitutes: development and clinical application, Yonsei Med J, 41 (2000) 774-779.

[56] K.V. Kavitha, S. Tiwari, V.B. Purandare, S. Khedkar, S.S. Bhosale, A.G. Unnikrishnan, Choice of wound care in diabetic foot ulcer: A practical approach, World Journal of Diabetes, 5 (2014) 546-556.

[57] A. Reyzelman, R.T. Crews, J.C. Moore, L. Moore, J.S. Mukker, S. Offutt, A. Tallis, W.B. Turner, D. Vayser, C. Winters, Clinical effectiveness of an acellular dermal regenerative tissue matrix compared to standard wound management in healing diabetic foot ulcers: a prospective, randomised, multicentre study, International wound journal, 6 (2009) 196-208.

[58] S. Bottcher-Haberzeth, T. Biedermann, E. Reichmann, Tissue engineering of skin, Burns, 36 (2010) 450-460.

[59] J.S. Pieper, T. Hafmans, P.B. van Wachem, M.J.A. van Luyn, L.A. Brouwer, J.H. Veerkamp, T.H. van Kuppevelt, Loading of collagen-heparan sulfate matrices with bFGF promotes angiogenesis and tissue generation in rats, Journal of Biomedical Materials Research, 62 (2002) 185-194.

[60] D.S. Thoma, N. Nänni, G.I. Benic, F.E. Weber, C.H.F. Hämmerle, R.E. Jung, Effect of platelet-derived growth factor-BB on tissue integration of cross-linked and non-cross-linked collagen matrices in a rat ectopic model, Clinical Oral Implants Research, 26 (2015) 263-270.

[61] K. Lee, E.A. Silva, D.J. Mooney, Growth factor delivery-based tissue engineering: general approaches and a review of recent developments, Journal of the Royal Society, Interface / the Royal Society, 8 (2011) 153-170.

[62] B. Buchberger, M. Follmann, D. Freyer, H. Huppertz, A. Ehm, J. Wasem, The importance of growth factors for the treatment of chronic wounds in the case of diabetic foot ulcers, GMS Health Technol Assess, 6 (2010) Doc12.

[63] Y.M. Elçin, V. Dixit, G. Gitnick, Extensive In Vivo Angiogenesis Following Controlled Release of Human Vascular Endothelial Cell Growth Factor: Implications for Tissue Engineering and Wound Healing, Artificial Organs, 25 (2001) 558-565.

[64] S.T.M. Nillesen, P.J. Geutjes, R. Wismans, J. Schalkwijk, W.F. Daamen, T.H. van Kuppevelt, Increased angiogenesis and blood vessel maturation in acellular collagen–heparin scaffolds containing both FGF2 and VEGF, Biomaterials, 28 (2007) 1123-1131.

[65] C.H. Lee, A. Singla, Y. Lee, Biomedical applications of collagen, International journal of pharmaceutics, 221 (2001) 1-22.

[66] D.G. Wallace, J. Rosenblatt, Collagen gel systems for sustained delivery and tissue engineering, Advanced drug delivery reviews, 55 (2003) 1631-1649.

[67] D. S., Global Markets and Technologies for Advanced Drug Delivery Systems, in, 2014, pp. 153.

[68] G. Kevin, Global markets for drug-device combinations, BCC Market Reserach Report, No. PHM045C, ISBN: 0-89336-243-3, in, 2013.

[69] D. Silcock, Collagen-based dressings as therapeutic agents for wound healing, in: L. Andrew (Ed.) Drug-Device Combination Products - Delivery Technologies and Applications, Woodhead Publishing, 2010, pp. 280-310.

[70] F. Peter, Collagen Structure and Mechanics, in: F. Peter (Ed.) Collagen Structure and Mechanics: an Introduction, Springer Science + Business Media, LLC, New York, 2008.

[71] K. Gelse, E. Poschl, T. Aigner, Collagens--structure, function, and biosynthesis, Advanced drug delivery reviews, 55 (2003) 1531-1546.

[72] D.G. Wallace, J. Rosenblatt, Collagen gel systems for sustained delivery and tissue engineering, Advanced Drug Delivery Reviews, 55 (2003) 1631-1649.

[73] K. Fujioka, M. Maeda, T. Hojo, A. Sano, Protein release from collagen matrices, Advanced Drug Delivery Reviews, 31 (1998) 247-266.

[74] M. Elder, Markets for Advanced Wound Management Technologies, in, BCC Research, Wellesley, MA, USA, 2014.

[75] S.H. De Paoli Lacerda, B. Ingber, N. Rosenzweig, Structure-release rate correlation in collagen gels containing fluorescent drug analog, Biomaterials, 26 (2005) 7164-7172.

[76] P.B. Malafaya, G.A. Silva, R.L. Reis, Natural-origin polymers as carriers and scaffolds for biomolecules and cell delivery in tissue engineering applications, Advanced drug delivery reviews, 59 (2007) 207-233.

[77] L. Ma, C. Gao, Z. Mao, J. Zhou, J. Shen, Enhanced biological stability of collagen porous scaffolds by using amino acids as novel cross-linking bridges, Biomaterials, 25 (2004) 2997-3004.

[78] K.P. Rao, Recent developments of collagen-based materials for medical applications and drug delivery systems, Journal of biomaterials science. Polymer edition, 7 (1995) 623-645.

[79] M.E. Nimni, D. Myers, D. Ertl, B. Han, Factors which affect the calcification of tissue-derived bioprostheses, Journal of biomedical materials research, 35 (1997) 531-537.

[80] L.L. Huang-Lee, D.T. Cheung, M.E. Nimni, Biochemical changes and cytotoxicity associated with the degradation of polymeric glutaraldehyde derived crosslinks, Journal of biomedical materials research, 24 (1990) 1185-1201.

[81] P.B. van Wachem, M.J. van Luyn, L.H. Olde Damink, P.J. Dijkstra, J. Feijen, P. Nieuwenhuis, Biocompatibility and tissue regenerating capacity of crosslinked dermal sheep collagen, Journal of biomedical materials research, 28 (1994) 353-363.

[82] S.A. Sell, P.S. Wolfe, K. Garg, J.M. McCool, I.A. Rodriguez, G.L. Bowlin, The Use of Natural Polymers in Tissue Engineering: A Focus on Electrospun Extracellular Matrix Analogues, Polymers, 2 (2010) 522-553.

[83] J.K. Law, J.R. Parsons, F.H. Silver, A.B. Weiss, An evaluation of purified reconstituted type 1 collagen fibers, Journal of biomedical materials research, 23 (1989) 961-977.

[84] M.J. Morykwas, In vitro properties of crosslinked, reconstituted collagen sheets, Journal of biomedical materials research, 24 (1990) 1105-1110.

[85] A. Simionescu, D. Simionescu, R. Deac, Lysine-enhanced glutaraldehyde crosslinking of collagenous biomaterials, J Biomed Mater Res, 25 (1991) 1495-1505.

[86] Q. Jiang, N. Reddy, S. Zhang, N. Roscioli, Y. Yang, Water-stable electrospun collagen fibers from a non-toxic solvent and crosslinking system, J Biomed Mater Res A, (2012).

[87] J.D. Berglund, M.M. Mohseni, R.M. Nerem, A. Sambanis, A biological hybrid model for collagen-based tissue engineered vascular constructs, Biomaterials, 24 (2003) 1241-1254.

[88] W.M. Elbjeirami, E.O. Yonter, B.C. Starcher, J.L. West, Enhancing mechanical properties of tissue-engineered constructs via lysyl oxidase crosslinking activity, Journal of biomedical materials research. Part A, 66 (2003) 513-521.

[89] M. Ehrbar, V.G. Djonov, C. Schnell, S.A. Tschanz, G. Martiny-Baron, U. Schenk, J. Wood, P.H. Burri, J.A. Hubbell, A.H. Zisch, Cell-demanded liberation of VEGF121 from fibrin implants induces local and controlled blood vessel growth, Circulation research, 94 (2004) 1124-1132.

[90] N.K. Mohtaram, A. Montgomery, S.M. Willerth, Biomaterial-based drug delivery systems for the controlled release of neurotrophic factors, Biomedical materials, 8 (2013) 022001.

[91] R.A. Brown, Direct collagen-material engineering for tissue fabrication, Tissue engineering. Part A, 19 (2013) 1495-1498.

[92] R.R. Chen, D.J. Mooney, Polymeric growth factor delivery strategies for tissue engineering, Pharmaceutical research, 20 (2003) 1103-1112.

[93] N.X. Wang, H.A. von Recum, Affinity-based drug delivery, Macromolecular bioscience, 11 (2011) 321-332.

[94] M. Markowicz, A. Heitland, G.C. Steffens, N. Pallua, Effects of modified collagen matrices on human umbilical vein endothelial cells, The International journal of artificial organs, 28 (2005) 1251-1258.

[95] A.L. Weiner, S.S. Carpenter-Green, E.C. Soehngen, R.P. Lenk, M.C. Popescu, Liposome-collagen gel matrix: a novel sustained drug delivery system, Journal of pharmaceutical sciences, 74 (1985) 922-925.

[96] M.J. Wissink, R. Beernink, J.S. Pieper, A.A. Poot, G.H. Engbers, T. Beugeling, W.G. van Aken, J. Feijen, Immobilization of heparin to EDC/NHS-crosslinked collagen. Characterization and in vitro evaluation, Biomaterials, 22 (2001) 151-163.

[97] M.J. Wissink, R. Beernink, A.A. Poot, G.H. Engbers, T. Beugeling, W.G. van Aken, J. Feijen, Improved endothelialization of vascular grafts by local release of growth factor from heparinized collagen matrices, Journal of controlled release : official journal of the Controlled Release Society, 64 (2000) 103-114.

[98] G.C. Steffens, C. Yao, P. Prevel, M. Markowicz, P. Schenck, E.M. Noah, N. Pallua, Modulation of angiogenic potential of collagen matrices by covalent incorporation of heparin and loading with vascular endothelial growth factor, Tissue engineering, 10 (2004) 1502-1509.

[99] G. Grieb, A. Groger, A. Piatkowski, M. Markowicz, G.C. Steffens, N. Pallua, Tissue substitutes with improved angiogenic capabilities: an in vitro investigation with endothelial cells and endothelial progenitor cells, Cells, tissues, organs, 191 (2010) 96-104.

[100] H. Bentz, J.A. Schroeder, T.D. Estridge, Improved local delivery of TGF-beta2 by binding to injectable fibrillar collagen via difunctional polyethylene glycol, Journal of biomedical materials research, 39 (1998) 539-548.

[101] R. Tu, S.H. Shen, D. Lin, C. Hata, K. Thyagarajan, Y. Noishiki, R.C. Quijano, Fixation of Bioprosthetic Tissues with Monofunctional and Multifunctional Polyepoxy Compounds, Journal of Biomedical Materials Research, 28 (1994) 677-684.

[102] L.H.H. Olde Damink, P.J. Dijkstra, M.J.A. van Luyn, P.B. van Wachem, P. Nieuwenhuis, J. Feijen, Cross-linking of dermal sheep collagen using a water-soluble carbodiimide, Biomaterials, 17 (1996) 765-773.

[103] W. Friess, Collagen – biomaterial for drug delivery1, European Journal of Pharmaceutics and Biopharmaceutics, 45 (1998) 113-136.

[104] Z. Ruszczak, W. Friess, Collagen as a carrier for on-site delivery of antibacterial drugs, Advanced Drug Delivery Reviews, 55 (2003) 1679-1698.

[105] S. Guo, L.A. DiPietro, Factors Affecting Wound Healing, Journal of Dental Research, 89 (2010) 219-229.

[106] A.K. Piez, Collagen, in: M.H. F. (Ed.) Encyclopedia of Polymer Science and Engineering, John Wiley and Sons, New York, 1985, pp. 699-727.

[107] D.I. Zeugolis, M. Raghunath, 2.215 - Collagen: Materials Analysis and Implant Uses, in: D. Editor-in-Chief: Paul (Ed.) Comprehensive Biomaterials, Elsevier, Oxford, 2011, pp. 261-278.

[108] J. Jokinen, E. Dadu, P. Nykvist, J. Käpylä, D.J. White, J. Ivaska, P. Vehviläinen, H. Reunanen, H. Larjava, L. Häkkinen, J. Heino, Integrin-mediated Cell Adhesion to Type I Collagen Fibrils, Journal of Biological Chemistry, 279 (2004) 31956-31963.

[109] A. Bhattacharjee, M. Bansal, Collagen structure: the Madras triple helix and the current scenario, IUBMB life, 57 (2005) 161-172.

[110] J.P. Borel, J.C. Monboisse, [Collagens: why such a structural complexity?], Comptes rendus des seances de la Societe de biologie et de ses filiales, 187 (1993) 124-142.

[111] C. Hellmich, F.J. Ulm, Are mineralized tissues open crystal foams reinforced by crosslinked collagen? Some energy arguments, Journal of biomechanics, 35 (2002) 1199-1212.

[112] R. Puxkandl, I. Zizak, O. Paris, J. Keckes, W. Tesch, S. Bernstorff, P. Purslow, P. Fratzl, Viscoelastic properties of collagen: synchrotron radiation investigations and structural model, Philosophical transactions of the Royal Society of London. Series B, Biological sciences, 357 (2002) 191-197.

[113] L. Bozec, M. Horton, Topography and mechanical properties of single molecules of type I collagen using atomic force microscopy, Biophysical journal, 88 (2005) 4223-4231.

[114] S. Ricard-Blum, F. Ruggiero, The collagen superfamily: from the extracellular matrix to the cell membrane, Pathologie-biologie, 53 (2005) 430-442.

[115] C.F. Whittington, Matrix-guided 3D lumenized vessel network formation and stabilization by endothelial colony forming cells: Role of collagen intermolecular cross-links, in, Purdue University, Ann Arbor, 2012, pp. 156.

[116] K.M. Blum, T. Novak, L. Watkins, C.P. Neu, J.M. Wallace, Z.R. Bart, S.L. Voytik-Harbin, Acellular and cellular high-density, collagen-fibril constructs with suprafibrillar organization, Biomaterials Science, 4 (2016) 711-723.

[117] B.d.C. J. Rossert, Type I collagen: structure, synthesis and regulation, in: L.G.R. J. P. Bilezkian, G. A. Rodan (Ed.) Principles in Bone Biology, Academic Press, Orlando, 2002, pp. 189-210.

[118] R.G. Paul, A.J. Bailey, Chemical stabilisation of collagen as a biomimetic, TheScientificWorldJournal, 3 (2003) 138-155.

[119] W.J.-J. Eyre David, Collagen Cross-Links, in: Top Curr Chem, Springer-Verlag Berlin Heidelberg, 2005, pp. 207-229.

[120] S.T. Kreger, B.J. Bell, J. Bailey, E. Stites, J. Kuske, B. Waisner, S.L. Voytik-Harbin, Polymerization and matrix physical properties as important design considerations for soluble collagen formulations, Biopolymers, 93 (2010) 690-707.

[121] C.F. Whittington, E. Brandner, K.Y. Teo, B. Han, E. Nauman, S.L. Voytik-Harbin, Oligomers Modulate Interfibril Branching and Mass Transport Properties of Collagen Matrices, Microscopy and microanalysis : the official journal of Microscopy Society of America, Microbeam Analysis Society, Microscopical Society of Canada, (2013) 1-11.

[122] K.E. Kadler, D.F. Holmes, J.A. Trotter, J.A. Chapman, Collagen fibril formation, The Biochemical journal, 316 (Pt 1) (1996) 1-11.

[123] C.F. Whittington, M.C. Yoder, S.L. Voytik-Harbin, Collagen-Polymer Guidance of Vessel Network Formation and Stabilization by Endothelial Colony Forming Cells In Vitro, Macromolecular bioscience, 13 (2013) 10.1002/mabi.201300128.

[124] A.L. Cronlund, B.D. Smith, H.M. Kagan, Binding of lysyl oxidase to fibrils of type I collagen, Connect Tissue Res, 14 (1985) 109-119.

[125] S.L. Voytik-Harbin, B. Han, Collagen-Cell Interactions in Three-Dimensional Microenvironments, in: Handbook of Imaging in Biological Mechanics, CRC Press, 2014, pp. 261-274.

[126] C.C.R. Fu, E. Shek, J.C. Fleitman, D.M.C. Leung, Collagen containing ophthalmic formulation, in, Google Patents, 1991.

[127] J.K. Milani, I. Verbukh, U. Pleyer, H. Sumner, S.A. Adamu, H.P. Halabi, H.J. Chou, D.A. Lee, B.J. Mondino, Collagen shields impregnated with gentamicin-dexamethasone as a potential drug delivery device, Am J Ophthalmol, 116 (1993) 622-627.

[128] H.-O. Ho, L.-H. Lin, M.-T. Sheu, Characterization of collagen isolation and application of collagen gel as a drug carrier, Journal of Controlled Release, 44 (1997) 103-112.

[129] G.J. Angella, M.B. Sherwood, L. Balasubramanian, J.W. Doyle, M.F. Smith, G. van Setten, M. Goldstein, G.S. Schultz, Enhanced short-term plasmid transfection of filtration surgery tissues, Investigative ophthalmology & visual science, 41 (2000) 4158-4162.

[130] C.E. Willoughby, M. Batterbury, S.B. Kaye, Collagen corneal shields, Surv Ophthalmol, 47 (2002) 174-182.

[131] Y. Agban, J. Lian, S. Prabakar, A. Seyfoddin, I.D. Rupenthal, Nanoparticle cross-linked collagen shields for sustained delivery of pilocarpine hydrochloride, International Journal of Pharmaceutics, 501 (2016) 96-101.

[132] R.B. Phinney, S.D. Schwartz, D.A. Lee, B.J. Mondino, Collagen-shield delivery of gentamicin and vancomycin, Arch Ophthalmol, 106 (1988) 1599-1604.

[133] M.R. Sawusch, T.P. O'Brien, J.D. Dick, J.D. Gottsch, Use of collagen corneal shields in the treatment of bacterial keratitis, Am J Ophthalmol, 106 (1988) 279-281.

[134] M.J. Taravella, J. Balentine, D.A. Young, P. Stepp, Collagen shield delivery of ofloxacin to the human eye, J Cataract Refract Surg, 25 (1999) 562-565.

[135] R.H. Marmer, Therapeutic and protective properties of the corneal collagen shield, J Cataract Refract Surg, 14 (1988) 496-499.

[136] T.P. Paul, R. Emmatty, J.J. Pulikkottil, A.A. Rahman, S.A. Kumar, N. George, Comparative Evaluation of Sustained Release Collagen Device Containing 5% Metronidazole (Metrogene) along With and Without Scaling and Root Planing at Regular Intervals with Treatment of Chronic Periodontitis: A Case Control Study, Journal of International Oral Health : JIOH, 7 (2015) 18-22.

[137] J. Choi, H. Park, T. Kim, Y. Jeong, M.H. Oh, T. Hyeon, A.A. Gilad, K.H. Lee, Engineered collagen hydrogels for the sustained release of biomolecules and imaging agents: promoting the growth of human gingival cells, International Journal of Nanomedicine, 9 (2014) 5189-5201.

[138] P.M. Royce, T. Kato, K. Ohsaki, A. Miura, The enhancement of cellular infiltration and vascularisation of a collagenous dermal implant in the rat by platelet-derived growth factor BB, Journal of dermatological science, 10 (1995) 42-52.

[139] M.G. Marks, C. Doillon, F.H. Silver, Effects of fibroblasts and basic fibroblast growth factor on facilitation of dermal wound healing by type I collagen matrices, Journal of biomedical materials research, 25 (1991) 683-696.

[140] G. Rath, T. Hussain, G. Chauhan, T. Garg, A.K. Goyal, Collagen nanofiber containing silver nanoparticles for improved wound-healing applications, J Drug Target, 24 (2016) 520-529.

[141] R. Sripriya, M.S. Kumar, M.R. Ahmed, P.K. Sehgal, Collagen bilayer dressing with ciprofloxacin, an effective system for infected wound healing, J Biomater Sci Polym Ed, 18 (2007) 335-351.

[142] L.G. Jorgensen, T.S. Sorensen, J.E. Lorentzen, Clinical and pharmacokinetic evaluation of gentamycin containing collagen in groin wound infections after vascular reconstruction, European journal of vascular surgery, 5 (1991) 87-91.

[143] H.J. Rutten, P.H. Nijhuis, Prevention of wound infection in elective colorectal surgery by local application of a gentamicin-containing collagen sponge, The European journal of surgery. Supplement. : = Acta chirurgica. Supplement, (1997) 31-35.

[144] V. Mendel, H.J. Simanowski, H.C. Scholz, H. Heymann, Therapy with gentamicin-PMMA beads, gentamicin-collagen sponge, and cefazolin for experimental osteomyelitis due to Staphylococcus aureus in rats, Arch Orthop Trauma Surg, 125 (2005) 363-368.

[145] S. Govender, C. Csimma, H.K. Genant, A. Valentin-Opran, Y. Amit, R. Arbel, H. Aro, D. Atar, M. Bishay, M.G. Borner, P. Chiron, P. Choong, J. Cinats, B. Courtenay, R. Feibel, B. Geulette, C. Gravel, N. Haas, M. Raschke, E. Hammacher, D. van der Velde, P. Hardy, M. Holt, C. Josten, R.L. Ketterl, B. Lindeque, G. Lob, H. Mathevon, G. McCoy, D. Marsh, R. Miller, E. Munting, S. Oevre, L. Nordsletten, A. Patel, A. Pohl, W. Rennie, P. Reynders, P.M. Rommens, J. Rondia, W.C. Rossouw, P.J. Daneel, S. Ruff, A. Ruter, S. Santavirta, T.A. Schildhauer, C. Gekle, R. Schnettler, D. Segal, H. Seiler, R.B. Snowdowne, J. Stapert, G. Taglang, R. Verdonk, L. Vogels, A. Weckbach, A. Wentzensen, T. Wisniewski, Recombinant human bone morphogenetic protein-2 for treatment of open tibial fractures: a prospective, controlled, randomized study of four hundred and fifty patients, The Journal of bone and joint surgery. American volume, 84-A (2002) 2123-2134.

[146] N. Morimoto, K. Yoshimura, M. Niimi, T. Ito, R. Aya, J. Fujitaka, H. Tada, S. Teramukai, T. Murayama, C. Toyooka, K. Miura, S. Takemoto, N. Kanda, K. Kawai, M. Yokode, A. Shimizu, S. Suzuki, Novel collagen/gelatin scaffold with sustained release of basic fibroblast growth factor: clinical trial for chronic skin ulcers, Tissue Eng Part A, 19 (2013) 1931-1940.

[147] M. Chvapil, Collagen sponge: theory and practice of medical applications, J Biomed Mater Res, 11 (1977) 721-741.

[148] M. Geiger, R.H. Li, W. Friess, Collagen sponges for bone regeneration with rhBMP-2, Adv Drug Deliv Rev, 55 (2003) 1613-1629.

[149] W. Friess, H. Uludag, S. Foskett, R. Biron, Bone regeneration with recombinant human bone morphogenetic protein-2 (rhBMP-2) using absorbable collagen sponges (ACS): influence of processing on ACS characteristics and formulation, Pharm Dev Technol, 4 (1999) 387-396.

[150] S.D. Glassman, L. Carreon, M. Djurasovic, M.J. Campbell, R.M. Puno, J.R. Johnson, J.R. Dimar, Posterolateral lumbar spine fusion with INFUSE bone graft, Spine J, 7 (2007) 44-49.

[151] S.L. Cusack, P. Reginald, L. Hemsen, E. Umerah, The pharmacokinetics and safety of an intraoperative bupivacaine-collagen implant (XaraColl(®)) for postoperative analgesia in women following total abdominal hysterectomy, Journal of Pain Research, 6 (2013) 151-159.

[152] M. Zilberman, J.J. Elsner, Antibiotic-eluting medical devices for various applications, Journal of Controlled Release, 130 (2008) 202-215.

[153] Y. Ikada, Challenges in tissue engineering, Journal of the Royal Society Interface, 3 (2006) 589-601.

[154] C. Dong, Y. Lv, Application of Collagen Scaffold in Tissue Engineering: Recent Advances and New Perspectives, Polymers, 8 (2016).

[155] F.J. O'Brien, Biomaterials & scaffolds for tissue engineering, Materials Today, 14 (2011) 88-95.

[156] M. Sahiner, D. Alpaslan, B. Bitlisli, Collagen-based hydrogel films as drug-delivery devices with antimicrobial properties, Polymer Bulletin, 71 (2014) 3017-3033.

[157] Z. Wachol-Drewek, M. Pfeiffer, E. Scholl, Comparative investigation of drug delivery of collagen implants saturated in antibiotic solutions and a sponge containing gentamicin, Biomaterials, 17 (1996) 1733-1738.

[158] J.M. Wu, Y.Y. Xu, Z.H. Li, X.Y. Yuan, P.F. Wang, X.Z. Zhang, Y.Q. Liu, J. Guan, Y. Guo, R.X. Li, H. Zhang, Heparin-functionalized collagen matrices with controlled release of basic fibroblast growth factor, J Mater Sci Mater Med, 22 (2011) 107-114.

[159] Z. Wachol-Drewek, M. Pfeiffer, E. Scholl, Comparative investigation of drug delivery of collagen implants saturated in antibiotic solutions and a sponge containing gentamicin, Biomaterials, 17 (1996) 1733-1738.

[160] W. Friess, G. Lee, M.J. Groves, Insoluble collagen matrices for prolonged delivery of proteins, Pharmaceutical development and technology, 1 (1996) 185-193.

[161] H. Sato, H. Kitazawa, I. Adachi, I. Horikoshi, Microdialysis assessment of microfibrous collagen containing a P-glycoprotein-mediated transport inhibitor, cyclosporine A, for local delivery of etoposide, Pharmaceutical research, 13 (1996) 1565-1569.

[162] A.O. Brightman, B.P. Rajwa, J.E. Sturgis, M.E. McCallister, J.P. Robinson, S.L. Voytik-Harbin, Time-lapse confocal reflection microscopy of collagen fibrillogenesis and extracellular matrix assembly in vitro, Biopolymers, 54 (2000) 222-234.

[163] Characterization and standardization of polymerizable collagen-based products and associated collagen-cell interactions, in, ASTM International: 2014, West Conshohocken, PA, 2014.

[164] N.T. Blum Kevin, Watkins Lauren, Neu Corey, Wallace Joseph, Bart Zachary, Voytik-Harbin Sherry, Acellular and cellular high-density, collagen-fibril constructs with suprafibrillar organization, Biomater. Sci., 4 (2016) 711-723.

[165] J. Siepmann, F. Siepmann, Modeling of diffusion controlled drug delivery, Journal of controlled release : official journal of the Controlled Release Society, 161 (2012) 351-362.

[166] B. Li, K.V. Brown, J.C. Wenke, S.A. Guelcher, Sustained release of vancomycin from polyurethane scaffolds inhibits infection of bone wounds in a rat femoral segmental defect model, Journal of Controlled Release, 145 (2010) 221-230.

[167] S. Dash, P.N. Murthy, L. Nath, P. Chowdhury, Kinetic modeling on drug release from controlled drug delivery systems, Acta poloniae pharmaceutica, 67 (2010) 217-223.

[168] K. Jørgensen, L. Jacobsen, Factorial design used for ruggedness testing of flow through cell dissolution method by means of Weibull transformed drug release profiles, International Journal of Pharmaceutics, 88 (1992) 23-29.

[169] F. Langenbucher, Parametric representation of dissolution-rate curves by the RRSBW distribution, Pharmazeutische Industie, 38 (1976) 472-477.

[170] V. Papadopoulou, K. Kosmidis, M. Vlachou, P. Macheras, On the use of the Weibull function for the discernment of drug release mechanisms, International journal of pharmaceutics, 309 (2006) 44-50.

[171] J.M. McPherson, D.G. Wallace, S.J. Sawamura, A. Conti, R.A. Condell, S. Wade, K.A. Piez, Collagen fibrillogenesis in vitro: a characterization of fibril quality as a function of assembly conditions, Coll Relat Res, 5 (1985) 119-135.

[172] S.T. Kreger, S.L. Voytik-Harbin, Hyaluronan concentration within a 3D collagen matrix modulates matrix viscoelasticity, but not fibroblast response, Matrix Biol, 28 (2009) 336-346.

[173] G.C. Wood, The formation of fibrils from collagen solutions. 2. A mechanism of collagen-fibril formation, Biochem J, 75 (1960) 598-605.

[174] G.C. Wood, M.K. Keech, The formation of fibrils from collagen solutions. 1. The effect of experimental conditions: kinetic and electron-microscope studies, The Biochemical journal, 75 (1960) 588-598.

[175] B.A. Roeder, K. Kokini, J.E. Sturgis, J.P. Robinson, S.L. Voytik-Harbin, Tensile mechanical properties of three-dimensional type I collagen extracellular matrices with varied microstructure, J Biomech Eng, 124 (2002) 214-222.

[176] K.E. Kadler, D.F. Holmes, J.A. Trotter, J.A. Chapman, Collagen fibril formation, Biochem J, 316 (Pt 1) (1996) 1-11.

[177] C.F. Whittington, E. Brandner, K.Y. Teo, B. Han, E. Nauman, S.L. Voytik-Harbin, Oligomers modulate interfibril branching and mass transport properties of collagen matrices, Microscopy and microanalysis : the official journal of Microscopy Society of America, Microbeam Analysis Society, Microscopical Society of Canada, 19 (2013) 1323-1333.

[178] E.A. Abou Neel, L. Bozec, J.C. Knowles, O. Syed, V. Mudera, R. Day, J.K. Hyun, Collagen — Emerging collagen based therapies hit the patient, Advanced Drug Delivery Reviews, 65 (2013) 429-456.

[179] C.F. Whittington, E. Brandner, K.Y. Teo, B. Han, E. Nauman, S.L. Voytik-Harbin, Oligomers Modulate Interfibril Branching and Mass Transport Properties of Collagen Matrices, Microscopy and Microanalysis, 19 (2013) 1323-1333.

[180] C.F. Whittington, M.C. Yoder, S.L. Voytik-Harbin, Collagen-Polymer Guidance of Vessel Network Formation and Stabilization by Endothelial Colony Forming Cells In Vitro, Macromolecular bioscience, (2013).

[181] S. Park, C. Whittington, S.L. Voytik-Harbin, B. Han, Microstructural Parameter-Based Modeling for Transport Properties of Collagen Matrices, Journal of Biomechanical Engineering, 137 (2015) 061003-061003.

[182] D. Fan, E.E. Creemers, Z. Kassiri, Matrix as an interstitial transport system, Circ Res, 114 (2014) 889-902.

[183] M. Miron-Mendoza, J. Seemann, F. Grinnell, The differential regulation of cell motile activity through matrix stiffness and porosity in three dimensional collagen matrices, Biomaterials, 31 (2010) 6425-6435.

[184] N.J. Trengove, M.C. Stacey, S. MacAuley, N. Bennett, J. Gibson, F. Burslem, G. Murphy, G. Schultz, Analysis of the acute and chronic wound environments: the role of proteases and their inhibitors, Wound Repair Regen, 7 (1999) 442-452.

[185] M. Romanelli, A.M. Gilligan, C.R. Waycaster, V. Dini, Difficult-to-heal wounds of mixed arterial/venous and venous etiology: a cost-effectiveness analysis of extracellular matrix, ClinicoEconomics and Outcomes Research: CEOR, 8 (2016) 153-161.

[186] A. Vasconcelos, A. Cavaco-Paulo, Wound dressings for a proteolytic-rich environment, Applied Microbiology and Biotechnology, 90 (2011) 445-460.

[187] I. Metzmacher, F. Radu, M. Bause, P. Knabner, W. Friess, A model describing the effect of enzymatic degradation on drug release from collagen minirods, European Journal of Pharmaceutics and Biopharmaceutics, 67 (2007) 349-360.

[188] R. Lobmann, A. Ambrosch, G. Schultz, K. Waldmann, S. Schiweck, H. Lehnert, Expression of matrix-metalloproteinases and their inhibitors in the wounds of diabetic and non-diabetic patients, Diabetologia, 45 (2002) 1011-1016.

[189] M.S. Ågren, C.J. Taplin, J.F. Woessner, W.H. Eagistein, P.M. Mertz, Collagenase in Wound Healing: Effect of Wound Age and Type, Journal of Investigative Dermatology, 99 (1992) 709-714.

[190] G. Koopmans, B. Hasse, N. Sinis, Chapter 19 The Role of Collagen in Peripheral Nerve Repair, in: International Review of Neurobiology, Academic Press, 2009, pp. 363-379.

[191] V. Ferraro, M. Anton, V. Santé-Lhoutellier, The "sisters" α-helices of collagen, elastin and keratin recovered from animal by-products: Functionality, bioactivity and trends of application, Trends in Food Science & Technology, 51 (2016) 65-75.

[192] C. Yao, M. Roderfeld, T. Rath, E. Roeb, J. Bernhagen, G. Steffens, The impact of proteinase-induced matrix degradation on the release of VEGF from heparinized collagen matrices, Biomaterials, 27 (2006) 1608-1616.

[193] J. Rosenblatt, W. Rhee, D. Wallace, The effect of collagen fiber size distribution on the release rate of proteins from collagen matrices by diffusion, Journal of Controlled Release, 9 (1989) 195-203.

[194] P.A. Vasquez, M.G. Forest, Complex Fluids and Soft Structures in the Human Body, in: E.S. Spagnolie (Ed.) Complex Fluids in Biological Systems: Experiment, Theory, and Computation, Springer New York, New York, NY, 2015, pp. 53-110.

[195] K.A. Watkins, R. Chen, pH-responsive, lysine-based hydrogels for the oral delivery of a wide size range of molecules, International Journal of Pharmaceutics, 478 (2015) 496-503.

[196] F.A. Radu, M. Bause, P. Knabner, G.W. Lee, W.C. Friess, Modeling of drug release from collagen matrices, Journal of pharmaceutical sciences, 91 (2002) 964-972.

[197] H. Nagase, J.F. Woessner, Matrix Metalloproteinases, Journal of Biological Chemistry, 274 (1999) 21491-21494.

[198] L.M. Coussens, Z. Werb, Matrix metal loproteinases and the development of cancer, Chemistry & Biology, 3 895-904.

[199] G. Rosenblum, P.E. Van den Steen, S.R. Cohen, A. Bitler, D.D. Brand, G. Opdenakker, I. Sagi, Direct Visualization of Protease Action on Collagen Triple Helical Structure, PLoS ONE, 5 (2010) e11043.

[200] L.M. Mullen, S.M. Best, R.A. Brooks, S. Ghose, J.H. Gwynne, J. Wardale, N. Rushton, R.E. Cameron, Binding and Release Characteristics of Insulin-Like Growth Factor-1 from a Collagen–Glycosaminoglycan Scaffold, Tissue Engineering. Part C, Methods, 16 (2010) 1439-1448.

[201] H.S. Nanda, S. Chen, Q. Zhang, N. Kawazoe, G. Chen, Collagen Scaffolds with Controlled Insulin Release and Controlled Pore Structure for Cartilage Tissue Engineering, BioMed Research International, 2014 (2014) 623805.

[202] I. d'Angelo, O. Oliviero, F. Ungaro, F. Quaglia, P.A. Netti, Engineering strategies to control vascular endothelial growth factor stability and levels in a collagen matrix for angiogenesis: The role of heparin sodium salt and the PLGA-based microsphere approach, Acta Biomaterialia, 9 (2013) 7389-7398.

[203] B. Wen, M. Karl, D. Pendrys, D. Shafer, M. Freilich, L. Kuhn, An evaluation of BMP-2 delivery from scaffolds with miniaturized dental implants in a novel rat mandible model, Journal of Biomedical Materials Research Part B: Applied Biomaterials, 97B (2011) 315-326.

[204] T. Kawashima, N. Nagai, H. Kaji, N. Kumasaka, H. Onami, Y. Ishikawa, N. Osumi, M. Nishizawa, T. Abe, A scalable controlled-release device for transscleral drug delivery to the retina, Biomaterials, 32 (2011) 1950-1956.

[205] N. Nagai, N. Kumasaka, T. Kawashima, H. Kaji, M. Nishizawa, T. Abe, Preparation and characterization of collagen microspheres for sustained release of VEGF, Journal of materials science. Materials in medicine, 21 (2010) 1891-1898.

[206] J.M. Wu, Y.Y. Xu, Z.H. Li, X.Y. Yuan, P.F. Wang, X.Z. Zhang, Y.Q. Liu, J. Guan, Y. Guo, R.X. Li, H. Zhang, Heparin-functionalized collagen matrices with controlled release of basic fibroblast growth factor, Journal of Materials Science: Materials in Medicine, 22 (2011) 107-114.

[207] R.A. Siegel, M.J. Rathbone, Overview of Controlled Release Mechanisms, in: J. Siepmann, R.A. Siegel, M.J. Rathbone (Eds.) Fundamentals and Applications of Controlled Release Drug Delivery, Springer US, Boston, MA, 2012, pp. 19-43.

[208] G. Frenning, Modelling drug release from inert matrix systems: From moving-boundary to continuous-field descriptions, International Journal of Pharmaceutics, 418 (2011) 88-99.

[209] N.A. Peppas, B. Narasimhan, Mathematical models in drug delivery: How modeling has shaped the way we design new drug delivery systems, Journal of Controlled Release, 190 (2014) 75-81.

[210] R.V. Joshi, C.E. Nelson, K.M. Poole, M.C. Skala, C.L. Duvall, Dual pH- and Temperature-responsive Microparticles for Protein Delivery to Ischemic Tissues, Acta biomaterialia, 9 (2013) 6526-6534.

[211] M. Ye, S. Kim, K. Park, Issues in long-term protein delivery using biodegradable microparticles, Journal of controlled release : official journal of the Controlled Release Society, 146 (2010) 241-260.

[212] M.V.S. Varma, A.M. Kaushal, A. Garg, S. Garg, Factors affecting mechanism and kinetics of drug release from matrix-based oral controlled drug delivery systems, American Journal of Drug Delivery, 2 (2004) 43-57.

[213] S. Dash, P.N. Murthy, L. Nath, P. Chowdhury, Kinetic modeling on drug release from controlled drug delivery systems, Acta Pol Pharm, 67 (2010) 217-223.

[214] M. Otsuka, H. Nakagawa, A. Ito, W.I. Higuchi, Effect of geometrical structure on drug release rate of a three-dimensionally perforated porous apatite/collagen composite cement, J Pharm Sci, 99 (2010) 286-292.

[215] R. Gurny, E. Doelker, N.A. Peppas, Modelling of sustained release of water-soluble drugs from porous, hydrophobic polymers, Biomaterials, 3 (1982) 27-32.

[216] N.A. Peppas, A model of dissolution-controlled solute release from porous drug delivery polymeric systems, J Biomed Mater Res, 17 (1983) 1079-1087.

[217] R.W. Korsmeyer, R. Gurny, E. Doelker, P. Buri, N.A. Peppas, Mechanisms of potassium chloride release from compressed, hydrophilic, polymeric matrices: effect of entrapped air, J Pharm Sci, 72 (1983) 1189-1191.

[218] N.A. Peppas, R. Gurny, [Relation between the structure of polymers and the controlled release of active ingredients], Pharm Acta Helv, 58 (1983) 2-8.

[219] T. Higuchi, Rate of Release of Medicaments from Ointment Bases Containing Drugs in Suspension, Journal of Pharmaceutical Sciences, 50 (1961) 874-875.

[220] P.L. Ritger, N.A. Peppas, A simple equation for description of solute release I. Fickian and non-fickian release from non-swellable devices in the form of slabs, spheres, cylinders or discs, Journal of Controlled Release, 5 (1987) 23-36.

[221] R.W. Korsmeyer, R. Gurny, E. Doelker, P. Buri, N.A. Peppas, Mechanisms of solute release from porous hydrophilic polymers, International Journal of Pharmaceutics, 15 (1983) 25-35.

[222] N.A. Peppas, J.J. Sahlin, A simple equation for the description of solute release. III. Coupling of diffusion and relaxation, International Journal of Pharmaceutics, 57 (1989) 169-172.

[223] J. Siepmann, N.A. Peppas, Modeling of drug release from delivery systems based on hydroxypropyl methylcellulose (HPMC), Adv Drug Deliv Rev, 48 (2001) 139-157.

[224] K. Kosmidis, E. Rinaki, P. Argyrakis, P. Macheras, Analysis of Case II drug transport with radial and axial release from cylinders, International Journal of Pharmaceutics, 254 (2003) 183-188.

[225] A. Dokoumetzidis, P. Macheras, A century of dissolution research: From Noyes and Whitney to the Biopharmaceutics Classification System, International Journal of Pharmaceutics, 321 (2006) 1-11.

[226] S. Giovagnoli, T. Tsai, P.P. DeLuca, Formulation and Release Behavior of Doxycycline–Alginate Hydrogel Microparticles Embedded into Pluronic F127 Thermogels as a Potential New Vehicle for Doxycycline Intradermal Sustained Delivery, AAPS PharmSciTech, 11 (2010) 212-220.

[227] A. Dokoumetzidis, P. Macheras, IVIVC of controlled release formulations: Physiological–dynamical reasons for their failure, Journal of Controlled Release, 129 (2008) 76-78.

[228] K. Adibkia, M.R.S. Shadbad, A. Nokhodchi, A. Javadzedeh, M. Barzegar-Jalali, J. Barar, G. Mohammadi, Y. Omidi, Piroxicam nanoparticles for ocular delivery: Physicochemical characterization and implementation in endotoxin-induced uveitis, Journal of Drug Targeting, 15 (2007) 407-416.

[229] U. Gbureck, E. Vorndran, J.E. Barralet, Modeling vancomycin release kinetics from microporous calcium phosphate ceramics comparing static and dynamic immersion conditions, Acta Biomaterialia, 4 (2008) 1480-1486.

[230] C.E. Nelson, M.K. Gupta, E.J. Adolph, J.M. Shannon, S.A. Guelcher, C.L. Duvall, Sustained local delivery of siRNA from an injectable scaffold, Biomaterials, 33 (2012) 1154-1161.

[231] A. Karewicz, K. Zasada, K. Szczubiałka, S. Zapotoczny, R. Lach, M. Nowakowska, "Smart" alginate–hydroxypropylcellulose microbeads for controlled release of heparin, International Journal of Pharmaceutics, 385 (2010) 163-169.

[232] J. Forsgren, E. Jämstorp, S. Bredenberg, H. Engqvist, M. Strømme, A ceramic drug delivery vehicle for oral administration of highly potent opioids, Journal of Pharmaceutical Sciences, 99 (2010) 219-226.

[233] S. Hesaraki, F. Moztarzadeh, R. Nemati, N. Nezafati, Preparation and characterization of calcium sulfate–biomimetic apatite nanocomposites for controlled release of antibiotics, Journal of Biomedical Materials Research Part B: Applied Biomaterials, 91B (2009) 651-661.

[234] H. Liu, C. Wang, Q. Gao, J. Chen, B. Ren, X. Liu, Z. Tong, Facile fabrication of well-defined hydrogel beads with magnetic nanocomposite shells, International Journal of Pharmaceutics, 376 (2009) 92-98.

[235] S. Hesaraki, R. Nemati, Cephalexin-loaded injectable macroporous calcium phosphate bone cement, Journal of Biomedical Materials Research Part B: Applied Biomaterials, 89B (2009) 342-352.

[236] A.S. da Silva, C.E. da Rosa Silva, F.R. Paula, F.E.B. da Silva, Discriminative Dissolution Method for Benzoyl Metronidazole Oral Suspension, AAPS PharmSciTech, 17 (2016) 778-786.

[237] A. Azadi, M. Hamidi, M.-R. Rouini, Methotrexate-loaded chitosan nanogels as 'Trojan Horses' for drug delivery to brain: Preparation and in vitro/in vivo characterization, International Journal of Biological Macromolecules, 62 (2013) 523-530.

[238] P.J. Critser, S.T. Kreger, S.L. Voytik-Harbin, M.C. Yoder, Collagen matrix physical properties modulate endothelial colony forming cell derived vessels in vivo, Microvascular research, 80 (2010) 23-30.

[239] S. Ramanujan, A. Pluen, T.D. McKee, E.B. Brown, Y. Boucher, R.K. Jain, Diffusion and convection in collagen gels: implications for transport in the tumor interstitium, Biophysical Journal, 83 (2002) 1650-1660.

[240] F.J. O'Brien, B.A. Harley, M.A. Waller, I.V. Yannas, L.J. Gibson, P.J. Prendergast, The effect of pore size on permeability and cell attachment in collagen scaffolds for tissue engineering, Technol Health Care, 15 (2007) 3-17.

[241] J.M. Stewart, D.S. Schultz, O.T. Lee, M.L. Trinidad, Exogenous collagen cross-linking reduces scleral permeability: modeling the effects of age-related cross-link accumulation, Invest Ophthalmol Vis Sci, 50 (2009) 352-357.

[242] J. Ambati, C.S. Canakis, J.W. Miller, E.S. Gragoudas, A.l. Edwards, D.J. Weissgold, I. Kim, F.o.C. Delori, A.P. Adamis, Diffusion of High Molecular Weight Compounds through Sclera, Investigative Ophthalmology & Visual Science, 41 (2000) 1181-1185.

[243] C. Nicholson, L. Tao, Hindered diffusion of high molecular weight compounds in brain extracellular microenvironment measured with integrative optical imaging, Biophys J, 65 (1993) 2277-2290.

[244] D.L. Gilbert, O. Teruo, M. Teruo, K. Sung Wan, Macromolecular diffusion through collagen membranes, International Journal of Pharmaceutics, 47 (1988) 79-88.

[245] J. Song, J.C. Odekerken, D.W. Lowik, P.M. Lopez-Perez, T.J. Welting, F. Yang, J.A. Jansen, S.C. Leeuwenburgh, Influence of the Molecular Weight and Charge of Antibiotics on Their Release Kinetics From Gelatin Nanospheres, Macromol Biosci, 15 (2015) 901-911.

[246] G. Teodora Tihan, C. Ungureanu, R. Constantin Barbaresso, R. Gabriela Zgârian, I. Rău, A. Meghea, M. Georgiana Albu, M. Violeta Ghica, Chloramphenicol collagen sponges for local drug delivery in dentistry, Comptes Rendus Chimie, 18 (2015) 986-992.

[247] H. Uludag, W. Friess, D. Williams, T. Porter, G. Timony, D. D'Augusta, C. Blake, R. Palmer, B. Biron, J. Wozney, rhBMP-Collagen Sponges as Osteoinductive Devices: Effects of in Vitro Sponge Characteristics and Protein pI on in Vivo rhBMP Pharmacokinetics, Annals of the New York Academy of Sciences, 875 (1999) 369-378.

[248] S.T. Kreger, B.J. Bell, J. Bailey, E. Stites, J. Kuske, B. Waisner, S.L. Voytik-Harbin, "Polymerization and Matrix Physical Properties as Important Design Considerations for Soluble Collagen Formulations", Biopolymers, 93 (2010) 690-707.

[249] in.

[250] J. Cupera, P. Lansky, Z. Sklubalova, Sampling times influence the estimate of parameters in the Weibull dissolution model, Eur J Pharm Sci, 78 (2015) 171-176.

[251] M.J.B. Wissink, R. Beernink, A.A. Poot, G.H.M. Engbers, T. Beugeling, W.G. van Aken, J. Feijen, Improved endothelialization of vascular grafts by local release of growth factor from heparinized collagen matrices, Journal of Controlled Release, 64 (2000) 103-114.

[252] G. Bhakta, Z.X.H. Lim, B. Rai, T. Lin, J.H. Hui, G.D. Prestwich, A.J. van Wijnen, V. Nurcombe, S.M. Cool, The influence of collagen and hyaluronan matrices on the delivery and bioactivity of bone morphogenetic protein-2 and ectopic bone formation, Acta Biomaterialia, 9 (2013) 9098-9106.

[253] R. Groning, C. Cloer, R.S. Muller, Development and in vitro evaluation of expandable gastroretentive dosage forms based on compressed collagen sponges, Pharmazie, 61 (2006) 608-612.

[254] K.M. Ivester, S.B. Adams, G.E. Moore, D.C. Van Sickle, T.B. Lescun, Gentamicin concentrations in synovial fluid obtained from the tarsocrural joints of horses after implantation of gentamicin-impregnated collagen sponges, American Journal of Veterinary Research, 67 (2006) 1519-1526.

[255] Q.L. Loh, C. Choong, Three-Dimensional Scaffolds for Tissue Engineering Applications: Role of Porosity and Pore Size, Tissue Engineering. Part B, Reviews, 19 (2013) 485-502.

[256] S. Lin, L. Hapach, C. Reinhart-King, L. Gu, Towards Tuning the Mechanical Properties of Three-Dimensional Collagen Scaffolds Using a Coupled Fiber-Matrix Model, Materials, 8 (2015) 5254.

[257] M.A. Urello, K.L. Kiick, M.O. Sullivan, A CMP-based method for tunable, cell-mediated gene delivery from collagen scaffolds, Journal of Materials Chemistry B, 2 (2014) 8174-8185.

[258] J. Choi, H. Park, T. Kim, Y. Jeong, M.H. Oh, T. Hyeon, A.A. Gilad, K.H. Lee, Engineered collagen hydrogels for the sustained release of biomolecules and imaging agents: promoting the growth of human gingival cells, International Journal of Nanomedicine, 9 (2014) 5189+.

[259] M. Maeda, S. Tani, A. Sano, K. Fujioka, Microstructure and release characteristics of the minipellet, a collagen-based drug delivery system for controlled release of protein drugs, Journal of controlled release : official journal of the Controlled Release Society, 62 (1999) 313-324.

[260] A. Kandamchira, S. Selvam, N. Marimuthu, S. Kalarical Janardhanan, N.N. Fathima, Influence of functionalized nanoparticles on conformational stability of type I collagen for possible biomedical applications, Materials Science and Engineering: C, 33 (2013) 4985-4988.

[261] I. Metzmacher, F. Radu, M. Bause, P. Knabner, W. Friess, A model describing the effect of enzymatic degradation on drug release from collagen minirods, European journal of pharmaceutics and biopharmaceutics : official journal of Arbeitsgemeinschaft fur Pharmazeutische Verfahrenstechnik e.V, 67 (2007) 349-360.

[262] D. Gopinath, M.S. Kumar, D. Selvaraj, R. Jayakumar, Pexiganan-incorporated collagen matrices for infected wound-healing processes in rat, Journal of Biomedical Materials Research Part A, 73A (2005) 320-331.

[263] M.-A. Lauzon, B. Marcos, N. Faucheux, Effect of initial pBMP-9 loading and collagen concentration on the kinetics of peptide release and a mathematical model of the delivery system, Journal of Controlled Release, 182 (2014) 73-82.

[264] K. Fujioka, Y. Takada, S. Sato, T. Miyata, Novel delivery system for proteins using collagen as a carrier material: the minipellet, Journal of Controlled Release, 33 (1995) 307-315.

[265] M. Maeda, K. Kadota, M. Kajihara, A. Sano, K. Fujioka, Sustained release of human growth hormone (hGH) from collagen film and evaluation of effect on wound healing in db/db mice, Journal of Controlled Release, 77 (2001) 261-272.

[266] N. Saeidi, K.P. Karmelek, J.A. Paten, R. Zareian, E. DiMasi, J.W. Ruberti, Molecular crowding of collagen: A pathway to produce highly-organized collagenous structures, Biomaterials, 33 (2012) 7366-7374.

[267] G. Mosser, A. Anglo, C. Helary, Y. Bouligand, M.-M. Giraud-Guille, Dense tissue-like collagen matrices formed in cell-free conditions, Matrix Biology, 25 (2006) 3-13.

[268] J.L. Puetzer, L.J. Bonassar, High density type I collagen gels for tissue engineering of whole menisci, Acta Biomaterialia, 9 (2013) 7787-7795.

[269] K.R. Johnson, J.L. Leight, V.M. Weaver, Demystifying the effects of a three-dimensional microenvironment in tissue morphogenesis, Methods Cell Biol, 83 (2007) 547-583.

[270] A. Nyga, M. Loizidou, M. Emberton, U. Cheema, A novel tissue engineered three-dimensional in vitro colorectal cancer model, Acta Biomater, 9 (2013) 7917-7926.

[271] A.M. Pizzo, K. Kokini, L.C. Vaughn, B.Z. Waisner, S.L. Voytik-Harbin, Extracellular matrix (ECM) microstructural composition regulates local cell-ECM biomechanics and fundamental fibroblast behavior: a multidimensional perspective, Journal of Applied Physiology, 98 (2005) 1909-1921.

[272] B.A. Roeder, K. Kokini, J.E. Sturgis, J.P. Robinson, S.L. Voytik-Harbin, Tensile Mechanical Properties of Three-Dimensional Type I Collagen Extracellular Matrices With Varied Microstructure, Journal of Biomechanical Engineering, 124 (2002) 214-222.

[273] H.C. Liang, Y. Chang, C.K. Hsu, M.H. Lee, H.W. Sung, Effects of crosslinking degree of an acellular biological tissue on its tissue regeneration pattern, Biomaterials, 25 (2004) 3541-3552.

[274] V. Perez-Puyana, A. Romero, A. Guerrero, Influence of collagen concentration and glutaraldehyde on collagen-based scaffold properties, Journal of Biomedical Materials Research Part A, 104 (2016) 1462-1468.

[275] I.V. Yannas, J.F. Burke, C. Huang, P.L. Gordon, Correlation of in vivo collagen degradation rate with in vitro measurements, Journal of Biomedical Materials Research, 9 (1975) 623-628.

[276] A. Francesko, D. Soares da Costa, R.L. Reis, I. Pashkuleva, T. Tzanov, Functional biopolymer-based matrices for modulation of chronic wound enzyme activities, Acta Biomaterialia, 9 (2013) 5216-5225.

[277] G.T. Tihan, I. Răpan, R.G. Zgârian, M.V. Ghica, Collagen-based biomaterials for ibuprofen delivery, Comptes Rendus Chimie, 19 (2016) 390-394.

[278] S.H. De Paoli Lacerda, B. Ingber, N. Rosenzweig, Structure−release rate correlation in collagen gels containing fluorescent drug analog, Biomaterials, 26 (2005) 7164-7172.

[279] J.L. Holloway, H. Ma, R. Rai, J.A. Burdick, Modulating hydrogel crosslink density and degradation to control bone morphogenetic protein delivery and in vivo bone formation, Journal of Controlled Release, 191 (2014) 63-70.

[280] S. Barrientos, H. Brem, O. Stojadinovic, M. Tomic-Canic, Clinical Application of Growth Factors and Cytokines in Wound Healing, Wound repair and regeneration : official publication of the Wound Healing Society [and] the European Tissue Repair Society, 22 (2014) 569-578.

[281] R.G. Frykberg, T. Zgonis, D.G. Armstrong, V.R. Driver, J.M. Giurini, S.R. Kravitz, A.S. Landsman, L.A. Lavery, J.C. Moore, J.M. Schuberth, D.K. Wukich, C. Andersen, J.V. Vanore, Diabetic Foot Disorders: A Clinical Practice Guideline (2006 Revision), The Journal of Foot and Ankle Surgery, 45 (2006) S1-S66.

[282] P.S. Briquez, J.A. Hubbell, M.M. Martino, Extracellular Matrix-Inspired Growth Factor Delivery Systems for Skin Wound Healing, Advances in Wound Care, 4 (2015) 479-489.

[283] S. Barrientos, H. Brem, O. Stojadinovic, M. Tomic-Canic, Clinical application of growth factors and cytokines in wound healing, Wound Repair and Regeneration, 22 (2014) 569-578.

[284] K.E. Johnson, T.A. Wilgus, Vascular Endothelial Growth Factor and Angiogenesis in the Regulation of Cutaneous Wound Repair, Advances in Wound Care, 3 (2014) 647-661.

[285] N. Ferrara, Vascular endothelial growth factor, European Journal of Cancer, 32 (1996) 2413-2422.

[286] G. Lauer, S. Sollberg, M. Cole, I. Flamme, J. Sturzebecher, K. Mann, T. Krieg, S.A. Eming, Expression and proteolysis of vascular endothelial growth factor is increased in chronic wounds, J Invest Dermatol, 115 (2000) 12-18.

[287] W.J. Jeffcoate, K.G. Harding, Diabetic foot ulcers, The Lancet, 361 (2003) 1545-1551.

[288] M.M. Martino, S. Brkic, E. Bovo, M. Burger, D.J. Schaefer, T. Wolff, L. Gürke, P.S. Briquez, H.M. Larsson, R. Gianni-Barrera, J.A. Hubbell, A. Banfi, Extracellular Matrix and Growth Factor Engineering for Controlled Angiogenesis in Regenerative Medicine, Frontiers in Bioengineering and Biotechnology, 3 (2015).

[289] D.L. Rabenstein, Heparin and heparan sulfate: structure and function, Natural Product Reports, 19 (2002) 312-331.

[290] S. Tessler, P. Rockwell, D. Hicklin, T. Cohen, B.Z. Levi, L. Witte, I.R. Lemischka, G. Neufeld, Heparin modulates the interaction of VEGF165 with soluble and cell associated flk-1 receptors, J Biol Chem, 269 (1994) 12456-12461.

[291] H. Gitay-Goren, S. Soker, I. Vlodavsky, G. Neufeld, The binding of vascular endothelial growth factor to its receptors is dependent on cell surface-associated heparin-like molecules, Journal of Biological Chemistry, 267 (1992) 6093-6098.

[292] C. Ruhrberg, H. Gerhardt, M. Golding, R. Watson, S. Ioannidou, H. Fujisawa, C. Betsholtz, D.T. Shima, Spatially restricted patterning cues provided by heparin-binding VEGF-A control blood vessel branching morphogenesis, Genes & Development, 16 (2002) 2684-2698.

[293] H. Gerhardt, M. Golding, M. Fruttiger, C. Ruhrberg, A. Lundkvist, A. Abramsson, M. Jeltsch, C. Mitchell, K. Alitalo, D. Shima, C. Betsholtz, VEGF guides angiogenic sprouting utilizing endothelial tip cell filopodia, The Journal of Cell Biology, 161 (2003) 1163-1177.

[294] N. Ferrara, Binding to the Extracellular Matrix and Proteolytic Processing: Two Key Mechanisms Regulating Vascular Endothelial Growth Factor Action, Molecular Biology of the Cell, 21 (2010) 687-690.

[295] P. Vempati, A.S. Popel, F. Mac Gabhann, Formation of VEGF isoform-specific spatial distributions governing angiogenesis: computational analysis, BMC Syst Biol, 5 (2011) 59.

[296] P.S. Briquez, L.E. Clegg, M.M. Martino, F.M. Gabhann, J.A. Hubbell, Design principles for therapeutic angiogenic materials, Nature Reviews Materials, 1 (2016) 15006.

[297] P.M. Kharkar, K.L. Kiick, A.M. Kloxin, Designing degradable hydrogels for orthogonal control of cell microenvironments, Chemical Society Reviews, 42 (2013) 7335-7372.

[298] S.E. Sakiyama-Elbert, Incorporation of heparin into biomaterials, Acta Biomaterialia, 10 (2014) 1581-1587.

[299] K. Vulic, M.S. Shoichet, Affinity-Based Drug Delivery Systems for Tissue Repair and Regeneration, Biomacromolecules, 15 (2014) 3867-3880.

[300] Y. Liang, K.L. Kiick, Heparin-functionalized polymeric biomaterials in tissue engineering and drug delivery applications, Acta Biomaterialia, 10 (2014) 1588-1600.

[301] Y.K. Joung, J.W. Bae, K.D. Park, Controlled release of heparin-binding growth factors using heparin-containing particulate systems for tissue regeneration, Expert Opinion on Drug Delivery, 5 (2008) 1173-1184.

[302] N. Ferrara, K.A. Houck, L.B. Jakeman, J. Winer, D.W. Leung, The vascular endothelial growth factor family of polypeptides, Journal of Cellular Biochemistry, 47 (1991) 211-218.

[303] M. Shibuya, Vascular Endothelial Growth Factor (VEGF) and Its Receptor (VEGFR) Signaling in Angiogenesis: A Crucial Target for Anti- and Pro-Angiogenic Therapies, Genes & Cancer, 2 (2011) 1097-1105.

[304] S. Ashikari-Hada, H. Habuchi, Y. Kariya, K. Kimata, Heparin Regulates Vascular Endothelial Growth Factor165-dependent Mitogenic Activity, Tube Formation, and Its Receptor Phosphorylation of Human Endothelial Cells: COMPARISON OF THE EFFECTS OF HEPARIN AND MODIFIED HEPARINS, Journal of Biological Chemistry, 280 (2005) 31508-31515.

[305] K.A. Houck, D.W. Leung, A.M. Rowland, J. Winer, N. Ferrara, Dual regulation of vascular endothelial growth factor bioavailability by genetic and proteolytic mechanisms, J Biol Chem, 267 (1992) 26031-26037.

[306] D. Krilleke, Y.-Shan E. Ng, David T. Shima, The heparin-binding domain confers diverse functions of VEGF-A in development and disease: a structure–function study, Biochemical Society Transactions, 37 (2009) 1201.

[307] J.-H. Kim, T.-H. Kim, M.S. Kang, H.-W. Kim, Angiogenic Effects of Collagen/Mesoporous Nanoparticle Composite Scaffold Delivering VEGF(165), BioMed Research International, 2016 (2016) 9676934.

[308] C. Yao, P. Prével, S. Koch, P. Schenck, E.M. Noah, N. Pallua, G. Steffens, Modification of Collagen Matrices for Enhancing Angiogenesis, Cells Tissues Organs, 178 (2004) 189-196.

[309] G. Grieb, A. Groger, A. Piatkowski, M. Markowicz, G.C.M. Steffens, N. Pallua, Tissue Substitutes with Improved Angiogenic Capabilities: An in vitro Investigation with Endothelial Cells and Endothelial Progenitor Cells, Cells Tissues Organs, 191 (2010) 96-104.

[310] C. Yao, M. Markowicz, N. Pallua, E. Magnus Noah, G. Steffens, The effect of cross-linking of collagen matrices on their angiogenic capability, Biomaterials, 29 (2008) 66-74.

[311] K.M. Brouwer, R.M. Wijnen, D. Reijnen, T.G. Hafmans, W.F. Daamen, T.H. van Kuppevelt, Heparinized collagen scaffolds with and without growth factors for the repair of diaphragmatic hernia, Organogenesis, 9 (2013) 161-167.

[312] G. Neufeld, T. Cohen, H. Gitay-Goren, Z. Poltorak, S. Tessler, R. Sharon, S. Gengrinovitch, B.-Z. Levi, Similarities and differences between the vascular endothelial growth factor (VEGF) splice variants, Cancer and Metastasis Reviews, 15 (1996) 153-158.

[313] D.W. Leung, G. Cachianes, W.J. Kuang, D.V. Goeddel, N. Ferrara, Vascular endothelial growth factor is a secreted angiogenic mitogen, Science, 246 (1989) 1306.

[314] J.E. Park, G.A. Keller, N. Ferrara, The vascular endothelial growth factor (VEGF) isoforms: differential deposition into the subepithelial extracellular matrix and bioactivity of extracellular matrix-bound VEGF, Molecular Biology of the Cell, 4 (1993) 1317-1326.

[315] T. Cohen, H. Gitay-Goren, R. Sharon, M. Shibuya, R. Halaban, B. Levi, G. Neufeld, VEGF121, a vascular endothelial growth factor (VEGF) isoform lacking heparin binding ability, requires cell-surface heparan sulfates for efficient binding to the VEGF receptors of human melanoma cells, Journal of Biological Chemistry, 270 (1995) 11322-11326.

[316] N. Vaisman, D. Gospodarowicz, G. Neufeld, Characterization of the receptors for vascular endothelial growth factor, J Biol Chem, 265 (1990) 19461-19466.

[317] Y. Tabata, M. Miyao, M. Ozeki, Y. Ikada, Controlled release of vascular endothelial growth factor by use of collagen hydrogels, Journal of Biomaterials Science, Polymer Edition, 11 (2000) 915-930.

[318] C. Yao, A. Li, W. Gao, N. Pallua, G. Steffens, Improving the angiogenic potential of collagen matrices by covalent incorporation of Astragalus polysaccharides, International Journal of Burns and Trauma, 1 (2011) 17-26.

[319] R.W. Farndale, D.J. Buttle, A.J. Barrett, Improved quantitation and discrimination of sulphated glycosaminoglycans by use of dimethylmethylene blue, Biochim Biophys Acta, 883 (1986) 173-177.

[320] S.L. Oke, M.B. Hurtig, R.A. Keates, J.R. Wright, J.H. Lumsden, Assessment of three variations of the 1,9-dimethylmethylene blue assay for measurement of sulfated glycosaminoglycan concentrations in equine synovial fluid, Am J Vet Res, 64 (2003) 900-906.

[321] C.H. Zheng, M.E. Levenston, Fact versus artifact: avoiding erroneous estimates of sulfated glycosaminoglycan content using the dimethylmethylene blue colorimetric assay for tissue-engineered constructs, Eur Cell Mater, 29 (2015) 224-236; discussion 236.

[322] D.H. Ausprunk, D.R. Knighton, J. Folkman, Vascularization of normal and neoplastic tissues grafted to the chick chorioallantois. Role of host and preexisting graft blood vessels, The American Journal of Pathology, 79 (1975) 597-628.

[323] M.L. Ponce, H.K. Kleinmann, The Chick Chorioallantoic Membrane as an In Vivo Angiogenesis Model, in: Current Protocols in Cell Biology, John Wiley & Sons, Inc., 2001.

[324] ICCVAM-Recommended Test Method Protocol: Hen's Egg Test – Chorioallantoic Membrane (HET-CAM) Test Method, in: NIH Publication No. 10-7553, NIH, 2010.

[325] D.C. West, W.D. Thompson, P.G. Sells, M.F. Burbridge, Angiogenesis assays using chick chorioallantoic membrane, Methods Mol Med, 46 (2001) 107-129.

[326] D. Ribatti, B. Nico, A. Vacca, M. Presta, The gelatin sponge-chorioallantoic membrane assay, Nat Protoc, 1 (2006) 85-91.

[327] J.M. McPherson, S.J. Sawamura, R.A. Condell, W. Rhee, D.G. Wallace, The effects of heparin on the physicochemical properties of reconstituted collagen, Coll Relat Res, 8 (1988) 65-82.

[328] J.D. San Antonio, A.D. Lander, M.J. Karnovsky, H.S. Slayter, Mapping the heparin-binding sites on type I collagen monomers and fibrils, J Cell Biol, 125 (1994) 1179-1188.

[329] S.M. Sweeney, C.A. Guy, G.B. Fields, J.D. San Antonio, Defining the domains of type I collagen involved in heparin- binding and endothelial tube formation, Proc Natl Acad Sci U S A, 95 (1998) 7275-7280.

[330] D.R. Stamov, T.A. Khoa Nguyen, H.M. Evans, T. Pfohl, C. Werner, T. Pompe, The impact of heparin intercalation at specific binding sites in telopeptide-free collagen type I fibrils, Biomaterials, 32 (2011) 7444-7453.

[331] M.K. Keech, The formation of fibrils from collagen solutions. IV. Effect of mucopolysaccharides and nucleic acids: an electron microscope study, J Biophys Biochem Cytol, 9 (1961) 193-209.

[332] C. Guidry, F. Grinnell, Heparin modulates the organization of hydrated collagen gels and inhibits gel contraction by fibroblasts, J Cell Biol, 104 (1987) 1097-1103.

[333] M.B. Mathews, L. Decker, The effect of acid mucopolysaccharides and acid mucopolysaccharide-proteins on fibril formation from collagen solutions, Biochem J, 109 (1968) 517-526.

[334] W.W. Kilarski, B. Samolov, L. Petersson, A. Kvanta, P. Gerwins, Biomechanical regulation of blood vessel growth during tissue vascularization, Nat Med, 15 (2009) 657-664.

[335] J.-H. Kim, T.-H. Kim, M.S. Kang, H.-W. Kim, Angiogenic Effects of Collagen/Mesoporous Nanoparticle Composite Scaffold Delivering VEGF165, BioMed Research International, 2016 (2016) 8.

[336] S.M. Jay, B.R. Shepherd, J.W. Andrejecsk, T.R. Kyriakides, J.S. Pober, W.M. Saltzman, Dual delivery of VEGF and MCP-1 to support endothelial cell transplantation for therapeutic vascularization, Biomaterials, 31 (2010) 3054-3062.

[337] E. Quinlan, A. López-Noriega, E.M. Thompson, A. Hibbitts, S.A. Cryan, F.J. O'Brien, Controlled release of vascular endothelial growth factor from spray-dried alginate microparticles in collagen–hydroxyapatite scaffolds for promoting vascularization and bone repair, Journal of Tissue Engineering and Regenerative Medicine, (2015) n/a-n/a.

[338] N. Nagai, N. Kumasaka, T. Kawashima, H. Kaji, M. Nishizawa, T. Abe, Preparation and characterization of collagen microspheres for sustained release of VEGF, J Mater Sci Mater Med, 21 (2010) 1891-1898.

[339] I. Wilcke, J.A. Lohmeyer, S. Liu, A. Condurache, S. Kruger, P. Mailander, H.G. Machens, VEGF(165) and bFGF protein-based therapy in a slow release system to improve angiogenesis in a bioartificial dermal substitute in vitro and in vivo, Langenbecks Arch Surg, 392 (2007) 305-314.

[340] Y.H. Shen, M.S. Shoichet, M. Radisic, Vascular endothelial growth factor immobilized in collagen scaffold promotes penetration and proliferation of endothelial cells, Acta Biomaterialia, 4 (2008) 477-489.

[341] D. Odedra, L.L.Y. Chiu, M. Shoichet, M. Radisic, Endothelial cells guided by immobilized gradients of vascular endothelial growth factor on porous collagen scaffolds, Acta Biomaterialia, 7 (2011) 3027-3035.

[342] L.L.Y. Chiu, M. Radisic, Scaffolds with covalently immobilized VEGF and Angiopoietin-1 for vascularization of engineered tissues, Biomaterials, 31 (2010) 226-241.

[343] Q. He, Y. Zhao, B. Chen, Z. Xiao, J. Zhang, L. Chen, W. Chen, F. Deng, J. Dai, Improved cellularization and angiogenesis using collagen scaffolds chemically conjugated with vascular endothelial growth factor, Acta Biomaterialia, 7 (2011) 1084-1093.

[344] Y. Miyagi, L.L.Y. Chiu, M. Cimini, R.D. Weisel, M. Radisic, R.-K. Li, Biodegradable collagen patch with covalently immobilized VEGF for myocardial repair, Biomaterials, 32 (2011) 1280-1290.

[345] K. Raghunath, G. Biswas, K.P. Rao, K.T. Joseph, M. Chvapil, Some characteristics of collagen-heparin complex, Journal of Biomedical Materials Research, 17 (1983) 613-621.

[346] M.B. Mathews, L. Decker, The effect of acid mucopolysaccharides and acid mucopolysaccharide−proteins on fibril formation from collagen solutions, Biochemical Journal, 109 (1968) 517-526.

[347] G.C. Wood, The formation of fibrils from collagen solutions. 3. Effect of chondroitin sulphate and some other naturally occurring polyanions on the rate of formation, Biochem J, 75 (1960) 605-612.

[348] D. Stamov, M. Grimmer, K. Salchert, T. Pompe, C. Werner, Heparin intercalation into reconstituted collagen I fibrils: Impact on growth kinetics and morphology, Biomaterials, 29 (2008) 1-14.

[349] Q. Tan, H. Tang, J. Hu, Y. Hu, X. Zhou, Y. Tao, Z. Wu, Controlled release of chitosan/heparin nanoparticle-delivered VEGF enhances regeneration of decellularized tissue-engineered scaffolds, International Journal of Nanomedicine, 6 (2011) 929-942.

[350] M.J.B. Wissink, R. Beernink, N.M. Scharenborg, A.A. Poot, G.H.M. Engbers, T. Beugeling, W.G. van Aken, J. Feijen, Endothelial cell seeding of (heparinized) collagen matrices: effects of bFGF pre-loading on proliferation (after low density seeding) and pro-coagulant factors, Journal of Controlled Release, 67 (2000) 141-155.

[351] S. Soker, S. Takashima, H.Q. Miao, G. Neufeld, M. Klagsbrun, Neuropilin-1 Is Expressed by Endothelial and Tumor Cells as an Isoform-Specific Receptor for Vascular Endothelial Growth Factor, Cell, 92 (1998) 735-745.

[352] M.A. Princz, H. Sheardown, Heparin-modified dendrimer crosslinked collagen matrices for the delivery of heparin-binding epidermal growth factor, Journal of Biomedical Materials Research Part A, 100A (2012) 1929-1937.

[353] A. Lode, A. Reinstorf, A. Bernhardt, C. Wolf-Brandstetter, U. König, M. Gelinsky, Heparin modification of calcium phosphate bone cements for VEGF functionalization, Journal of Biomedical Materials Research Part A, 86A (2008) 749-759.

[354] C. Wolf-Brandstetter, A. Lode, T. Hanke, D. Scharnweber, H. Worch, Influence of modified extracellular matrices on TI6AL4V implants on binding and release of VEGF, Journal of Biomedical Materials Research Part A, 79A (2006) 882-894.

[355] S. Knaack, A. Lode, B. Hoyer, A. Rösen-Wolff, A. Gabrielyan, I. Roeder, M. Gelinsky, Heparin modification of a biomimetic bone matrix for controlled release of VEGF, Journal of Biomedical Materials Research Part A, 102 (2014) 3500-3511.

[356] U. Konig, A. Lode, P.B. Welzel, Y. Ueda, S. Knaack, A. Henss, A. Hauswald, M. Gelinsky, Heparinization of a biomimetic bone matrix: integration of heparin during matrix synthesis versus adsorptive post surface modification, J Mater Sci Mater Med, 25 (2014) 607-621.

[357] Y.-T. Hou, H. Ijima, T. Takei, K. Kawakami, Growth factor/heparin-immobilized collagen gel system enhances viability of transplanted hepatocytes and induces angiogenesis, Journal of Bioscience and Bioengineering, 112 (2011) 265-272.

[358] R.L. Jackson, S.J. Busch, A.D. Cardin, Glycosaminoglycans: molecular properties, protein interactions, and role in physiological processes, Physiol Rev, 71 (1991) 481-539.

[359] I. Capila, R.J. Linhardt, Heparin-protein interactions, Angew Chem Int Ed Engl, 41 (2002) 391-412.

[360] K.M. Keller, J.M. Keller, K. Kühn, The C-terminus type I collagen is a major binding site for heparin, Biochimica et Biophysica Acta (BBA) - General Subjects, 882 (1986) 1-5.

[361] B. ÖBrink, A Study of the Interactions between Monomeric Tropocollagen and Glycosaminoglycans, European Journal of Biochemistry, 33 (1973) 387-400.

[362] M.B. Mathews, The interaction of collagen and acid mucopolysaccharides. A model for connective tissue, Biochemical Journal, 96 (1965) 710.

[363] A.Y. Wang, C.A. Foss, S. Leong, X. Mo, M.G. Pomper, S.M. Yu, Spatio-Temporal Modification of Collagen Scaffolds Mediated by Triple Helical Propensity, Biomacromolecules, 9 (2008) 1755-1763.

[364] R.J. Lee, M.L. Springer, W.E. Blanco-Bose, R. Shaw, P.C. Ursell, H.M. Blau, VEGF Gene Delivery to Myocardium, Circulation, 102 (2000) 898.

[365] M.L. Springer, A.S. Chen, P.E. Kraft, M. Bednarski, H.M. Blau, VEGF Gene Delivery to Muscle: Potential Role for Vasculogenesis in Adults, Molecular Cell, 2 (1998) 549-558.

[366] C.J. Drake, C.D. Little, Exogenous vascular endothelial growth factor induces malformed and hyperfused vessels during embryonic neovascularization, Proceedings of the National Academy of Sciences, 92 (1995) 7657-7661.

[367] A.H. Zisch, M.P. Lutolf, J.A. Hubbell, Biopolymeric delivery matrices for angiogenic growth factors, Cardiovascular Pathology, 12 (2003) 295-310.

[368] C. Wong, E. Inman, R. Spaethe, S. Helgerson, Fibrin-based biomaterials to deliver human growth factors, Thrombosis and Haemostasis, 89 (2003) 573-582.

[369] N.S. Moiemen, E. Vlachou, J.J. Staiano, Y. Thawy, J.D. Frame, Reconstructive Surgery with Integra Dermal Regeneration Template: Histologic Study, Clinical Evaluation, and Current Practice, Plastic and Reconstructive Surgery, 117 (2006) 160S-174S.

[370] A. Cuadra, G. Correa, R. Roa, J.L. Piñeros, H. Norambuena, S. Searle, R.L. Heras, W. Calderón, Functional results of burned hands treated with Integra^{®}, Journal of Plastic, Reconstructive & Aesthetic Surgery, 65 228-234.

[371] M. Ehrbar, A. Metters, P. Zammaretti, J.A. Hubbell, A.H. Zisch, Endothelial cell proliferation and progenitor maturation by fibrin-bound VEGF variants with differential susceptibilities to local cellular activity, Journal of Controlled Release, 101 (2005) 93-109.

[372] R.B. Rema, K. Rajendran, M. Ragunathan, Angiogenic efficacy of Heparin on chick chorioallantoic membrane, Vascular Cell, 4 (2012) 8-8.

[373] D. Ribatti, L. Roncali, B. Nico, M. Bertossi, Effects of exogenous heparin on the vasculogenesis of the chorioallantoic membrane, Acta Anat (Basel), 130 (1987) 257-263.

[374] S. Pacini, M. Gulisano, S. Vannucchi, M. Ruggiero, Poly-l-lysine/Heparin Stimulates Angiogenesis in Chick Embryo Chorioallantoic Membrane, Biochemical and Biophysical Research Communications, 290 (2002) 820-823.

[375] W.J. Fairbrother, M.A. Champe, H.W. Christinger, B.A. Keyt, M.A. Starovasnik, Solution structure of the heparin-binding domain of vascular endothelial growth factor, Structure, 6 (1998) 637-648.

[376] K.G. Harding, H.L. Morris, G.K. Patel, Healing chronic wounds, BMJ, 324 (2002).

[377] D. Ribatti, Chicken Chorioallantoic Membrane Angiogenesis Model, in: X. Peng, M. Antonyak (Eds.) Cardiovascular Development: Methods and Protocols, Humana Press, Totowa, NJ, 2012, pp. 47-57.

[378] D. Ribatti, The chick embryo chorioallantoic membrane (CAM). A multifaceted experimental model, Mechanisms of Development, 141 (2016) 70-77.

[379] M.J.B. Wissink, R. Beernink, J.S. Pieper, A.A. Poot, G.H.M. Engbers, T. Beugeling, W.G. van Aken, J. Feijen, Immobilization of heparin to EDC/NHS-crosslinked collagen. Characterization and in vitro evaluation, Biomaterials, 22 (2001) 151-163.

[380] C.J. Robinson, S.E. Stringer, The splice variants of vascular endothelial growth factor (VEGF) and their receptors, Journal of Cell Science, 114 (2001) 853.

[381] B. Hoier, M. Walker, M. Passos, P.J. Walker, A. Green, J. Bangsbo, C.D. Askew, Y. Hellsten, Angiogenic response to passive movement and active exercise in individuals with peripheral arterial disease, J Appl Physiol (1985), 115 (2013) 1777-1787.

[382] B. Hoier, N. Nordsborg, S. Andersen, L. Jensen, L. Nybo, J. Bangsbo, Y. Hellsten, Pro- and anti-angiogenic factors in human skeletal muscle in response to acute exercise and training, J Physiol, 590 (2012) 595-606.

[383] C. Kut, F. Mac Gabhann, A.S. Popel, Where is VEGF in the body? A meta-analysis of VEGF distribution in cancer, Br J Cancer, 97 (2007) 978-985.

[384] B.A. Bladergroen, B. Siebum, K.G.C. Siebers-Vermeulen, T.H. Van Kuppevelt, A.A. Poot, J. Feijen, C.G. Figdor, R. Torensma, In Vivo Recruitment of Hematopoietic Cells Using Stromal Cell–Derived Factor 1 Alpha–Loaded Heparinized Three-Dimensional Collagen Scaffolds, Tissue Engineering Part A, 15 (2008) 1591-1599.

[385] L. Ravanti, V.M. Kahari, Matrix metalloproteinases in wound repair (review), Int J Mol Med, 6 (2000) 391-407.

[386] C. Mauch, B. Adelmann-Grill, A. Hatamochi, T. Krieg, Collagenase gene expression in fibroblasts is regulated by a three-dimensional contact with collagen, FEBS Letters, 250 (1989) 301-305.

[387] C. Helary, A. Foucault-Bertaud, G. Godeau, B. Coulomb, M.M. Giraud Guille, Fibroblast populated dense collagen matrices: cell migration, cell density and metalloproteinases expression, Biomaterials, 26 (2005) 1533-1543.

[388] S. Baiguera, P. Macchiarini, D. Ribatti, Chorioallantoic membrane for in vivo investigation of tissue-engineered construct biocompatibility, Journal of Biomedical Materials Research Part B: Applied Biomaterials, 100B (2012) 1425-1434.

[389] G.C. Hughes, S.S. Biswas, B. Yin, R.E. Coleman, T.R. DeGrado, C.K. Landolfo, J.E. Lowe, B.H. Annex, K.P. Landolfo, Therapeutic angiogenesis in chronically ischemic porcine myocardium: comparative effects of bFGF and VEGF, The Annals of Thoracic Surgery, 77 (2004) 812-818.

[390] L. Lu, H.M. Arbit, J.L. Herrick, S.G. Segovis, A. Maran, M.J. Yaszemski, Tissue Engineered Constructs: Perspectives on Clinical Translation, Annals of biomedical engineering, 43 (2015) 796-804.

[391] P. Velander, C. Theopold, T. Hirsch, O. Bleiziffer, B. Zuhaili, M. Fossum, D. Hoeller, R. Gheerardyn, M. Chen, S. Visovatti, H. Svensson, F. Yao, E. Eriksson, Impaired wound healing in an acute diabetic pig model and the effects of local hyperglycemia, Wound Repair and Regeneration, 16 (2008) 288-293.

[392] J. Haier, F. Schmidt, In Vivo Animal Models in Tissue Engineering, in: U. Meyer, J. Handschel, H.P. Wiesmann, T. Meyer (Eds.) Fundamentals of Tissue Engineering and Regenerative Medicine, Springer Berlin Heidelberg, Berlin, Heidelberg, 2009, pp. 773-779.

[393] A.L. Rubin, K.H. Stenzel, T. Miyata, M.J. White, M. Dunn, Collagen as a vehicle for drug delivery. Preliminary report, Journal of clinical pharmacology, 13 (1973) 309-312.

[394] S. Premaraj, B.L. Mundy, D. Morgan, P.L. Winnard, M.P. Mooney, A.M. Moursi, Sustained delivery of bioactive cytokine using a dense collagen gel vehicle collagen gel delivery of bioactive cytokine, Archives of oral biology, 51 (2006) 325-333.

[395] C. Kojima, T. Suehiro, K. Watanabe, M. Ogawa, A. Fukuhara, E. Nishisaka, A. Harada, K. Kono, T. Inui, Y. Magata, Doxorubicin-conjugated dendrimer/collagen hybrid gels for metastasis-associated drug delivery systems, Acta biomaterialia, 9 (2013) 5673-5680.

[396] S.E. Fu C. R., Fleitman J. S., De Leung M. C., , Collagen containing ophthalmic formulation, in: E. Patent (Ed.), 1990.

[397] Y. Pang, H.P. Greisler, Using a type 1 collagen-based system to understand cell-scaffold interactions and to deliver chimeric collagen-binding growth factors for vascular tissue engineering, Journal of investigative medicine : the official publication of the American Federation for Clinical Research, 58 (2010) 845-848.

[398] R.B. Phinney, S.D. Schwartz, D.A. Lee, B.J. Mondino, Collagen-shield delivery of gentamicin and vancomycin, Archives of ophthalmology, 106 (1988) 1599-1604.

[399] J.V. Aquavella, J.J. Ruffini, J.A. LoCascio, Use of collagen shields as a surgical adjunct, Journal of cataract and refractive surgery, 14 (1988) 492-495.

[400] T. Takezawa, T. Takeuchi, A. Nitani, Y. Takayama, M. Kino-oka, M. Taya, S. Enosawa, Collagen vitrigel membrane useful for paracrine assays in vitro and drug delivery systems in vivo, Journal of Biotechnology, 131 (2007) 76-83.

[401] D. Thacharodi, K.P. Rao, Rate-controlling biopolymer membranes as transdermal delivery systems for nifedipine: development and in vitro evaluations, Biomaterials, 17 (1996) 1307-1311.

[402] B. Rossler, J. Kreuter, D. Scherer, Collagen microparticles: preparation and properties, Journal of microencapsulation, 12 (1995) 49-57.

[403] B.M. Gebhardt, H.E. Kaufman, Collagen as a delivery system for hydrophobic drugs: studies with cyclosporine, Journal of ocular pharmacology and therapeutics : the official journal of the Association for Ocular Pharmacology and Therapeutics, 11 (1995) 319-327.

[404] L.P. Brewster, C. Washington, E.M. Brey, A. Gassman, A. Subramanian, J. Calceterra, W. Wolf, C.L. Hall, W.H. Velander, W.H. Burgess, H.P. Greisler, Construction and characterization of a thrombin-resistant designer FGF-based collagen binding domain angiogen, Biomaterials, 29 (2008) 327-336.

[405] J.S. Kay, B.S. Litin, M.A. Jones, A.W. Fryczkowski, M. Chvapil, J. Herschler, Delivery of antifibroblast agents as adjuncts to filtration surgery--Part II: Delivery of 5-fluorouracil and bleomycin in a collagen implant: pilot study in the rabbit, Ophthalmic surgery, 17 (1986) 796-801.

[406] S. Suzuki, K. Matsuda, N. Isshiki, Y. Tamada, K. Yoshioka, Y. Ikada, Clinical evaluation of a new bilayer "artificial skin" composed of collagen sponge and silicone layer, British journal of plastic surgery, 43 (1990) 47-54.

[407] J.F. Burke, I.V. Yannas, W.C. Quinby, Jr., C.C. Bondoc, W.K. Jung, Successful use of a physiologically acceptable artificial skin in the treatment of extensive burn injury, Annals of surgery, 194 (1981) 413-428.

[408] F. Lefebvre, P. Pilet, N. Bonzon, G. Daculsi, M. Rabaud, New preparation and microstructure of the EndoPatch elastin-collagen containing glycosaminoglycans, Biomaterials, 17 (1996) 1813-1818.

[409] C.J. Doillon, F.H. Silver, Collagen-based wound dressing: effects of hyaluronic acid and fibronectin on wound healing, Biomaterials, 7 (1986) 3-8.

[410] M. Chvapil, Considerations on manufacturing principles of a synthetic burn dressing: a review, Journal of biomedical materials research, 16 (1982) 245-263.

[411] I.V. Yannas, J.F. Burke, P.L. Gordon, C. Huang, R.H. Rubenstein, Design of an artificial skin. II. Control of chemical composition, Journal of biomedical materials research, 14 (1980) 107-132.

[412] B.A. Weissman, D.A. Lee, Oxygen transmissibility, thickness, and water content of three types of collagen shields, Archives of ophthalmology, 106 (1988) 1706-1708.

[413] C. Chai, K.W. Leong, Biomaterials approach to expand and direct differentiation of stem cells, Molecular therapy : the journal of the American Society of Gene Therapy, 15 (2007) 467-480.

[414] S. Hong, H.J. Hsu, R. Kaunas, J. Kameoka, Collagen microsphere production on a chip, Lab on a chip, 12 (2012) 3277-3280.

[415] M. Monaghan, S. Browne, K. Schenke-Layland, A. Pandit, A Collagen-based Scaffold Delivering Exogenous MicroRNA-29B to Modulate Extracellular Matrix Remodeling, Molecular Therapy, 22 (2014) 786-796.

[416] S. Koch, C. Yao, G. Grieb, P. Prével, E.M. Noah, G.C.M. Steffens, Enhancing angiogenesis in collagen matrices by covalent incorporation of VEGF, Journal of Materials Science: Materials in Medicine, 17 (2006) 735-741.

[417] M. Ragothaman, T. Palanisamy, C. Kalirajan, Collagen–poly(dialdehyde) guar gum based porous 3D scaffolds immobilized with growth factor for tissue engineering applications, Carbohydrate Polymers, 114 (2014) 399-406.

[418] E.O. Osidak, M.S. Osidak, D.E. Sivogrivov, T.S. Portnaya, T.M. Grunina, L.A. Soboleva, V.G. Lunin, A.S. Karyagina, S.P. Domogatskii, Regulation of the binding of the BMP-2 growth factor with collagen by blood plasma fibronectin, Applied Biochemistry and Microbiology, 50 (2014) 200-205.

[419] H.S. Nanda, N. Kawazoe, Q. Zhang, S. Chen, G. Chen, Preparation of collagen porous scaffolds with controlled and sustained release of bioactive insulin, Journal of Bioactive and Compatible Polymers: Biomedical Applications, 29 (2014) 95-109.

[420] E. Quinlan, A. López-Noriega, E. Thompson, H.M. Kelly, S.A. Cryan, F.J. O'Brien, Development of collagen–hydroxyapatite scaffolds incorporating PLGA and alginate microparticles for the controlled delivery of rhBMP-2 for bone tissue engineering, Journal of Controlled Release, 198 (2015) 71-79.

[421] B. Wen, M. Karl, D. Pendrys, D. Shafer, M. Freilich, L. Kuhn, An evaluation of BMP-2 delivery from scaffolds with miniaturized dental implants in a novel rat mandible model, J Biomed Mater Res B Appl Biomater, 97 (2011) 315-326.

[422] P. Prabu, N. Dharmaraj, S. Aryal, B.M. Lee, V. Ramesh, H.Y. Kim, Preparation and drug release activity of scaffolds containing collagen and poly(caprolactone), Journal of Biomedical Materials Research Part A, 79A (2006) 153-158.

[423] N. Shanmugasundaram, J. Sundaraseelan, S. Uma, D. Selvaraj, M. Babu, Design and delivery of silver sulfadiazine from alginate microspheres-impregnated collagen scaffold, Journal of Biomedical Materials Research Part B: Applied Biomaterials, 77B (2006) 378-388.

[424] M. Schlapp, W. Friess, Collagen/PLGA microparticle composites for local controlled delivery of gentamicin, Journal of Pharmaceutical Sciences, 92 (2003) 2145-2151.

[425] A.L. Weiner, S.S. Carpenter-Green, E.C. Soehngen, R.P. Lenk, M.C. Popescu, Liposome–collagen gel matrix: A novel sustained drug delivery system, Journal of Pharmaceutical Sciences, 74 (1985) 922-925.

[426] T. Kitajima, H. Terai, Y. Ito, A fusion protein of hepatocyte growth factor for immobilization to collagen, Biomaterials, 28 (2007) 1989-1997.

[427] E. Jeon, Y.-R. Yun, H.-W. Kim, J.-H. Jang, Engineering and application of collagen-binding fibroblast growth factor 2 for sustained release, Journal of Biomedical Materials Research Part A, 102 (2014) 1-7.

[428] W. Sun, C. Sun, H. Lin, H. Zhao, J. Wang, H. Ma, B. Chen, Z. Xiao, J. Dai, The effect of collagen-binding NGF-β on the promotion of sciatic nerve regeneration in a rat sciatic nerve crush injury model, Biomaterials, 30 (2009) 4649-4656.

[429] Y. Yang, Y. Zhao, B. Chen, Q. Han, W. Sun, Z. Xiao, J. Dai, Collagen-binding human epidermal growth factor promotes cellularization of collagen scaffolds, Tissue Eng Part A, 15 (2009) 3589-3596.

[430] J. Zhang, L. Ding, Y. Zhao, W. Sun, B. Chen, H. Lin, X. Wang, L. Zhang, B. Xu, J. Dai, Collagen-targeting vascular endothelial growth factor improves cardiac performance after myocardial infarction, Circulation, 119 (2009) 1776-1784.

[431] N. Ohkawara, H. Ueda, S. Shinozaki, T. Kitajima, Y. Ito, H. Asaoka, A. Kawakami, E. Kaneko, K. Shimokado, Hepatocyte Growth Factor Fusion Protein Having Collagen-Binding Activity (CBD-HGF) Accelerates Re-endothelialization and Intimal Hyperplasia in Balloon-injured Rat Carotid Artery, Journal of Atherosclerosis and Thrombosis, 14 (2007) 185-191.

[432] W. Sun, H. Lin, B. Chen, W. Zhao, Y. Zhao, Z. Xiao, J. Dai, Collagen scaffolds loaded with collagen-binding NGF-beta accelerate ulcer healing, J Biomed Mater Res A, 92 (2010) 887-895.

[433] C. Shi, W. Chen, Y. Zhao, B. Chen, Z. Xiao, Z. Wei, X. Hou, J. Tang, Z. Wang, J. Dai, Regeneration of full-thickness abdominal wall defects in rats using collagen scaffolds loaded with collagen-binding basic fibroblast growth factor, Biomaterials, 32 (2011) 753-759.

[434] J. Zhao, M. Shinkai, T. Takezawa, S. Ohba, U.-i. Chung, T. Nagamune, Bone regeneration using collagen type I vitrigel with bone morphogenetic protein-2, Journal of Bioscience and Bioengineering, 107 (2009) 318-323.

APPENDIX A. TYPE I COLLAGEN BASED DRUG DELIVERY FORMATS

Table A: Examples of Type I Collagen-based Drug Delivery in Research

1. Gels		
Molecules delivered	***In vitro/vivo* Applications**	**Drug binding approach**
Pilocarpine [393] TGF-β3 [394] Doxorubicin [395] Keterolac [396]	Ophthalmic treatment Craniocynostosis treatment Cancer chemotherapy Treating inflammation	*Physical:* Direct Admixing in collagen solution, then allowing collagen to polymerize into gel by incubation in 37°C.
Transforming growth factor TGF-β2 [100]	Facilitating tissue repair	*Chemical:* Covalent binding to collagen through difunctional PEG
growth factor R136K-CBD [397]	Smooth Muscle Cell Proliferation	Chemical: Chimeric collagen binding domain based attachment
2. Shields		
Plasmid DNA [129]	Gene therapy for healing after glaucoma surgery	*Physical:* Plasmid absorbed into the collagen shield
Gentamicin GA and Vancomycin VA [398] Tobramycin, Pilocarpine [399]	Antibiotic therapy through collagen contact lenses Keratoplasty treatment	*Physical:* Presoaking collagen shield in drug solution right before application
3. Membrane/Sheet		
Vascular Endothelial Growth Factor VEGF [400] Nifedipine [401]	Useful for paracrine assays and angiogenesis Transdermal delivery devices for wound dressings	*Physical:* Admixing in collagen gel followed by vitrification *Physical:* Mixing in alginate and then into collagen membrane

Table A (continued)

4. Microspheres/nanoparticles		
Retinol, tretinoin, or tetracaine and lidocaine in free base form [402]	Carriers for lipophilic drugs	*Physical:* Drug encapsulated by emulsion into cross-linked collagen microspheres
Cyclosporines [403]	Delivery to the ocular surface to prevent corneal graft rejection	*Physical:* Collagen-particles encapsulating cyclosporine suspended in methyl cellulose
5. Sponge		
Retinoic acid RA [404]	Endothelial regeneration in prosthetic bypass grafts	*Chemical:* Chimeric domain binding to sponge
5-Fluorouracil [405] Gentamicin [143] [142] rhBMP-2 [145]	Reduces intraocular pressure wound healing Bone remodeling	*Physical:* Lyophilized sponge rehydrated and soaked in drug/growth factor solution

It can be seen from above table that the versatility of collagen lends itself well to a variety of medical applications including but not limited to wound care, oral surgery, cardiovascular systems, neurology, urology, and orthopedics. The formats of collagen used in these applications are many, and selective examples are described below.

Sponges: Collagen sponges were originally developed as wound dressings due to their ability to absorb large quantities of tissue exudates, adherence to wet wound bed with preservation of low moist environment and shielding against mechanical harm and secondary bacterial infection [406]. Growth factors have been coated on collagen sponge to give recovery from dermal and epidermal wounds [138, 139]. Collagen sponges are generally prepared by lyophilizing aqueous collagen preparations [4] which yields collagen sponges with high porosity and fibril interconnectivity. The porosity of the lyophilized collagen can be altered by varying the collagen concentration and the freezing rate, which allows for some degree of control over the design of the sponge [407].

Another method of loading lyophilized sponge, apart from coating them with drug solution, is to soak the sponge in aqueous drug formulations prior to implantation. For example, porous collagen sponges have been soaked in antibiotic solutions (e.g., gentamicin) [142, 143] and in growth factor solutions (e.g. rhBMP) for delivery to tissue of interest [145]. In addition, collagen can be combined with other materials like such as elastin [408], fibronectin and hyaluronate [409] or glycoaminoglycans [410, 411] to aid in the delivery of drugs which do not interact well with collagen. The starting collagen material can be cross-linked with agents like glutaraldehyde and dehydrothermal treatments (DHT) in order to achieve highly resilient materials [410, 411]. However, the use of such cross-linking agents is not always effective as discussed in section 6. Sponges also suffer from the problem of releasing the entrapped factors quickly [159], giving a burst release profile in most cases [4].

Gels: Collagen gels are primarily used in aqueous injectable systems that are initially liquid but solidify after administration to the tissue. In situ polymerization methods offer an advantage of injectability and spatial control with better mechanical properties over other collagen-based devices such as implantable collagen sponges or sheets. For most gel formulations, the drug is admixed or physically entrapped with collagen in liquid form at a certain ratio, and then allowed to gel when the temperature is raised to 37 °C (body temperature), as is the case with drugs such as pilocarpine, TGF-β, doxorubicine and ketorolac (Table 2) [393-396]. Although such collagen gel systems show promise in drug delivery, their open pore structure cause diffusion-dominated release, which is undesirable due to little or no control over drug release rates.

Shields: Collagen shields have been primarily used as therapeutic devices for ophthalmological conditions such as plasmid delivery for glaucoma treatment or contact lenses to promote corneal epithelial healing and deliver hydro soluble drugs [129]. Shields typically start in a dehydrated form and have to be soaked with drugs in liquid solution prior to application. The thin collagen films conform to the shape of the cornea when applied to the eye and are able to provide sufficient oxygen transmission, as well as act as short term bandage lenses [412]. As the shields dissolve, they provide a layer of collagen solution that lubricates the surface of the eye, minimizes rubbing of the lids on the cornea, and fosters epithelial healing [65]. However, some disadvantages still limit

the application of collagen shields such as incomplete transparency, slight discomfort, complex insertion technique, and short period of working before dissolution. For mechanical strength imparting reason, cross-linking is performed on shields already loaded with drugs, but that endangers the chemical integrity of the active substance [160].

Microspheres: Collagen microparticulate systems have been used for encapsulating number of antibiotics, steroids, growth factors, and hydrophilic and hydrophobic drugs for therapeutic purposes due to their small particle size, large surface area, and ability to disperse in water to form colloidal solutions [65]. Microspheres can provide regulation of release by controlling the shell material and protection of drug until its delivery is needed [413]. Moreover, microspheres can create gradients in the concentration of growth factors that can direct cell migration, create patterns of cell differentiation an direct tissue organization into complex structures such as branching networks of vascular systems [107].

Despite many successful studies on collagen microspheres, the transition to collagen as the primary biomaterial for microsphere technology is hindered by limitations in manufacturing material, methods, and use of solvents due to risks of collagen denaturation. Most of the methods of formulation are tedious, requiring that each step (i.e. droplet generation, gelation, and extraction) be performed separately [414]. Furthermore, microsphere prepared have to be cross-linked exogenously in most cases, in order to avoid the possibility of losing the mechanical integrity and shape of device, but that leads to detrimental effects of exogenous cross-links.

APPENDIX B. STATE-OF-THE-ART METHODS OF TUNING COLLAGEN BASED MOLECULAR RELEASE

Table B: Strategies of tuning molecular release from collagen based materials and their limitations

Strategy	Example	Molecule delivered	Release period	Ref.	Limitation
Varying extent of exogenous crosslinking	Crosslinking with Glutaraldehyde	Vascular Endothelial Growth Factor (VEGF)	30 days	[317]	Detrimental effects on cells and tissues, such as cytotoxicity or tissue calcification;
	Crosslinking with four-arm poly (ethylene glycol) terminated succinimidyl glutarate (4S-StarPEG)	siRNA	10 days	[415]	Release requires hydrolysis of a linking bond which is different from *in-vivo* proteolytic degradation;
	Crosslinking with N-(3-dimethylaminopropyl)-N′-ethylcarbodiimide (EDC) and N-hydroxysuccinimide (NHS).	heparin	11 days	[379]	Crosslinking with additives increases complexity of system
	Crosslinking with metal oxide nanoparticles (NPs) and PVP capped ZnO (ZnO/PVP) in addition to UV crosslinking	pilocarpine hydrochloride (PHCl)	14 days	[131]	Crosslinking reagents can also react with and affect non-collagen structural proteins, glycosaminoglycans, growth factors and other bioactive compounds, or cells

Table B (continued)

Chemical modification of collagen to enable ionic bonding between drug and collagen	Succinylating collagen sponge and film with drug dispersed in poly (N-vinyl-2-pyrrolidione) (PVP) solution	Ciprofloxacin (a cationic fluoroquinilone antibiotic).	5 days	[141]	Succinylated collagen gels do not appear to have a long lifetime *in vivo*, usually disappearing within 24 h depending on the degree of succinylation
Covalent immobilization of drug	Crosslinking with di-functional or multi-functional succinimidyl ester polyethylene glycol (PEG, 3.4 to 10 kDa)	transforming growth factor beta-2 (TGF-beta2)	5 days	[100]	Covalent conjugation can be difficult to control, produce poor reaction yields, and even compromise the biochemical features of the protein/drug or collagen itself
	Crosslinking with SS-PEG-SS	VEGF	72 hrs	[416]	
	Poly(dialdehyde) guar gum (PDAGG) based covalent crosslinking of biomolecules with collagen	platelet derived growth factor (PDGF)	13 days	[417]	
Adding intermediate proteins with affinity for collagen and protein of interest	Heparin	basic fibroblast growth factor (bFGF)	10 days	[94]	Binding interactions are specific to each drug and hard to predict;
	Fibronectin	Recombinant human bone morphogenic factor 2 (rhBMP-2)	7 days	[418]	Very little tuning if the binding interaction is weak

Table B (continued)

Mixing collagen with other synthetic or natural polymers	Hybrid scaffolds of collagen and poly (lactic-co-glycolic acid) microbeads were prepared by introducing insulin-releasing poly (lactic-co-glycolic acid) microbeads into collagen porous scaffolds. Pore structure was controlled using ice particulates.	Insulin	4 weeks	[419]	Reduction in material's cell-instructive capacity and its inability to integrate with host tissue, can make the clinical translation of products very difficult
	Collagen–hydroxyapatite scaffolds combined with either alginate or poly(lactic-co-glycolic acid) (PLGA) microparticles	rhBMP-2	28 days	[420]	
	Addition of BMP-2 into soft PEG hydrogels before infusion in to the solid collagen/HA sponges	BMP-2	40% release observed in 15 days	[421]	
	collagen and poly-(caprolactone)	gentamicin and amikacin	60 hrs	[422]	
	collagen impregnated with drug loaded alginate microspheres	antibacterial agent silver sulfadiazine (AgSD)	66.8% released in 72 hrs	[423]	
	lyophilizing solution of suspended PLGA microparticles in a collagen dispersion	gentamicin	7 days	[424]	
	Drug containing liposome sequestration in collagen gel	Insulin Growth hormone	5 day 14 day	[425]	

Table B (continued)

Engineering peptides with collagen binding domain (CBD)	Fusion protein consisting of hepatocyte growth factor (HGF; an angiogenic factor) and a collagen-binding domain (CBD) polypeptide of fibronectin was produced in a baculovirus expression system	Hepatocyte growth factor (HGF)	1 week	[426-433] [426]	Complexity of such systems is a disadvantage from a commercial perspective
Addition of collagen mimetic peptides (CMPs)	CMP-modified polyplexes are bound to collagen via thermally induced annealing that induces CMP strand invasion and CMP-collagen triple helical hybridization	Gene	1 month	[257]	Native collagen microstructure is modified
Vitrification of collagen membrane	Collagen gel was dried for 2 weeks to convert into a rigid glass-like material, which was rehydrated with PBS containing VEGF	VEGF	14 days	[400]	Native collagen microstructure is modified
	After gelation, collagen membranes were formed by vitrification for 2 days, followed by rehydration with PBS containing BMP-2	BMP-2	>80% retained even after 15 days	[434]	

Table B (continued)

Increasing collagen density	Collagen content varied from 1.5% to 2.0% and 2.5%, pexiganan release from collagen was found to be extended from 24 h to 48 h and 72 h respectively	FITC coupled Pexiganan (a 22 amino acid antimicrobial peptide)	72 h	[262]	Can limit cell migration/ infiltration into the densified collagen
	A membrane consisting of photo polymerized polyethylene glycol dimethacrylate (PEGDM) and interconnected collagen microparticles (COLs) was used and collagen concentration varied from 100 mg/ml to 300 and 500 mg/ml	40-kDa FITC-dextran, and recombinant human brain-derived neurotrophic factor (rhBDNF)	42 days	[204]	
	Concentration of type I collagen hydrogels was varied from 1.5 to 4.5 mg/ml; drug interaction also played a role in tuning the release	pBMP-9	72 h	[263]	

VITA

Rucha received her BS in Biotechnology from Kolhapur, India and thereafter came to Vanderbilt University to work on her MS developing smart bio-materials for drug delivery applications. Rucha is interested in solving cutting edge biomedical problems related to wound healing, tissue regeneration and drug delivery.

Her interests in STEM started at young age when she developed a process for developing low calorie biscuits from banana peel pulp as a school project. Later she presented this innovative idea at variety of national and international forums such as-National Children Science Congress, Pune, India; Young Inventors Exhibition in Japan, and Joint Indo-Russian Technology Summit, Delhi, India. She was awarded patent for this invention and also presented a paper at the Solid Waste Management Conference in 2007 at Philadelphia. In order to motivate other Indian students towards STEM pursuits she later wrote a book summarizing her experiences. This book was awarded literature award by the Maharashtra State Government, India. For her inventions and STEM popularization efforts, she was invited by the late president of India, Dr. APJ Abdul Kalam to inaugurate 15th National Children's Science Congress. After coming to the U.S., Rucha continued her pursuit of excellence and received several prestigious scholarships and awards such as the Ross fellowship for outstanding PhD applicants, and Burton D. Morgan Fellowship for thought leadership, entrepreneurship, & community engagement in. She is motivated to pursue her passion in research, teaching, and STEM popularization upon graduation.

In her free time, Rucha likes to involve herself in community enrichment activities. She is an active member and was the president of Purdue Marathi Mandal, a student organization promoting Indian cultural activities at Purdue. She was also involved in "save river expedition" spreading awareness about pollution of Godavari River in India, and created a documentary to increase people's awareness about this issue. Apart from these activities, she enjoys SCUBA diving, badminton, writing, and hiking.